

การเพิ่มสมรรถนะของเว็บกราฟเพื่อจำลองสารสนเทศอุทกธรณีวิทยา



นายรุ่งวิทย์ หลายชูไทย

สถาบันวิทยบริการ จุฬาลงกรณ์มหาวิทยาลัย

วิทยานิพนธ์นี้เป็นส่วนหนึ่งของการศึกษาตามหลักสูตรปริญญาวิศวกรรมศาสตรมหาบัณฑิต


สาขาวิชาวิศวกรรมคอมพิวเตอร์ ภาควิชาวิศวกรรมคอมพิวเตอร์

คณะวิศวกรรมศาสตร์ จุฬาลงกรณ์มหาวิทยาลัย

ปีการศึกษา 2549

ลิขสิทธิ์ของจุฬาลงกรณ์มหาวิทยาลัย

AN ENHANCEMENT OF REEB GRAPH FOR MODELING HYDROGEOLOGICAL
INFORMATION



Mr.Rungwit Laichuthai

สถาบันวิทยบริการ

จุฬาลงกรณ์มหาวิทยาลัย

A Thesis Submitted in Partial Fulfillment of the Requirements

for the Degree of Master of Engineering Program in Computer Engineering

Department of Computer Engineering

Faculty of Engineering

Chulalongkorn University

Academic Year 2006

Copyright of Chulalongkorn University

รุ่งวิทย์ หลายชูไทย : การเพิ่มสมรรถนะของเรบกกราฟเพื่อจำลองสารสนเทศอุทกธรณีวิทยา (AN ENHANCEMENT OF REEB GRAPH FOR MODELING HYDROGEOLOGICAL INFORMATION) อ.ที่ปรึกษา : ดร.พิชญ์ คนองชัยยศ, อ.ที่ปรึกษาร่วม : รศ. ดร.สุจิตต์ คุณธนกุลวงศ์, 78 หน้า.

การสร้างภาพนามธรรมในระบบสามมิติมีความสำคัญสำหรับในระบบสารสนเทศภูมิศาสตร์อย่างมาก อย่างไรก็ตามวิธีการสร้างภาพนามธรรมในคอมพิวเตอร์กราฟิกส์ทั่วไปมักไม่สามารถแทนสารสนเทศภูมิศาสตร์หลายชั้นได้อย่างเหมาะสม เนื่องจากโครงสร้างภายในแบบจำลองสารสนเทศภูมิศาสตร์ทั่วไปไม่สามารถแสดงความสัมพันธ์ หรือการเชื่อมต่อระหว่างชั้นดินได้ ทำให้เกิดความคลาดเคลื่อนของการประมาณตำแหน่งชั้นดิน และการจัดแบ่งประเภทของชั้นดินที่เกิดขึ้นซึ่งไม่ตรงตามข้อมูลจริง งานวิจัยนี้นำเสนอวิธีเพิ่มสมรรถนะของเรบกกราฟเพื่อสร้างภาพนามธรรมของข้อมูลสารสนเทศภูมิศาสตร์แบบหลายชั้นในระบบสามมิติ ซึ่งสามารถแสดงโครงสร้างภายในที่ซับซ้อนของการจัดแบ่งประเภทของชั้นดินได้และคำนวณข้อมูลสารสนเทศภูมิศาสตร์ที่ต้องการได้ เช่น ตำแหน่งของชั้นดิน ภาพตัดขวางของชั้นดิน และเส้นรอบขอบตามระดับความสูงในระบบภูมิศาสตร์ได้อย่างเหมาะสมใกล้เคียงกับข้อมูลจริง การวิจัยเริ่มจากการเพิ่มสมรรถนะแบบจำลองเรบกกราฟโดยเปลี่ยนจากความสัมพันธ์ระหว่างจุดยอดบนเรบกกราฟกับเส้นรอบขอบตามปกติให้เป็นความสัมพันธ์ระหว่างจุดยอดบนเรบกกราฟกับเขตของเส้นรอบขอบแทนและสร้างวิธีการประมาณพื้นผิวในช่วงของเขตของเส้นรอบขอบขึ้นใหม่ หลังจากนั้นนำแบบจำลองเรบกกราฟที่ปรับแล้วไปใช้โดยการระบุตำแหน่งของชั้นดิน และสร้างพื้นผิวของชั้นดินแต่ละในช่วงตำแหน่งของชั้นดินที่รับเข้ามา แล้วนำมาสร้างภาพตัดขวางของชั้นดินของแต่ละชั้นดิน ณ ตำแหน่งความสูงที่เป็นจุดวิกฤตทั้งหมดตามทฤษฎีเมอร์สเพื่อสร้างเรบกกราฟรูปแบบใหม่ ท้ายสุดพื้นผิวที่สร้างขึ้นสามารถแทนโครงสร้างภายในทั้งหมดของข้อมูลสารสนเทศภูมิศาสตร์ได้ โดยผลการทดลองแสดงให้เห็นว่าวิธีที่นำเสนอสามารถเก็บ และแสดงโครงสร้างภายในของชั้นดินตลอดจนการภาพตัดขวางของชั้นดินของข้อมูลสารสนเทศอุทกธรณีวิทยาได้อย่างมีประสิทธิภาพ

ภาควิชา.....วิศวกรรมคอมพิวเตอร์.....ลายมือชื่อนิสิต..... *รุ่งวิทย์ หลายชูไทย*
 สาขาวิชา.....วิศวกรรมคอมพิวเตอร์.....ลายมือชื่ออาจารย์ที่ปรึกษา..... *พิชญ์ คนองชัยยศ*
 ปีการศึกษา2549.....ลายมือชื่ออาจารย์ที่ปรึกษาร่วม..... *สุจิตต์ คุณธนกุลวงศ์*

4870440821 : MAJOR COMPUTER ENGINEERING

KEY WORD : THREE DIMENTIONAL MODEL / CROSS SECTIONAL DATA / REEB GRAPH / HYDROGEOLOGICAL INFORMATION

RUNGWIT LAICHUTHAI : AN ENHANCEMENT OF REEB GRAPH FOR MODELING HYDROGEOLOGICAL INFORMATION. THESIS ADVISOR : PIZZANU KANONGCHAIYOS, Ph.D., THESIS CO-ADVISOR : ASSOC.PROF.SUCHARIT KOONTANAKULVONG, Ph.D., 78 pp.

Three-dimensional visualization has been useful for several geological information systems. Typical visualization methods in computer graphics usually cannot properly represent the multi-layer geographical data because of the lack of relation between each soil layer. In addition, some errors in the estimated position of soil layers and in the classification of soil layers can occur. This research, therefore, presents an enhancement of Reeb graph method for three-dimensional geological information providing the complex internal structure of soil layers. Proposed method can calculate major geological information, such as the positions of soil layers, the cross-sectional contours of soil layers at each height level corresponding to the input data. Firstly, the original Reeb graph is enhanced by changing from the relation between Reeb node and its contour to the relation between each Reeb node and its set of contours. Then, the surface is constructed from the set of contours. After specifying the position of each soil layer and constructing each surface for each soil layer according to the input depth, the cross-sectional contours of each soil layer at every critical height are then calculated using Morse theory. Next the enhanced Reeb graph is generated. Finally, the reconstructed surfaces represent the complete internal structure of the geological information. The experimental result shows that the proposed method can be efficiently applied for storing and displaying the cross-sectional data and the structure of soil layers of the hydrogeological information.

Department.....Computer Engineering.....Student's signature.....*รุ่งวิทย์ ลาชัยอยู่*.....
 Field of study...Computer Engineering....Advisor's signature.....*[Signature]*.....
 Academic year...2006.....Co-advisor's signature.....*Sucharit K*.....

ACKNOWLEDGMENTS

It is a great pleasure to acknowledge my thesis advisors, Dr. Pizzanu Kanongchaiyos and Associate Professor Dr. Sucharit Koontanakulvong, for their intellectual advice and valuable assistance throughout this research. I would also like to express my grateful thanks to my thesis committee, Dr. Proadpran Punyabukkana, Dr. Daricha Sutivong and Associate Professor Dr. Pavadee Sompagdee for their beneficial guidance and suggestions.

I am thankful for the scholarship of Chulalongkorn University that my research had been published in the 2006 International Conference on Cyberworlds (CW2006), which was held on November 28-29, 2006, EPFL, Lausanne, Switzerland, pages 93-96. The paper title is An Enhancement of Reeb Graph for Modeling Hydrogeological Information. In addition, in proceedings of 1st National Applied Statistics Conference (ASCONF2006), Bangkok, Thailand, August 10-11, 2006, pages 275-285. The paper title is Visualization of hydrogeological Information Using Reeb Graph. Moreover, Poster session presented at the 1st Thai-Japanese Student Exchange Meeting (TJSE2006), Osaka University, Osaka, Japan, November 2-3, 2006. The poster title is An Algorithm for Multi-layer Three Dimensional Object Modeling.

I want to extend my thanks to all research members especially my associates in computer graphic and animation lab (CG & A Lab) for their generous help, encouragement and relationships which made my life through the course filled with amusements and happiness.

Finally, I deeply wish to thank my parents for their love, understanding and invaluable support throughout my graduate study.

TABLE OF CONTENTS

	Page
ABSTRACT (THAI)	iv
ABSTRACT (ENGLISH)	v
ACKNOWLEDGMENTS	vi
TABLE OF CONTENTS	vii
LIST OF FIGURES	x
LIST OF TABLES	xiv
CHAPTER I INTRODUCTION	1
1.1 Background and Statement of Problems	1
1.2 Objectives	2
1.3 Scope of Study	2
1.4 Research Procedure	3
1.5 Expected Benefits	3
1.6 Thesis Structure	3
1.7 Publication	4
CHAPTER II THEORETICAL BACKGROUND AND RELATED WORKS	5
2.1 Theoretical Background	5
2.1.1 Mathematical Fundamentals	5
2.1.1.1 Differentiable Manifold	5
2.1.1.2 Morse Theory	6
2.1.1.3 Reeb Graph	7
2.1.1.3.1 Reeb Graph on Height Function	7
2.1.1.3.2 Enhanced Reeb Graph	8

2.1.1.4 Homotopy.....	10
2.1.2 Surface Constructions	11
2.1.2.1 Implementation of Enhanced Reeb Graph	11
2.1.2.1.1 Adopted Curves	11
2.1.2.1.2 Edge of Enhanced Reeb Graph	14
2.1.2.1.3 Contour of Enhanced Reeb Graph	14
2.1.2.2 Toroidal Graph.....	15
2.1.2.2.1 Discrete Toroidal Graph	16
2.1.2.2.2 Continuous Toroidal Graph.....	17
2.1.2.2.3 Distance Function	18
2.1.2.2.4 Closest Pair Vertex	19
2.1.2.3 Surface Construction	19
2.1.2.3.1 Correspondence between Contours.....	20
2.1.2.3.2 Contour Interpolation by Homotopy.....	22
2.1.2.3.3 Contour Interpolate by Sliding Homotopy	23
2.1.2.4 Branch Handling	26
2.1.2.4.1 Guiding Curve.....	27
2.1.2.4.2 Continuity near Critical Point.....	29
2.2 Related Works	31
2.2.1 Surface Reconstruction	31
2.2.2 Three-Dimensional Model Creation with Reeb Graph.....	33

	Page
CHAPTER III ENHANCED REEB GRAPH FOR MODELING HYDROGEOLOGICAL INFORMATION.....	37
3.1 Enhanced Reeb graph.....	37
3.2 Set of contours.....	38
3.3 Surface reconstruction.....	39
CHAPTER IV EXPERIMENTAL RESULTS	40
4.1 Tool Development.....	40
4.1.1 Requirement	40
4.1.2 Analysis and Design	42
4.1.3 Implement	43
4.1.4 Result Testing	47
4.2 Sample Results	67
4.3 Discussion	71
CHAPTER V CONCLUSION AND FUTURE WORK.....	73
5.1 Conclusion.....	73
5.2 Future Work	73
REFERENCES	74
BIOGRAPHY	77

LIST OF FIGURES

Figure	Page
2-1. A torus and its Reeb graph on a height function is presented	8
2-2. Two tori that differ about their shape have the same Reeb graph	8
2-3. Each torus has the different enhanced Reeb graph.....	10
2-4. The upper contour is transformed to the lower contour by homotopy	11
2-5. The difference between a Cardinal Spline and a Catmull-Rom Spline is displayed	14
2-6. A spline curve is approximated by a polygon to determine the parameter	15
2-7. A discrete toroidal graph is presented. The upper contour has six vertices and the lower contour has five vertices	17
2-8. Triangular patches are determined by the above discrete toroidal graph.....	17
2-9. A continuous toroidal graph is presented	18
2-10. A contour on $ax+by+cz+d=0$ is transformed to the contour on a plane parallel to the xy -plane.....	20
2-11. The rectangle that encloses the contour is searched and mapped to a unit square	21
2-12. The correspondence between the mapped contours is determined.....	21
2-13. The correspondence between the contours is determined	21
2-14. The different edges are given to the same pair of contours.....	23
2-15. The edge that have the same shape pass through the same pair of contours at the different points	24
2-16. An edge vector is presented.....	25
2-17. A homotopy vector is presented	25

Figure	Pag ๓
2-18. Sliding homotopy is presented. First, the top contour and the bottom contour are giving. Then contours are interpolated by homotopy. Next sliding vector is calculated. And contours are shifted by the sliding vector	26
2-19. Contours are transformed by an attached guiding curve	27
2-20. The new parameters are given to the merged contour	29
2-21. The new parameters are given to the divided contours	29
2-22. This is an example of a merge case. Two upper contours and one lower contour are given.....	30
2-23. The contour f at the critical point is interpolated by the guiding curve homotopy	30
2-24. Parametric Surface Reconstructions	31
2-25. Volumetric Surface Reconstructions	31
2-26. Delaunay-Based Surface Reconstructions.....	32
2-27. Incremental Surface Reconstructions	32
2-28. Interactive Surface Reconstructions	33
2-29. Cross-sectional Contour and Reeb graph	34
2-30. Show contour of Cochlea	34
2-31. Cross-sectional model and Reeb graph	34
2-32. Bi-Torus (a) cross-sectional and contour (b) Reeb graph.....	35
2-33. Show the critical region of Manifold M , which is from the differential manifold. This region is constructed using Delauney triangulation from height function.	35
2-34. Structure Reeb graph of heart model.....	36
3-1. Nodes and connecting lines of extended Reeb graph with its sets of contours .	37
3-2. Cross section and contours of each soil layer.....	38

Figure	Page
4-1. Surface reconstruction of hydrogeological information from 52 sample drill holes	41
4-2. Cross section of each soil layer and categorization of soil layer.....	41
4-3. Flowchart of Process for 3D Modeling Hydrogeological Information	42
4-4. Soil layer position model.....	43
4-5. Geographical surface model according to the category of soil layer.....	44
4-6. Cross section of soil layers in each category	45
4-7. Surface reconstruction by creating the Reeb graph.....	46
4-8. Model of the surface and internal structure of geographical information	46
4-9. Soil layer model in example 1 from all four sides.....	63
4-10. Soil layer model after computation with small number of boreholes in example one.....	64
4-11. Soil layer model after computation with large number of boreholes in example one.....	64
4-12. Soil layer model in example 2 from all four sides.....	65
4-13. Soil layer model after computation with small number of boreholes in example two.....	65
4-14. Soil layer model after computation with large number of boreholes in example two.....	66
4-15. Mesh layers of soil layers	67
4-16. Internal structure of soil layers	68
4-17. Another view of internal structure of soil layers.	68
4-18. Cross-sectional top view of soil layers.....	69
4-19. Cross-sectional side view of soil layers.....	69
4-20. Subdivision of soil layer shown with 20 layers.....	70

Figure	Page
4-21. Reeb graph for subdivision with 20 layers	70
4-22. Different arrangement of soil layers.....	71



สถาบันวิทยบริการ
จุฬาลงกรณ์มหาวิทยาลัย

LIST OF TABLES

Table	Page
4.1 Format of collecting soil layers information.....	40
4.2 Result of compare from example one with $Z - test$	49
4.3 Result of compare from example two with $Z - test$	50
4.4 Result of compare from example three with $Z - test$	51
4.5 Conclusion of compare from example one, two and three with Z -test.....	53
4.6 Difference between the interpolated depth from our model and the original survey depth from example one with each soil layer.....	55
4.7 Difference between the interpolated depth from our model and the original survey depth from example one with all soil layer	56
4.8 Difference between the interpolated depth from our model and the original survey depth from example two with each soil layer	57
4.9 Difference between the interpolated depth from our model and the original survey depth from example two with all soil layer.....	58
4.10 Difference between the interpolated depth from our model and the original survey depth from example three with each soil layer	59
4.11 Difference between the interpolated depth from our model and the original survey depth from example three with all soil layer.....	61
4.12 Conclusion of difference between the interpolated depth from our model and the original survey depth from example one, two and three.....	63

CHAPTER I

INTRODUCTION

1.1 Background and Statement of Problems

Computer aided calculations have a major role in assisting geographical information systems, such as surveying underground water sources. These include geological environmental modeling, and processing geographical information, and displaying the soil layers with three-dimensional graphics. Also, there are many types of tools to help create various types of geological models, for example, diagramming, organizing geological systems, displaying a model of soil layers and the cross section of a geological area, and estimating contour lines for the data in a given range of relations between soil layers.

Creating a model of geographical information by using geometrical methods will display using typical computer graphics methods. Creating a model of underground water in 3D, or creating a model of a geological surface [1, 2, 3, 4] usually cannot display the complete relationships of the geological data accurately and appropriately, as there are no standard geological models, and creating or estimating the surface of each soil layer is independent, due to the lack of data for the internal structure. In addition, we cannot display the geological relations or connections between each soil layer. In some instances, analysis and calculation of partial data to create a sufficiently accurate display may not be possible. In addition, there are inaccuracies in the soil layer positions and inaccurate categorization of soil layers.

Therefore, this research presents a 3D model for hydrological and geological information, which can display relations between various types of geographical information, for example, coordinates on a surface, coordinates under soil layers, and categories of soil layers. Also, it can display the internal structure of soil layers categorization and can calculate required geographical information, such as the position of soil layer, cross section of soil layer, contours, and geological maps accurately and consistent with the actual data. We utilize the Morse theory, which refers to the general sense of variant calculus, which explains every case of the relation between a point on a continuous real-number function and the general topology of a manifold. Here we replace

the manifold with a data set of a geographical surface. The calculation begins by specifying each location of a soil layer. In addition, creating the surface by estimating from the input depths of the layer to create the cross section of each soil layer at all critical positions obtained using the Morse theory [5, 6, 7], in order to create the extended Reeb graph for creating the surfaces and complete internal structure of the geographical data. Next, we compare the results from the model with the actual data, which will be within the limits that cover all the received depth data. This conceptual model can be displayed as a 3D model where we can retrieve the internal structure of soil layer to view, as well as display the cross section of the soil layer, and can be used to represent and store systematically geographical information for efficient retrieval or search.

1.2 Objectives

To propose an enhancement of Reeb graph modeling for representing 3D geographical information model displaying internal structures appropriately for accurate data analysis, by processing cross sections to find the limit of the research area in the geological model accurately, as well as approximating the soil layer heights correctly, and categorizing soil layers correctly as well, to create proper relations between soil layers and drill holes.

1.3 Scope of Study

1. This research is to test the modeling system for hydrogeological information. The data for testing can be obtained with two methods: creating boreholes by randomizing the coordinates and depth (52 boreholes), and creating boreholes by using data from surveys water resource engineering (200 boreholes covering a provincial area).
2. This research had to input data format which importing a file of numerical data, stored as an Excel file that data of depth and co-ordinate of each soil layer from exploration of water resource engineering.
3. The presented modeling system has the following capabilities: display three-dimensional imagery, the cross-sectional soil layers, categorizing soil layers with multiple viewing angles, and display the relations of the soil layer with the borehole.

1.4 Research Procedure

Procedure of research that consist of seven parts

1. Review literature

This research can explain related-theories.

- The Fundamental Mathematical Theories
- Surface Reconstruction Theories
- Reeb Graph Theories
- Morse Theories

Previous research studies, articles, books, online information technology.

2. Design an algorithm.

3. Program development

4. Model evaluation

5. Implementation

6. Analysis

7. Deliverables and conclusion

1.5 Expected Benefits

Proposed Enhances Reeb Graph Model can represent geographic information from water resource engineering. The model can be applied for displaying the geographical data in the three dimensional images, and representing the relationship of internal structure and analyzing the geographical data.

1.6 Thesis Structure

This thesis has five chapters: Introduction, Theoretical background and related works, Enhanced Reeb Graph for Modeling Hydrogeological Information, Experimentation results and Conclusion and Future work.

The first chapter provides background and statement of problems, objectives, scope of study, research procedure, expected benefits, thesis structure and publications. Chapter 2 gives a brief description of Mathematical Fundamentals and Surface Constructions, Differentiable Manifold, Morse theory and explains how to represent objects with Reeb graph. In addition, discusses on previous works regarding representating three-dimensional model (3D) and Surface Reconstruction. In chapter 3 explains improving the performance of Reeb graph to model hydrological and geological

information. Chapter 4 explains experimental results and Chapter 5 explains the results and possible paths for further development.

1.7 Publications

Some parts of this research had been published in the 2006 International Conference on Cyberworlds (CW2006), which was held on November 28-29, 2006, EPFL, Lausanne, Switzerland. The paper title is An Enhancement of Reeb Graph for Modeling Hydrogeological Information. The authors are Rungwit Laichuthai and Pizzanu Kanongchaiyos. In addition, in proceedings of 1st National Applied Statistics Conference (ASCONF2006), Bangkok, Thailand, August 10-11, 2006, pages 275-285. The paper title is Visualization of hydrogeological Information Using Reeb Graph. Moreover, Poster session presented at the 1st Thai-Japanese Student Exchange Meeting (TJSE), Osaka University, Osaka, Japan, November 2-3, 2006. The poster title is An Algorithm for Multi-layer Three Dimensional Object Modeling.



สถาบันวิทยบริการ
จุฬาลงกรณ์มหาวิทยาลัย

CHAPTER II

THEORETICAL BACKGROUND AND RELATED WORKS

This chapter explains the mathematical fundamentals. In addition, subject discusses on previous works regarding Reeb Graph Construction and Surface Reconstruction Model.

2.1 Theoretical Background

This section explains the mathematical fundamentals that compose the basis of three-dimensional model of surface reconstruction and Three Dimensional Model Creation with Reeb Graph.

2.1.1 Mathematical Fundamentals

This section explains the mathematical fundamentals that compose the basis of this modeling system. First, the concept manifold is presented. Second, Morse theory is explained. This is a backbone about surface construction of this system. Then a Reeb graph is introduced. This graph is the topological concept that has structural information of an object. Finally, homotopy is mentioned. It is utilized to contour interpolation.

2.1.1.1 Differentiable Manifold

Let S be a set. A chart is a bijection φ from a subset U to S to an open subset of Banach space. A C^k atlas is a family of charts $A = \{(U_i, \varphi_i) \mid i \in I\}$ such that

1. $S = \cup \{U_i \mid i \in I\}$
2. Any two charts in A are compatible in the sense that the overlap maps between members of A are C^k diffeomorphisms : for two charts (U_i, φ_i) and (U_j, φ_j) with $U_i \cap U_j \neq \emptyset$, we form the overlap map : $\varphi_{ji} = \varphi_j \circ \varphi_i^{-1} \mid \varphi_i(U_i \cap U_j)$. We require that $\varphi_i(U_i \cap U_j)$ is open and that φ_{ji} be a C^k diffeomorphism.

Two C^k atlases A_1 and A_2 are equivalent if $A_1 \cup A_2$ is a C^k atlas. A C^k differentiable structure D on S is an equivalence class on S . The union of the atlases in D , $A_D = \cup\{A \mid A \in D\}$ is the maximal atlases on D , and a chart $(U, \varphi) \in A_D$ is an admissible local chart. If A is a C^k atlas on S , the union of all atlases equivalent to A is called the C^k structure generated by A . A differentiable manifold M is a pair (S, D) where S is a set and D is a C^k differentiable structure on S . A differentiable manifold M is an n -manifold when every chart has values in an n -dimensional vector space. Thus for every point $a \in M$, there is an admissible local chart (U, φ) with $a \in \mathbb{R}^n$, where $n = \dim M$ [8, 9].

2.1.1.2 Morse Theory

Let f be a mapping from an n dimensional manifold M to a set of real number R . If the point p is a non-degenerate critical point of f , the function is approximated by quadratic form based on second order partial derivatives in the neighborhood of p as follows:

$$H(i, j) = \frac{\partial^2 f}{\partial x_i \partial y_j}$$

This matrix is called a Hessian matrix. If the Hessian matrix of the critical point p is regular, the point is called non-degenerate. The index of f at p is the number of negative Eigen values of the Hessian matrix. A function f is called a Morse function if the following two conditions are satisfied.

1. None of its critical points is degenerate.
2. The values of f at one critical point differs from those of the other critical points.

Since the critical points of a Morse function are isolated, the number of critical points is finite as long as M is compact.

Let M be a compact differentiable manifold and f be a Morse function from M to R . If the critical points of f are p_1, p_2, \dots, p_k and their indices are r_1, r_2, \dots, r_k , respectively. M is homotopy equivalent to the finite CW complex that is composed of

an r_1 -dimensional cell, a r_2 -dimensional cell, ..., and a r_n -dimensional cell. In other words, the following is satisfied.

$$M \simeq e^{r_1} \cup e^{r_2} \cup \Lambda \cup e^{r_n}$$

Morse theory states that the homotopy type of an object is determined by the above formula. Users can therefore construct a desired surface attaching cells corresponding to the critical points of its Morse function. However, Morse theory cannot determine the topological structure of surface completely. For instance, the connectivity, the existence of knots, and the existence of links are not distinguished. These ambiguities are the limitation [7, 10].

2.1.1.3 Reeb Graph

A Reeb graph is introduced in this section. A Reeb graph is proposed by G.Reeb and it represents the topological structure of an object. This graph is defined as follows [11, 12, 13, 14, 15].

Let $f: M \rightarrow R$ be a function on a compact manifold M . The Reeb graph of f is the quotient space of the graph of f in $M \times R$ by the equivalence relation given below:

$$(X_1, f(X_1)) \sim (X_2, f(X_2)) \Leftrightarrow f(X_1) = f(X_2)$$

where X_1, X_2 are in the same connected component of $f^{-1}(f(X_1))$

2.1.1.3.1 Reeb Graph on Height Function

Now a Reeb graph on height function is explained. A Reeb graph on height function has topological information of an object as follows.

1. Its node corresponds to critical point of an object.
2. Its edge corresponds with a connected component of an object.
3. Its point of an edge corresponds with a contour on a cross-sectional plane.

For instance, the Reeb graph of a torus is presented in figure 2.1. Since a Reeb graph on height function has the topological information of an object, the graph can be utilized to a three-dimensional object construction.

However, the graph has no information about shape of an object. Consequently, we cannot construct three-dimensional objects by utilizing only Reeb graph. An example is shown in figure 2.1. There are two tori in the figure 2.2. One is regular torus and the

other is a distorted torus. They are different about their shape but they have the same Reeb graph in the figure 2.2 because they have the same topological structure.

Thus, in the modeling system that introduces a Reeb graph as the structure of an object, some geometrical information about must be attached to the topological graph later.

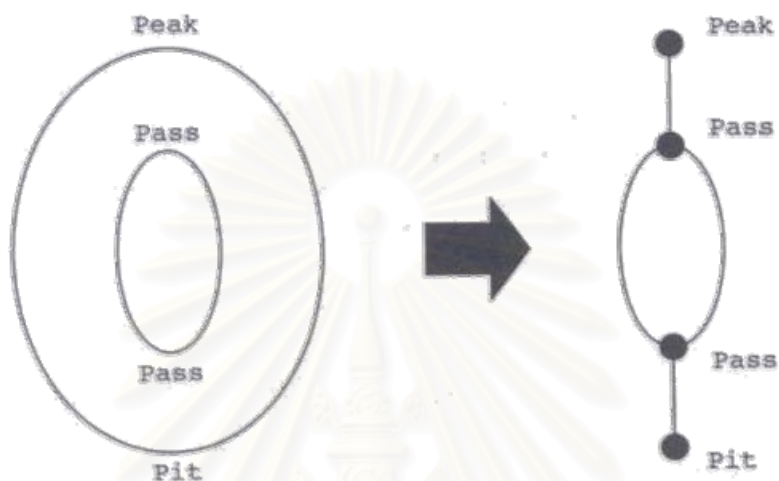


Figure 2.1: A torus and its Reeb graph on a height function is presented.

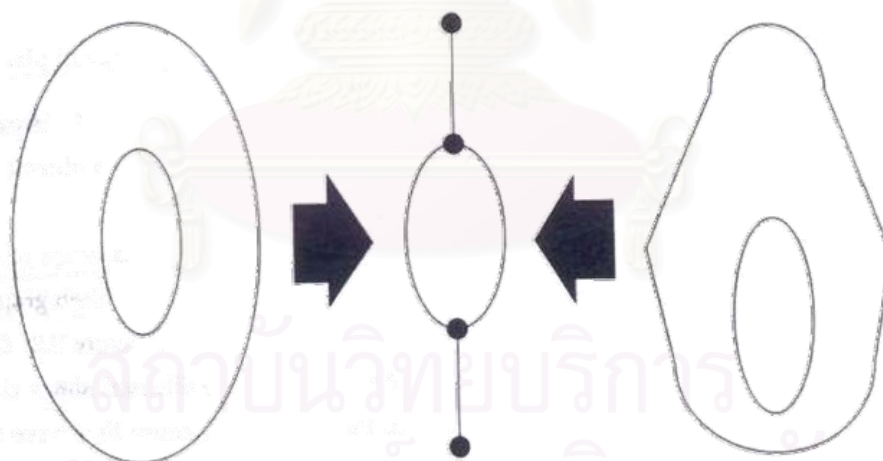


Figure 2.2: Two tori that differ about their shapes but have the same Reeb graph.

2.1.1.3.2 Enhanced Reeb graph

In this section, an enhanced Reeb graph is defined. This graph is an extension of an original Reeb graph on a height function that is previously explained. The enhanced Reeb graph is extended to hold both topological information and geometrical information of an object. Its node has the coordinates of a critical point. Its edge has information of

the shape about the connective components of an object. In addition, the graph has cross-sectional information of object.

An enhanced Reeb graph R consists of three sets below.

1. Let N be a finite set. Each element of is a point of N the vector space R^3 and called the *node* of. R . N is called the *node set* of R^3 .
2. Let I be a closed set such that $I=[0,1]$. Let E be a finite set. Each element of E is a continuous mapping from I to R^3 and is called the *edge* of R . E is called the *edge set* of R .

An edge of R must satisfy the following conditions.

- There exist such nodes n_i and n_j that $e(0)=n_i, e(1)=n_j$ and $i \neq j$.
 - The z value of $e(t)$ increases or decreases monotonically for all $t \in [0,1]$.
3. Let I be such a closet set that $I=[0,1]$. Let C be a finite set. Each element of C is a continuous mapping from I to R^3 and is called the *contour* of R .

A contour c of R must satisfy the following conditions.

- A contour c is a closed curve. i.e. $c(0)=c(1)$ must be satisfied.
- A contour c does not intersect itself. i.e. $c(s) \neq c(t)$ must be satisfied for all s and t .
- A contour c does not intersect any other contour of the graph R .
- Contours of the graph R are oriented in the same direction.

An enhanced Reeb graph consists of a tripple (N, E, C) . The graph is considered as the Reeb graph that has geometrical information of an object.

For instance, the enhanced Reeb graph of the two tori in figure 2.2 is presented in figure 2.3.

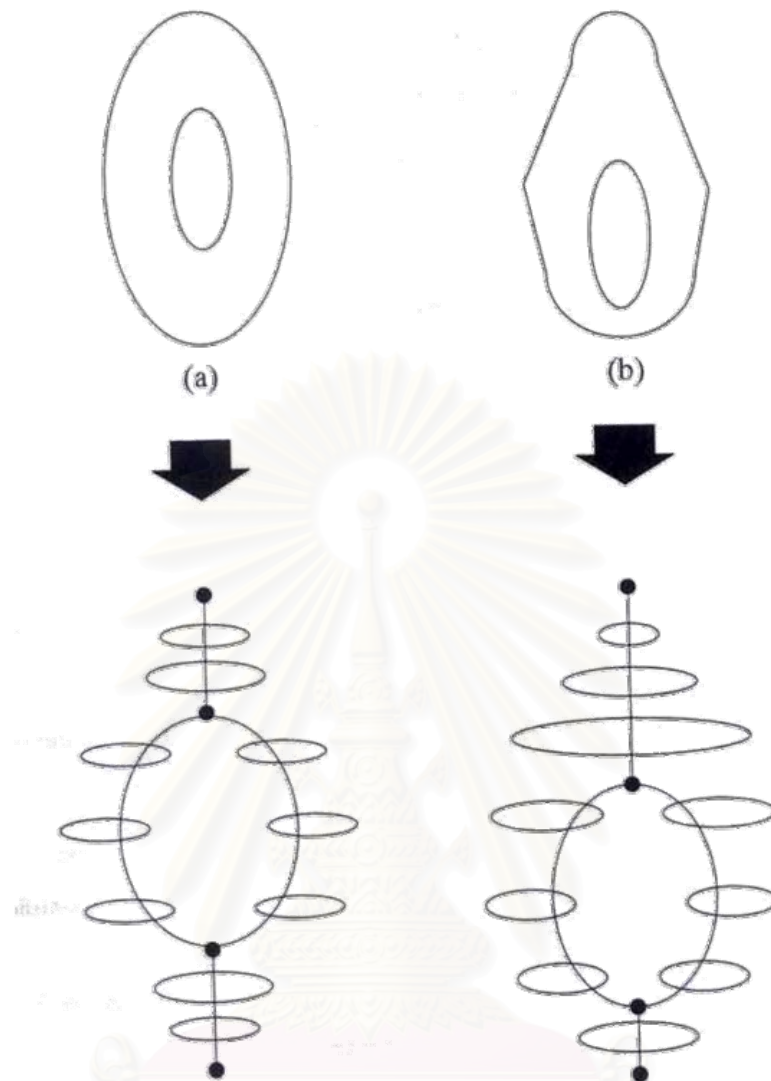


Figure 2.3: Each torus has the different enhanced Reeb graph.

2.1.1.4 Homotopy

In this section, homotopy is explained. Homotopy is a topological concept about mappings. Homotopy is formulated below [16, 17].

Let $f, g: X \rightarrow Y$ be maps where X and Y are two topological spaces. Then f is homotopic to g if there exists a map $H: X \times I \rightarrow Y$ such that $H(x, 0) = f(x)$ and $H(x, 1) = g(x)$ for all points $x \in X$. Here $I = [0, 1] \subset \mathbb{R}$. This map H is called a homotopy from f to g and is notated as $f \simeq g$. If for some subsets A of X

$$H(a, t) = f(a) \quad \forall a \in A, \quad \forall t \in I$$

Then, f is said to be homotopic to g relative to A and is written $f \simeq g \text{ rel } A$

For example, the transformation of homotopy is presented in figure 2.4. The upper contour is presented by the function f and the lower by g

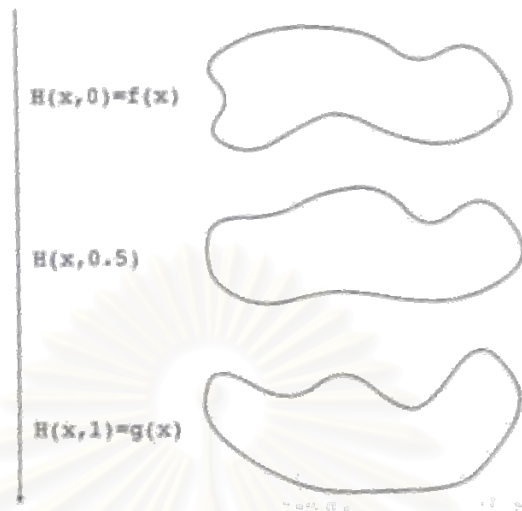


Figure 2.4: The upper contour is transformed to the lower contour by homotopy.

2.1.2 Surface Constructions

This chapter explains the implementation of enhanced Reeb graph and homotopy. First, the implementation of enhanced Reeb graphs is explained. Next, the toroidal graph is introduced. Finally, the way is represented that homotopy is implemented.

2.1.2.1 Implementation of Enhanced Reeb Graph

This section of implementation of enhanced Reeb graph for 3D object consist of three portions: Adopted curves, Edge of enhanced Reeb graph and Contour of enhanced Reeb graph.

2.1.2.1.1 Adopted Curves

This part explains the curves adopted by the system. Further studies about these curves are written in [7].

Bezier

An n-dimensional Bezier curve is defined as follows.

$$f(t) = \sum_{k=0}^n B_k^n(t) p_i \quad (0 \leq t \leq 1, p_i \in R^3)$$

where is called the Bernstein function and it is expressed by this formula.

$$\text{where } B_k^n(t) = \binom{n}{k} t^k (1-t)^{n-k}$$

This formulation is called the Bernstein form of a Bezier curve. The curve is specified by an ordered set named *control points*. The curve has convex hull properties and is invariant under affine maps.

NURBS

A NURBS (Non Uniform Rational B-Spline) curve is defined by this formula.

$$f(t) = \frac{\sum_{i=0}^n N_{i,k}(t) w_i p_i}{\sum_{i=0}^n N_{i,k}(t) w_i}$$

where w_i is a weight associated with control points. And the function is a polynomial of degree k call a B-Spline basis function. Is called *knot vector*.

$$N_{i,k}(t) = \frac{(t - x_i) N_{i,k-1}(t)}{x_{i+k} - x_i} + \frac{(x_{i+k+1} - t) N_{i+1,k-1}(t)}{x_{i+k+1} - x_{i+1}} \quad (2 \leq k \leq n+1)$$

$$N_{i,0}(t) = \begin{cases} 1 & (x_i \leq t < x_{i+1}) \\ 0 & \text{otherwise} \end{cases}$$

A NURBS curve has these features. It can represent a quadratic surface accurately. And it has a local approximation property. If a control point is moved or if a weight value associated with a control point is changed, the shape of surface changes only in its neighborhood.

NURBS is adopted by a standard data exchange format called IGES (Initial Graphic Exchanged Specification) and is extensively utilized in a great number of CAD systems.

Cardinal Spline

A Cardinal spline curve is defined by this formula.

$$C(t) = \begin{bmatrix} t^3 & t^2 & t & 1 \end{bmatrix} \begin{bmatrix} -a & 2-a & -2+a & a \\ 2a & -3+a & 3-2a & -a \\ -a & 0 & a & 0 \\ 0 & 1 & 0 & 0 \end{bmatrix} \begin{bmatrix} p_{i-1} \\ p_i \\ p_{i+1} \\ p_{i+2} \end{bmatrix}$$

where p_i is a control point.

The Cardinal spline curve represents the curved segment i between p_i and p_{i+1} that passes through both p_i and p_{i+1} . In addition, the segment i at $t=1$ joins with positional and tangent continuity to segment $i+1$ at $t=0$. This curve can express the everywhere C^1 continuous curve that passes through the control points. This feature is of use for this system. This curve is discussed further in the technical report [18].

Catmull-Rom Spline

A catmull-Rom spline curve is defined as follows.

$p_{i-1}, p_i, p_{i+1}, p_{i+2}$ are given control points.

$$CR(t) = \begin{bmatrix} w_{i-1} & w_i & w_{i+1} & w_{i+2} \end{bmatrix} \begin{bmatrix} p_i \\ p_{i+1} \\ d_i \\ d_{i+2} \end{bmatrix}$$

where d_i and d_{i+1} are

$$d_i = (1-a)(p_i - p_{i-1}) + a(p_{i+1} - p_i)$$

$$d_{i+1} = (1-b)(p_{i+1} - p_i) + b(p_{i+2} - p_{i+1})$$

And w_{i-1}, w_i, w_{i+1} and w_{i+2} are

$$\begin{bmatrix} w_{i-1} \\ w_i \\ w_{i+1} \\ w_{i+2} \end{bmatrix} = \begin{bmatrix} t^3 & t^2 & t & 1 \end{bmatrix} \begin{bmatrix} 2 & -2 & 1 & 1 \\ -3 & 3 & -2 & -1 \\ 0 & 0 & 1 & 0 \\ 1 & 0 & 0 & 0 \end{bmatrix}$$

A Catmull-Rom Spline curve is an extension of a Cardinal Spline curve. This curve expresses the curved segment i between the control points p_i and p_{i+1} that passes through p_i and p_{i+1} . In addition, this curve has the same features as the Cardinal Spline. The difference between a Cardinal Spline and a Catmull-Rom Spline is the degree of winding as presented in figure 2.5. Further discussion is in [19, 20]

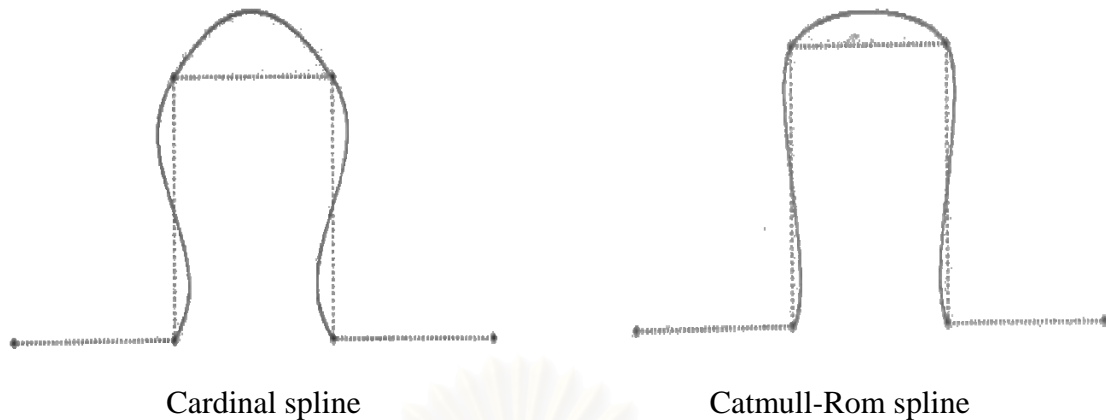


Figure 2.5: The difference between a Cardinal Spline and a Catmull-Rom Spline is displayed.

2.1.2.1.2 Edge of Enhanced Reeb Graph

In this part, the implementation of edges is explained. Reviewing the definition of an edge e , e is a function like this. Let I be a closed set $I=[0,1]$. e is a function $e : I \rightarrow R^3$ and its z value increase or decrease monotonically.

Cardinal Spline curves, Catmull-Rom Spline curves or line segments in the implementation represent an edge. To satisfy the conditions above, z value of control point must increase or decrease monotonously. If an edge does not satisfy this, this system considers the edge as an invalid edge. However, this condition is not a sufficient condition because a Cardinal Spline curves or a Catmull-Rom spline curves do not change monotonously if its control points are an ordered set about its z values.

2.1.2.1.3 Contour of Enhanced Reeb Graph

In this part, the implementation of contours is explained. A contour is defined as follows. Let I be a closed set $I=[0,1]$. A contour c is a function $I \rightarrow R^3$ and is a closed curve.

To satisfy this condition, the implementation is as follows. First, the type of a contour is determined. This system supports these types.

- *Polygon*: gives the shape of a polygon that connects the given vertices.
- *Circle*: gives the shape of a circle based on the coordinates of the center and the radius.
- *Bezier*: gives the shape of a Bezier curve determined by the given control points.

- *NURBS*: gives the shape of a NURBS curve determined by the given control points.
- *Cardinal Spline*: gives the shape of a Cardinal Spline curve determined by the given control points.
- *Catmull-Rom Spline*: gives the shape of a Catmull-Rom Spline curve determined by the given control points.

The next step is to give the contour parameters. The method of determining parameters depends on the type of contour. The method of determining parameters is divided into the three types; a polygon, a circle and a spline curve.

- *Polygon*: If a contour is polygonal, the perimeter is utilized as the parameter. The parameter is proportional to the perimeter.
- *Circle*: If a contour is a circle, determining parameters is very simple. Let (c_x, c_y, c_z) be the given coordinate of the center of the circle and r be the given radius. The parameter is the same as with a cylindrical coordinate system.
- *Spline curve*: If a contour is a spline curve, determining parameters is not easy. Though the arc length should be utilized as the parameter, it is difficult to calculate the length. Then linear line segments in figure 2.6 approximate each spline curve. Instead of the arc length, the approximated perimeter is utilized as the parameter.



Figure 2.6: A spline curve is approximated by a polygon to determine the parameter.

2.1.2.2 Toroidal Graph

How we can construct the natural surface when triangular patches are created between two contours? The problem is discussed in the section. To solve the problem,

first the original toroidal graph is introduced. This graph is proposed by Fuchs et al [21]. Next, the continuous toroidal graph is explained [17].

2.1.2.2.1 Discrete Toroidal Graph

Consider that there are two contours. One contour is called the upper contour and the other is called the lower contour. Assume the following conditions.

- The contours are approximated by linear line segment.
- The upper contour is defined by distinct points u_0, u_1, \dots, u_{n-1} .
- The lower contour is defined by distinct points l_0, l_1, \dots, l_{m-1} .
- The loops of the contours are oriented in the same direction.

When triangular patches are created, the triangulation method must satisfy the following conditions [22].

1. If two nodes of the same contour are to be defined as the vertices of the same triangle, they must neighbor each other on the contour line.
2. No more than two vertices of any triangle may be recruited from the same contour line.

Fuchs et al. proposed the graph that supports these two conditions. It is the toroidal graph on a two-dimensional torus.

In a toroidal graph, vertices correspond to the set of all possible spans between the points of the upper contour and the points of the lower contour. The arcs correspond to the set of all the possible triangles.

In figure 2.7, an example of a discrete toroidal graph is presented. Moreover, in figure 2.8, the patch determined by the toroidal graph is represented.

จุฬาลงกรณ์มหาวิทยาลัย

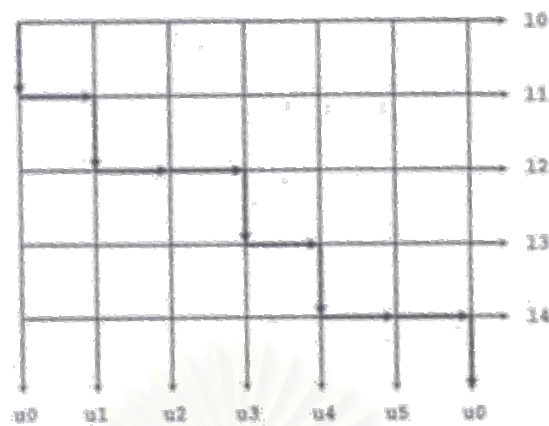


Figure 2.7: A discrete toroidal graph is presented. The upper contour has six vertices and the lower contour has five vertices.

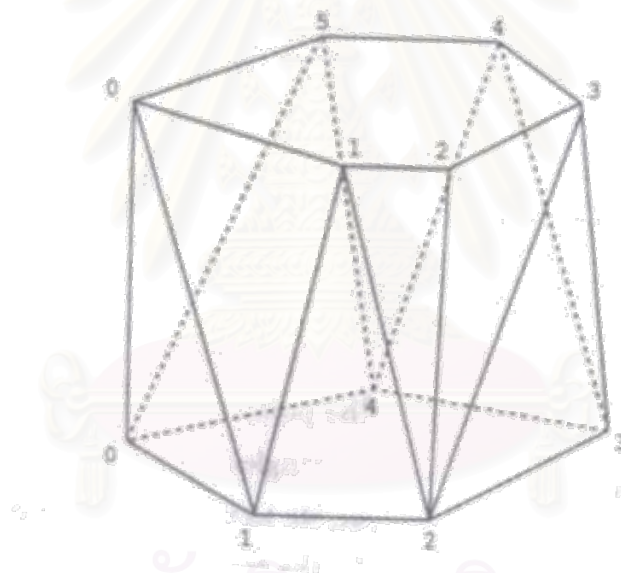


Figure 2.8: Triangular patches are determined by the above discrete toroidal graph.

2.1.2.2.2 Continuous Toroidal Graph

In an enhanced Reeb Graph, a contour is defined as a parametric closed curve. It is desired that a toroidal graph can deal with a parametric curve. Shinagawa & Kunii proposed a continuous toroidal graph [17]. In this section, the continuous version of a discrete toroidal graph is introduced.

Let f, g be contours of an enhanced Reeb Graph. In a continuous toroidal graph, the horizontal and vertical distances between the two vertices represent the differences of the parameter values between the two vertices.

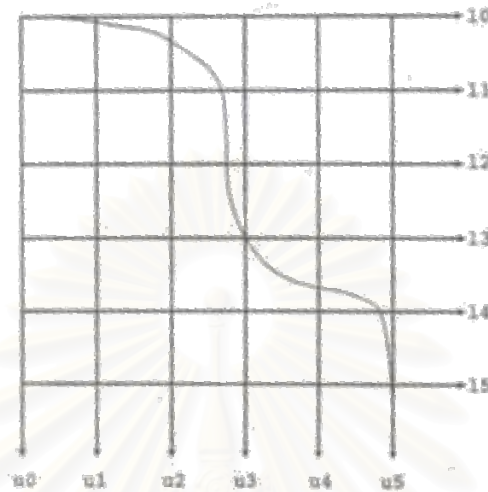


Figure 2.9: A continuous toroidal graph is presented.

The acceptable path of the continuous graph is represented as a monotonously increasing multi-valued function. The path is representing as the concatenation of these functions.

- $\alpha_i : [u_{2i}, u_{2i+1}] \rightarrow I \quad (0 = u_0 \leq u_1 \leq \Lambda < u_{2n-1} < 1)$
- $\beta_i : [l_{2i}, l_{2i+1}] \rightarrow I \quad (0 = l_0 \leq l_1 \leq \Lambda < l_{2n-1} < 1)$
- $\alpha_0(0) = \beta_{2n-1}(1), \alpha_i(u_{2i+1}) = \beta_i(l_{2i+1}), \beta_i(l_{2i+2}) = \alpha_{i+1}(u_{2i+2})$

The representation is the generalization of a monotonously increasing function.

The discrete toroidal graph is the special case of this continuous graph. The discrete toroidal graph is the concatenation of that of $u = u_i$ and $l = l_i$.

2.1.2.2.3 Distance Function

In order to create natural surfaces, the path of the toroidal graph should be shorter. Some measure is necessary to create patches. In addition, the correspondence between contours should be determined.

The two distance functions of the toroidal graph are defined here. These functions are also utilized when the correspondence between contours are determined.

Euclidean Distance Function

A Euclidean distance function is the function that returns the Euclidean distance between the two vertices. This function can be utilized on the two toroidal graphs.

$$d_E(u, v) = \sqrt{(u_x - v_x)^2 + (u_y - v_y)^2 + (u_z - v_z)^2}$$

Parametrical Distance Function

A parametric distance function is the function that returns the difference of the parametrical value between the two vertices. This function is defined on the continuous toroidal graph.

$$d_p(u, v) = |s - t|$$

where the parametrical values of u and v are s and t , respectively.

2.1.2.2.4 Closest Pair Vertex

Here a closest pair vertex is defined. This is not a distance function but the concept is based on the functions. This concept is utilized when contours are interpolated by some homotopy function. Let d be a distance between (u_i, l_j) . A vertex on a toroidal graph (u_i, l_j) is called a closest pair vertex if the vertex satisfies the following two conditions.

$$d(u_i, l_j) = \min_k d(u_i, l_k)$$

$$d(u_i, l_j) = \min_k d(u_k, l_j)$$

Then the closest vertex pair is searched. The closest pair vertex is the closest vertex pair whose distance is the shortest of the all. In the continuous graph, proper points are sampled and the closest vertex pair is defined.

2.1.2.3 Surface Construction

The surface creation takes four steps. First, correspondence between the two contours is determined. Then homotopy of the two contours is determined. Next *sliding homotopy* is created by the edge of an enhanced Reeb graph and the homotopy. Finally, triangular patches are made between the interpolated contours and a curved surface is created.

2.1.2.3.1 Correspondence between Contours

The correspondence between contours is determined. Let be f, g contours of an enhanced Reeb graph. The correspondence takes the next steps.

1. Proper points of a continuous contour f are sampled. The sampled points are determined at regular intervals in this implementation.
2. Assume that f is on a plane $ax+by+cz+d=0$. The contour f is rotated and on a plane $z=e$. The rectangles that enclose the contour f is searched. Δx and Δy is the lengths of the rectangle. A mapped contour is defined according to the following formula. Let (α_s, β_s) be a point of a mapped contour. Let $X = \max_{s \in I}(x_s)$ and $Y = \max_{s \in I}(y_s)$.

$$\alpha_s = \frac{X - x_s}{\Delta x} \quad \beta_s = \frac{Y - y_s}{\Delta y}$$

3. Let be mf and mg contours obtained by f and g being mapped to the xy -plane. The correspondence between the two contour mf and mg is determined. Let the most closet pair vertex (U, L) on the Euclidean distance function. The parameter of each contour is redefined. If the value of the parameter is greater than U then the value is changed to $u-U$. Otherwise, the value is changed to $1.0 - u + U$. The same procedure is done to the lower contour. The correspondence between the two contours f and g is determined by the correspondence between the mapped contours.

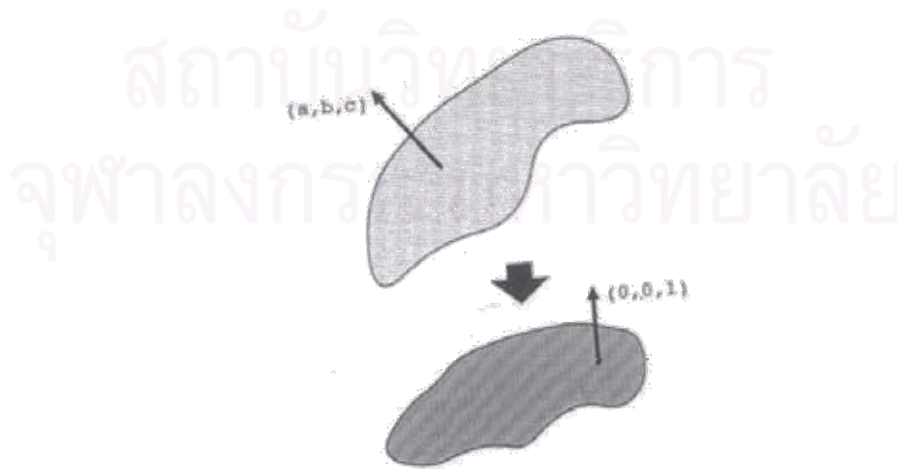


Figure 2.10: A contour on $ax+by+cz+d=0$ is transformed to the contour on a plane parallel to the xy -plane

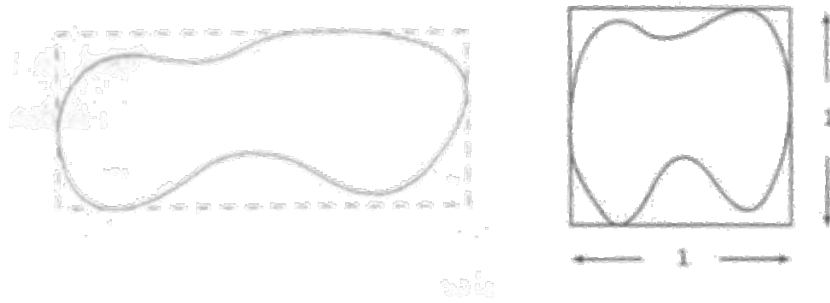


Figure 2.11: The rectangle that encloses the contour is searched and mapped to a unit square.

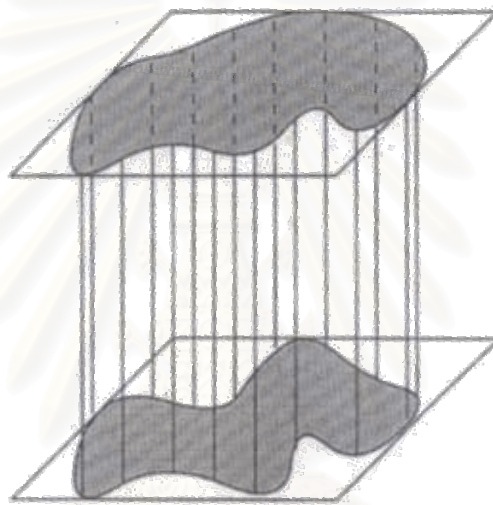


Figure 2.12: The correspondence between the mapped contours is determined.

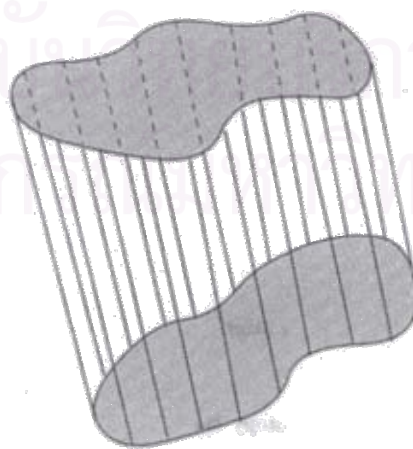


Figure 2.13: The correspondence between the contours is determined.

2.1.2.3.2 Contour Interpolation by Homotopy

After the correspondence between the upper contour and the lower contour is determined, the contours between them are interpolated by utilizing homotopy. There are a lot of homotopy functions and this system supports three primitive functions; linear, parabolic and quadrant. And two peculiar functions; Cardinal Spline and Catmull-Rom spline.

These homotopies is mentioned in detail below. Let be the upper contour $f(s)$ and the lower contour $g(s)$.

- Linear: $Linear(s,t) = (1-t)f(s) + tg(s)$

Linear homotopy is also called straight-line homotopy. This is the most primitive homotopy and interpolated contours linearly.

- Parabola: $Parabola(s,t) = (1-t^2)f(s) + t^2g(s)$

Parabolic homotopy creates parabolic surfaces.

- Quadrant: $Quadrant(s,t) = \sqrt{1-t^2}f(s) + (1-\sqrt{1-t^2})g(s)$

A quadrant means a quarter of a circle. This homotopy is mainly used between a critical point of an e_0 or e_2 cell and a contour. If this homotopy is used in this situation, the shape of a created object is like a ball.

- Cardinal Spline:

Cardinal Spline homotopy creates Cardinal Spline surfaces. As this curve is mentioned previously, this curve can express an everywhere c^1 continuous curve that passes through the control points. The facts enable this homotopy to create c^1 continuous surfaces that include given contour completely. The defect in this homotopy is that at least four contours are necessary to create a Cardinal Spline surface. If there are less than four contours, this system creates virtual contours by utilizing existing contours.

- Catmull-Rom Spline:

Catmull-Rom Spline homotopy creates Catmull-Rom Spline surfaces. The feature of this homotopy is similar to the Cardinal Spline homotopy. This

homotopy can create surface that do not wind more than the Cardinal Spline homotopy.

2.1.2.3.3 Contour Interpolate by Sliding Homotopy

In the previous part, the contour interpolation based on homotopy is explained. But an enhanced Reeb graph has both the shape of connective components as the edge and the cross-sectional information as a contour. It is useless to interpolate contours by utilizing normal homotopy.

Some problems are presented below when an enhance Reeb is interpreted to construct an object.

- When a user gives the system an edge and some contours, the problem occurs that the points where the given edge passes through the given contours. In other word, the problem is whether a user can give the points arbitrarily or the system determines the points automatically.
- If two contour and two different edges are given, the problem occurs that the difference of the reconstructed shapes when the different edges are given to the contours. This case is presented in figure 2.14.
- If the two contours and an edge, the problem occurs that the difference of the reconstructed shapes when the edge passes through the contours at different point. This case is presented in figure 2.15.



Figure 2.14: The different edges are given to the same pair of contours.

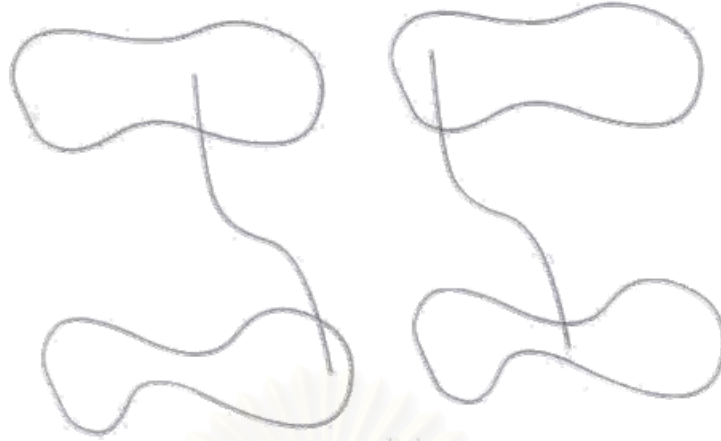


Figure 2.15: The edges that have the same shape passes through the same pair of contours at the different points.

Sliding homotopy can solve these problems above. With sliding homotopy, a user can give the system an enhanced Reeb graph arbitrarily. The graph is interpreted properly to create three-dimensional objects. Assume that two contours and an edge that pass through the contours are given. Assume one contour is represented as $f(s)$ and the order as $g(s)$. Some new functions are introduced and the sliding homotopy is defined.

Edge Vector An edge vector of an edge is defined as follows. Let e be an edge of a enhanced Reeb graph. The edge is a function $I \rightarrow R^3$. An edge vector $ev(t)$ is a function $I \rightarrow R^3$ where

$$ev(t) = e(t) - e(0)$$

An edge vector has c^1 continuity if the edge is represented by a Cardinal Spline curve or a Catmull-Rom Spline curve.

Homotopy Vector A homotopy vector is defined as follows. Let H be homotopy from f to g . Assume that N corresponding points on the $H(s,t)$ and $H(s,0)$ are selected. Homotopy vector $hv(t)$ is a function $I \rightarrow R^3$ where

$$hv(t) = \frac{1}{N} \sum_{i=0}^{N-1} \{H(s_i, t) - H(s_i, 0)\}$$

A homotopy vector is c^1 continuous if homotopy is represented by cardinal Spline homotopy or Catmull-Rom Spline homotopy.

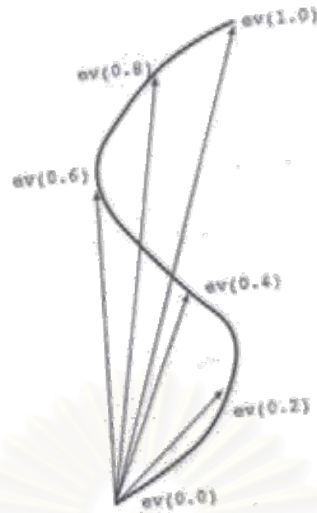


Figure 2.16: An edge vector is presented.



Figure 2.17: A homotopy vector is presented.

Sliding Vector A sliding vector is defined as follows. Let $ev(t)$ be an edge vector and $hv(t)$ be a homotopy vector. Let $k(t)$ be a function $I \rightarrow R$ that satisfy these condition.

$$k(0) = k(1) = 0, \quad 0 \leq k(t) \leq 1$$

A sliding vector $sv(t)$ is a function $I \rightarrow R^3$ where

$$sv(t) = k(t)\{ev(t) - hv(t)\}$$

A sliding vector is c^1 continuous and satisfies $sv(0) = sv(1) = 0$. This is important for sliding homotopy.

$k(t)$ is a weight function. There are many functions for the weight $k(t)$ but $k(t)$ is desirable to satisfy $k'(0) = k'(1) = 0$. In the current implementation,

$$k(t) = \frac{1}{2}(1 - \cos 2\pi t)$$

is selected.

Sliding Homotopy Sliding homotopy $SH(s,t)$ is the semantics of an enhanced Reeb graph to reconstruct an object. Let $H(s,t)$ be some homotopy and $sv(t)$ be a sliding vector. The sliding homotopy is formulated as follows.

$$SH(s,t) = H(s,t) + sv(t)$$

$SH(s,0) = H(s,0) = f(s)$ and $SH(s,1) = H(s,1) = g(s)$ are satisfied because a sliding vector $sv(t)$ satisfied the condition $sv(0) = sv(1) = 0$. This homotopy can create c^1 continuous surfaces if H and sv are c^1 continuous.



Figure 2.18: Sliding homotopy is presented. First, the top contour and the bottom contour are given. Then contours are interpolated by homotopy. Next sliding vector is calculated. And contours are shifted by the sliding vector.

2.1.2.4 Branch Handling

In the systems that construct surfaces by utilizing a series of cross-sectional information, branch handling is a big problem. If the contour at a critical point is not given, the contour is estimated by some means.

There is a simple method proposed by Christiansen HN and Sederberg TW but this method fails if the shape of contours is complex [22]. There is another method proposed by A.B.Ekoule et.al. This method deals with branches by creating a virtual

contour at a critical point but created surface is not c^1 continuous. Komatsu et.al proposed the shrinking boundary that the based on the diffusion equation. This method can create c^1 continuous surfaces naturally but cannot be applied to all cases of branch handling.

It is not easy c^1 continuous surfaces if they have some branches in this system. As is mentioned previously, c^1 continuous surfaces can be using Cardinal spline homotopy or Catmull-Rom spline homotopy but four contours are necessary to create smooth surfaces by utilizing these homotopies. There are not enough contours to create smooth surfaces in the neighborhood of critical points as is represented in the figure 2.22.

Moreover, the following condition is necessary at the critical point.

$$\frac{\partial f}{\partial x} = \frac{\partial f}{\partial y} = 0$$

The tangent vector at the critical point must be parallel to the xy -plane.

In this section, some assistant idea is explained to create c^1 continuous surfaces in the neighborhood of critical points.

2.1.2.4.1 Guiding Curve

A guiding curve is one of homotopy function that can interpolate contours along the points that the curve passes through. A guiding curve is defined as follows [23].

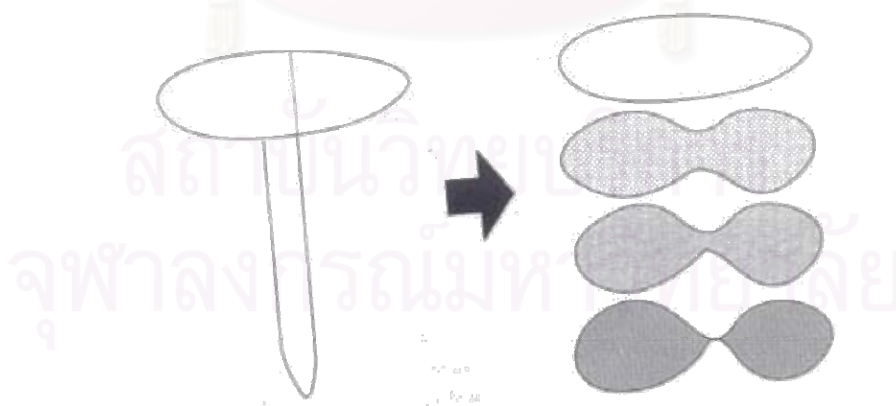


Figure 2.19: Contours are transformed by an attached guiding curve.

$$H(s,t) = (1 - \text{weight}(s, s_i))f(s,t) + \text{weight}(s, s_i)F(s_i,t)$$

where *weight* is a weight function like this.

$$weight(s, s_i) = \begin{cases} \frac{s - s_i + a_l}{a_l} & (s_i - a_l \leq s \leq s_i) \\ \frac{s_i + a_u - s}{a_u} & (s_i \leq s \leq s_i + a_u) \\ 0 & otherwise \end{cases}$$

This function satisfies

$$0 \leq weight(s, s_i) \leq 1 \quad weight(s_i, s_i) = 1$$

This curve is attached to the contours at any point. Several guiding curves can be attached to one contour.

If some proper function is selected as a guiding curve, the contour at the critical point whose tangent vector can be parallel to the xy -plane. In this system, this is achieved by the quadrant guiding curve c_p that is defined below.

for $0 \leq t \leq 1/2$,

$$c_q(t) = \begin{bmatrix} \left(1 - \sqrt{1 - (2t)^2}\right) c_q(0)_x + \left(1 - \sqrt{1 - (2t)^2}\right) c_q(1/2)_x \\ \left(1 - \sqrt{1 - (2t)^2}\right) c_q(0)_y + \left(1 - \sqrt{1 - (2t)^2}\right) c_q(1/2)_y \\ (1 - 2t) c_q(0)_z + 2t c_q(1/2)_z \end{bmatrix}$$

and for $1/2 \leq t \leq 1$,

$$c_q(t) = \begin{bmatrix} \left(1 - \sqrt{1 - (2-2t)^2}\right) c_q(1/2)_x + \left(1 - \sqrt{1 - (2-2t)^2}\right) c_q(1)_x \\ \left(1 - \sqrt{1 - (2-2t)^2}\right) c_q(1/2)_y + \left(1 - \sqrt{1 - (2-2t)^2}\right) c_q(1)_y \\ (2-2t) c_q(1/2)_z + (2t-1) c_q(1)_z \end{bmatrix}$$

Merge Case: When the two contour f_0 and f_1 are merged, the guiding curve is attached to the points of the points the contours and the critical point. $c_p(0)$ is the point of the contour f_0 and $c_p(1)$ is the point of the contour f_1 . $c_p(1/2)$ is the critical point. Then the interpolated contour created by the guiding curve is given new parameters. Then the new parameters are given by tracing the two contours.

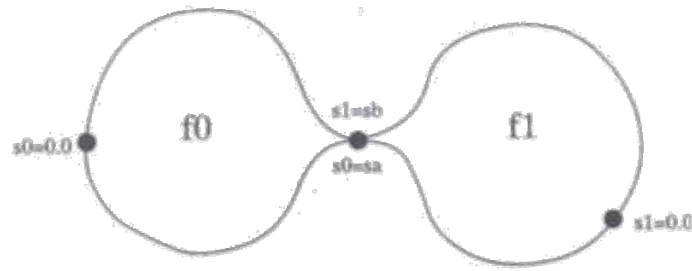


Figure 2.20: The new parameters are given to the merged contour.

Divide Case: When the contour f is divided, the guiding curve is attached to the two points of the contour and the critical point. $c_p(0)$ and $c_p(1)$ is the point of the contour f . $c_p(1/2)$ is the critical point. Then the interpolated contour created by the guiding curve is given new parameters. First the arc length of the interpolated contour is calculated. Then the new parameters are given by tracing the contour.



Figure 2.21: The new parameters are given to the divided contours.

2.1.2.4.2 Continuity near Critical Point

c^1 continuous surfaces can not be created by utilizing the guiding curve homotopy. A guiding curve can create surface whose tangent vector of a saddle point is parallel to xy -plane. However, it dose not confirm the continuity near the critical points.

Let us consider the case represented in the figure 2.22. Two upper contours f_1 and f_2 are given. In addition, one lower contour g is given. First, a guiding curve is attached to the upper contours and a new contour that includes the critical point is interpolated. This case is expressed in the figure 2.23.

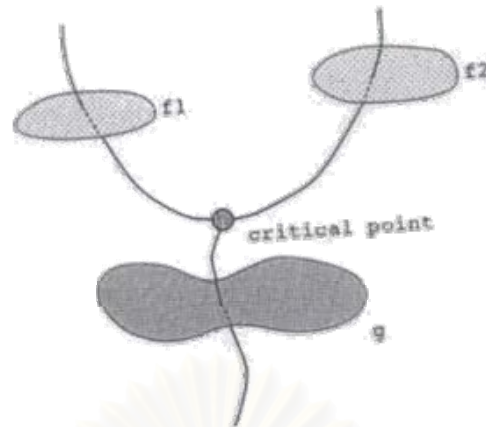


Figure 2.22: This is an example of a merge case. Two upper contours and one lower contour are given.



Figure 2.23: The contour f at the critical point is interpolated by the guiding curve homotopy.

Then the surface between f_1 and f , between f_2 and f and, between f and g are created by utilizing Cardinal spline homotopy or Catmull-Rom spline homotopy, respectively. The created surface will not be continuous in the neighborhood of the critical points because there is no positive proof of the c^1 continuity.

In order to create smooth surfaces, some special procedure is done to the surfaces. This procedure is not implemented yet. One method is that more than one enhanced Reeb graph is utilizing in creating objects. Even if a point is a critical point for one function, that is not a critical point for another. An object is constructed by homotopy in the several directions.

2.2 Related Works

This related work can categorize in two sections, which is surface reconstruction that created for hydrogeological information and three-dimensional model creation with Reeb graph.

2.2.1 Surface Reconstruction

Surface reconstruction can categorize in five sections: parametric surface reconstructions, volumetric surface reconstructions, delaunay-based surface reconstructions, Incremental Surface Reconstructions and Interactive Surface Reconstructions.

2.2.1.1 Parametric Surface Reconstructions [4]

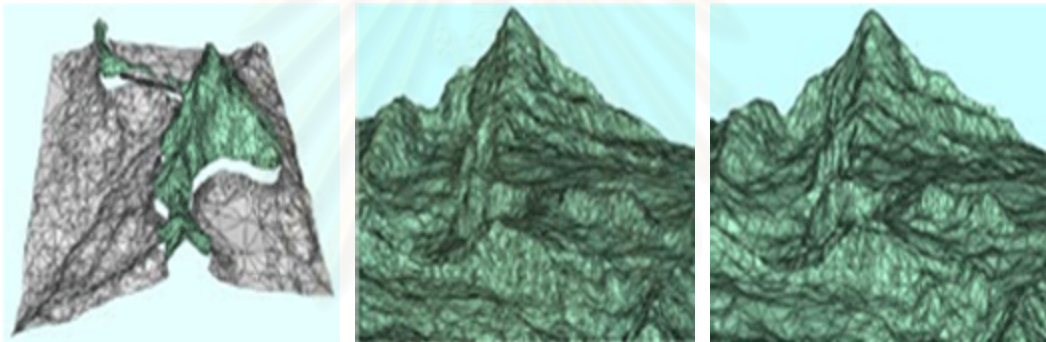


Figure 2.24: Parametric Surface Reconstructions

There are many surface reconstruction techniques such as B-Spline function and NURBS. Although, these methods can easily interpolate the surface value, they are not suitable for complex topology surfaces are shown figure 2.24.

2.2.1.2 Volumetric Surface Reconstructions [3]



Figure 2.25: Volumetric Surface Reconstructions

Volumetric surface reconstruction can render internal object information. These method store information as 3D array, which each element is called voxel. Direct rendeing volumetric data results in low resolution of the object surface. Thus, it is not suitable for application, which require high-resolution surface. The volumetric surface uses great amount of memory to store data. The rendering time is also slow. The 3D voxel can be converted to polygonal mesh using Marching cube algorithm. By rendering the volumetric surface with polygon, the object surface becomes smoother are shown in figure 2.25.

2.2.1.3 Delaunay-Based Surface Reconstructions [2]

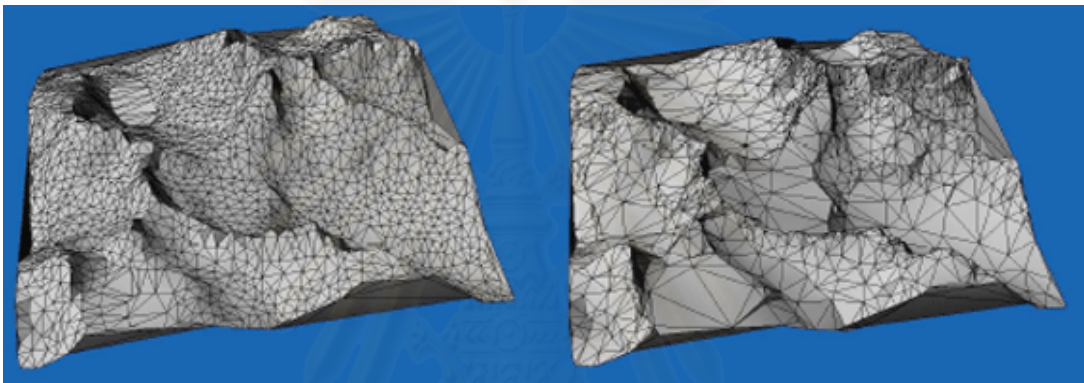


Figure 2.26: Delaunay-Based Surface Reconstructions

Delauney triangulation is the method to construct the surface by using surface vertices. It can be used with complex surfaces. However, it needs a great amount of memory and takes long computational time. In addition, Delauney triangulation is not suitable for surface with high varying surface slopness are shown figure 2.26.

2.2.1.4 Incremental Surface Reconstructions [1]

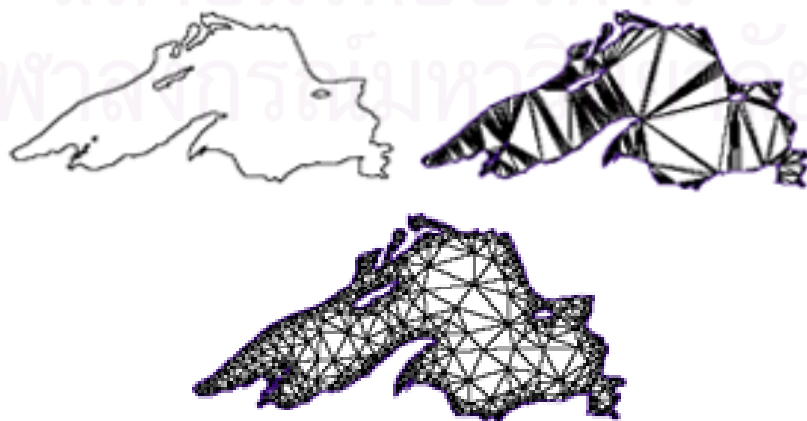


Figure 2.27: Incremental Surface Reconstructions

Incremental surface reconstruction constructs the surface by incrementally place a vertex to the surface. The new vertices are then join together to form triangle mesh. This technique is suitable for input surface with low number of vertex. Thus, it is not appropriate for large area surface are shown figure 2.27.

2.2.1.5 Interactive Surface Reconstructions [24]

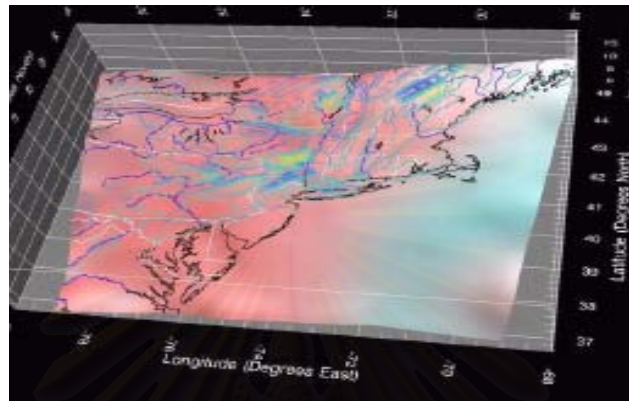


Figure 2.28: Interactive Surface Reconstructions

Interactive surface reconstruction downsamplings the input data to lower resolution. It also pre-computed some information that will be used later in interactive rendering. This technique depends heavily on graphic hardware capability. The result image may appear blocky due to low-resolution data are shown figure 2.28.

2.2.2 Three-Dimensional Model creation with Reeb Graph

This section creation three-dimensional model with Reeb graph can categorize in six portions.

2.2.2.1 Constructing a Reeb Graph Automatically from Cross Sections

This research builds Reeb graph [15] from the cross sections of the model. It is used in the complex medical imaging, such as Cochlea images and Smicircular Canals images. The Reeb graph can be computed automatically. The algorithm analyzes the model topology, such as holes and components of the model, to construct the object's contour shapes. The contours are then used to build Reeb graph.

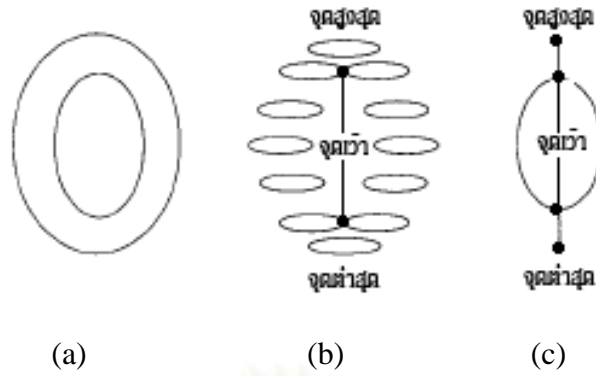


Figure 2.29: Cross-sectional, Contour and Reeb graph

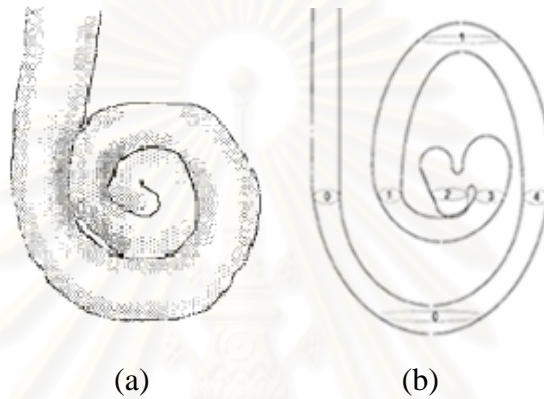


Figure 2.30: Show contour of Cochlea

2.2.2.2 Homotopy Modeling Based on Enhanced Reeb Graph

Enhanced Reeb Graph [16], ERG, adds the height function to the original Reeb graph model. The height function is used to represent the internal structure of the object. ERG has both geometrical datas and topological datas of the object. This research has presented a way to modelling an object with ERG. It also explain how to compute the Homotopy, the function which maps the object contours with Reeb graph, of the object.

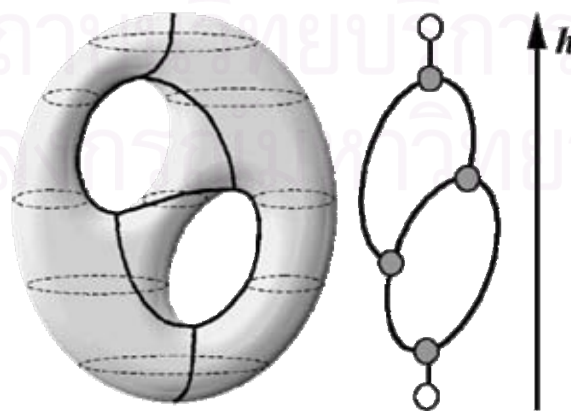


Figure 2.31: Cross-sectional model and Reeb graph

2.2.2.3 Extended Reeb Graphs for Surface Understanding and Description

This research uses Extended Reeb Graphs [25] for representing surfaces. It is using the topology coding techniques. This method can solve the degenerating non-simple critical points problems. It has control levels to automatically constructing the ERG for non-continuous surfaces. This method can represent the surfaces correctly.

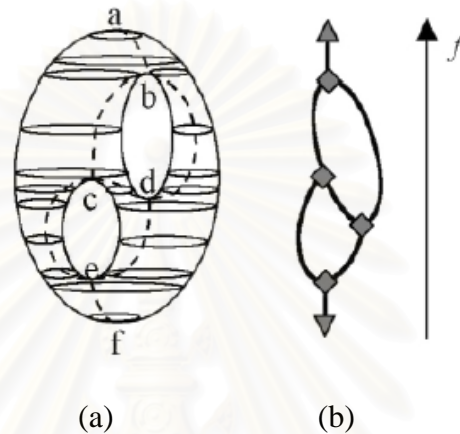


Figure 2.32: Bi-Torus (a) cross-sectional and contour (b) Reeb graph



Figure 2.33: Show the critical region of Manifold M, which is from the differential manifold. This region is constructed using Delauney triangulation from height function.

2.2.2.4 Loops in Reeb Graphs of 2-Manifolds

This research constructs Reeb graph [8] by joining the two-connected components of level sets. The algorithm uses the Morse function to do the computation. This method can handle 2-Manifold topological objects. The asymptotic complexity is $O(n \log n)$, when n is the number of edges.

2.2.2.5 Topological Modeling of Illuminated Surfaces Using Reeb Graph

In this research, the Topological modeling [11] is used for illuminating surfaces. It encodes object in the form of Reeb graph by using object topology information. First, the critical points are identified using Morse Theorem. Then, the algorithm does the cross

section to obtain the contours of the object. The contours are sent to the Reeb graph using height function. This method proves that the height function is nearly the same as topological transformation.

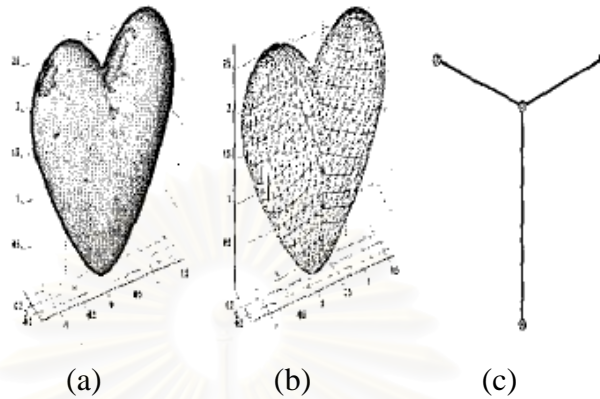


Figure 2.34: Structure Reeb graph of heart model

2.2.2.6 3D-Object Reconstruction System Using Cross-Sectional Data

This research studies 3D object representation [13]. The representation includes the internal object structure. The system builds from this research can render many types of objects specified by the user need. However, the storage structure is quite complicated. Some part of the surface may not be rendered. It uses Level sets and Fast-Marching method to render the model. The performance is quite good and can use with Reeb graph with branching.

CHAPTER III

ENHANCED REEB GRAPH FOR MODELING HYDROGEOLOGICAL INFORMATION

In this section, a modeling technique using Enhancing the Reeb graph for representing surface of Hydrogeology Information is described. In addition, this technique is comprised with three main portions: the enhanced Reeb graph, which improves on the original Reeb graph for representations that are more complex in section 3.1. The contour set in section 3.2. Finally, the surface reconstructions, creating the plane surface between sets of contours with the Reeb graph, with the manifold sets represented with geographical surfaces are shown in section 3.3.

3.1. Enhanced Reeb graph

The definition of enhanced Reeb Graph will be considered at the same height on the hydrogeological surface. We specify a function $f : \{M_1, M_2, M_3, \dots, M_n\} \rightarrow R$ as a real-number function on the set of manifolds $\{M_1, M_2, M_3, \dots, M_n\}$, which transmits values to the Reeb graph of the set of manifolds $\{M_1, M_2, M_3, \dots, M_n\}$ that depend on function f defined as the spatial quotient of $\{M_1, M_2, M_3, \dots, M_n\} \times R$ which have equivalence relations, as in section 2.1.1.3 and showing the representation with Reeb graph in Figure 3.1.

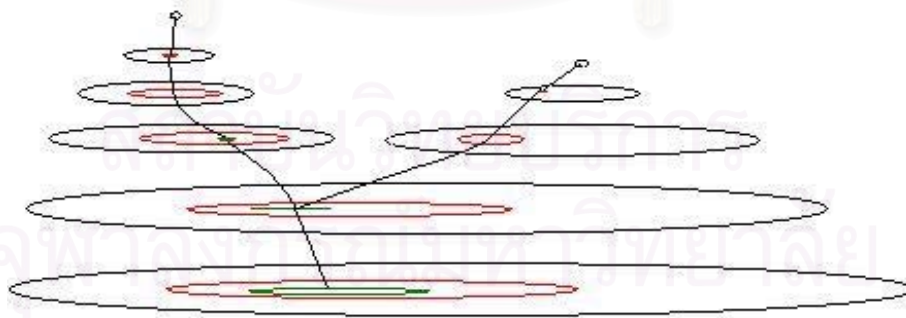


Figure 3.1: Nodes and connecting lines of extended Reeb graph with its sets of contours

3.2. Set of contours

The set s of contours is obtained from the cross sections of each layer of the hydrogeological surface. A contour c at any given height is a set of points on a surface layer.

Creating a more detailed surface is achievable by interpolation of the contour between two object layers, which can be achieved in 2 methods: in the vertical axis and the horizontal axis. Approximation in vertical and horizontal axes can be used to calculate the approximate contours on both the outside and the inside of the surface. For approximating values in contour ranges calculated from the inside of the surface we consider at the same height, i.e., calculating by the horizontal. After the correspondence between the upper contour and the lower contour is determined, the contour between them will be interpolated. Approximating the contour from calculating from the outside of the surface results in an extra contour between each layer of the hydrogeological surface in Figure 3.2. In this research, Natural Cubic Spline method used to interpolate the corresponding contours is described as following.

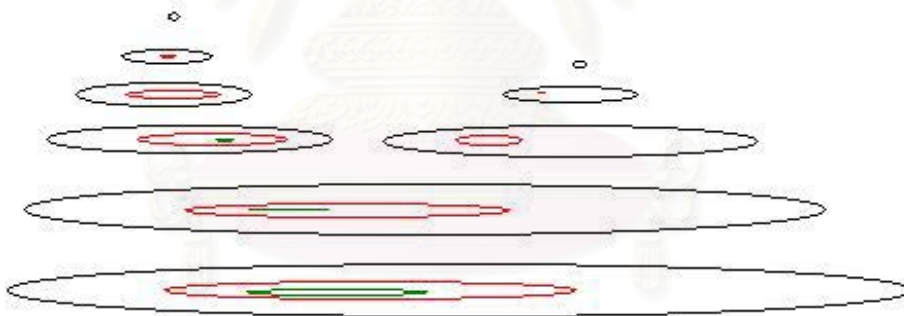


Figure 3.2: Cross section and contours of each soil layer

Suppose that $\{(x_k, y_k)\}_{k=0}^n$ are $n+1$ corresponding contour points, where $a = x_0 < x_1 < \dots < x_n = b$. The n cubic polynomial $S_k(x)$ with coefficients $S_{k,0}, S_{k,1}, S_{k,2}$, and $S_{k,3}$ has to satisfy the properties:

$$S_k(x) = S_{k,0} + S_{k,1}(x - x_k) + S_{k,2}(x - x_k)^2 + S_{k,3}(x - x_k)^3$$

for $x \in [x_k, x_{k+1}]$ and $k = 0, 1, \dots, n$

- The spline passes through each data point.

$$S_k(x) = y_k \text{ for } k = 0, 1, \dots, n$$

- The spline forms a continuous function over.

$$S_k(x_{k+1}) = S_{k+1}(x_{k+1}) \text{ for } k = 0, 1, \dots, n$$

- The spline forms a smooth function.

$$S'_k(x_{k+1}) = S'_{k+1}(x_{k+1}) \text{ for } k = 0, 1, \dots, n$$

- The second derivative is continuous.

$$S''_k(x_{k+1}) = S''_{k+1}(x_{k+1}) \text{ for } k = 0, 1, \dots, n$$

The natural cubic spline has zero second derivatives on one or both of its boundaries.

3.3. Surface reconstruction

Each surface reconstruction in a layer will be assembled a surface between corresponding the contours obtained in Section 3.2 with the Enhanced Reeb graph obtained in Section 3.1. Three adjacent points on the set of contours of hydrogeological surface are formed as a triangular-shape mesh. When triangular patches are created, if two points of the same contour are to be defined as the vertices of the same triangle, they must neighbor each other on the contour's perimeter. Therefore, no more than two vertices of any triangle may be recruited from the same contour. The surface can be simply constructed when all points are covered with meshes. Additionally, to make smooth the surface, normal vector of each point has to be averaged with normal vectors of the other points around it.

CHAPTER IV

EXPERIMENTAL RESULTS

This section shows the experimental results of the proposed to enhanced Reeb graph for modeling hydrogeological information. The number of boreholes for tested model is 52 boreholes. The three-dimensional model is also provided.

4.1 Tool Development

These sections consist of four portions: requirement, Analysis and Design, Implement and Testing.

4.1.1 Requirement

The system is Intel Pentium M Processor 1.73 GHz with 1 GB of memory, using a RADEON X600 with 256 MB of memory or higher. In addition, this program to use in this research developed by Microsoft Visual C++ and Open GL, which run on window XP.

Table 4.1: Format of collecting soil layers information

	A	B	C	D	E	F	G	H	I
1	-135	155	120	1	116.5085	2	158.9445	3	133.192
2	-80	160	43	1	143.1933	2	143.1313	3	133.6151
3	-30	155	5	1	110.0747	2	129.3209	3	133.6043
4	30	160	-60	1	152.8694	2	149.0617	3	141.0505
5	135	160	50	1	164.6239	2	131.1234	3	124.5423
6	-70	110	50	1	162.5552	2	137.3255	3	124.8085
7	-5	105	-20	1	155.7039	2	153.4564	3	112.428
8	20	115	-22	1	159.6474	2	118.8387	3	110.5694
9	20	135	-40	1	120.8199	2	144.6781	3	123.0786
10	90	130	30	1	126.5447	2	143.4838	3	114.1664

Input information format is importing a file of numerical data, stored as an Excel File, which Data of depth and co-ordinate of each soil layer from exploration of water resource engineering as a Table 4.1.

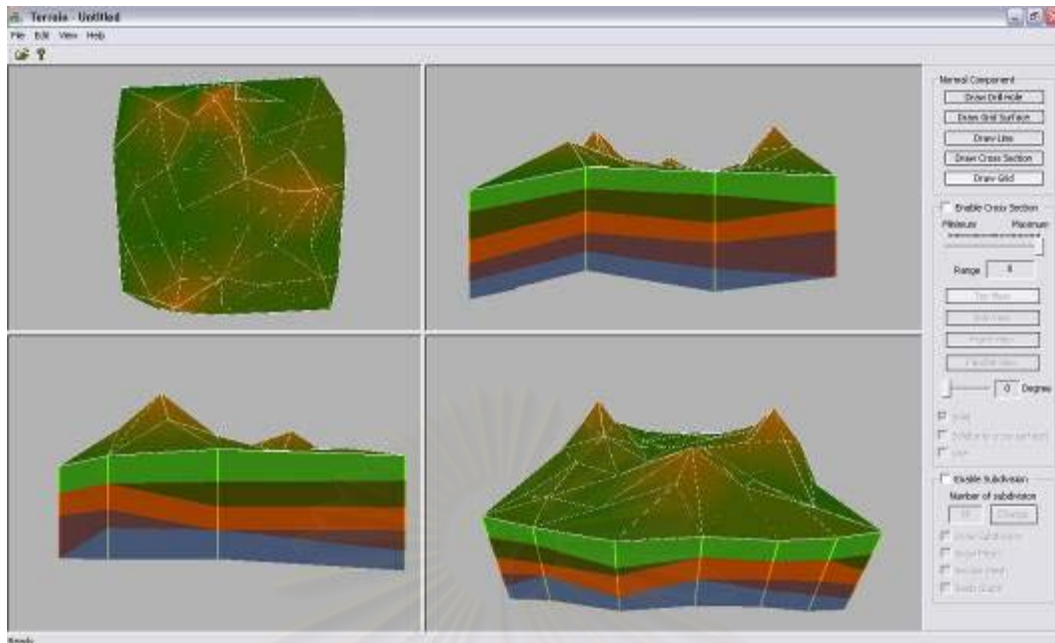


Figure 4.1: Surface reconstruction of hydrogeological information from 52 sample drill holes

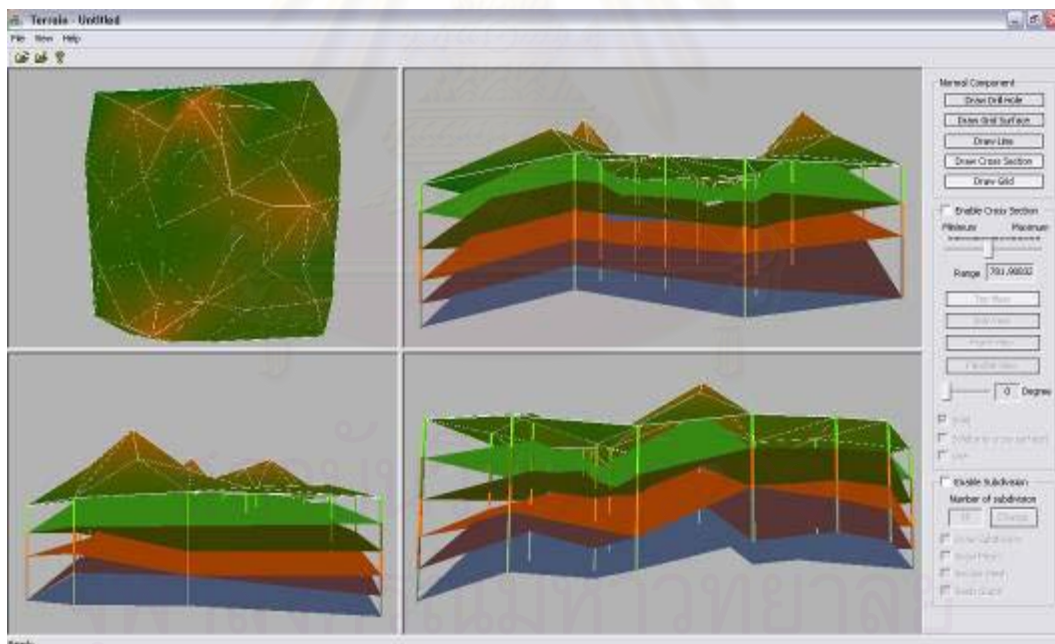


Figure 4.2: Cross section of each soil layer and categorization of soil layer

Result format is able to show three dimensional model as a figure 4.1 and cross section of each soil layer and categorization of soil layer as a figure 4.2.

4.1.2 Analysis and Design

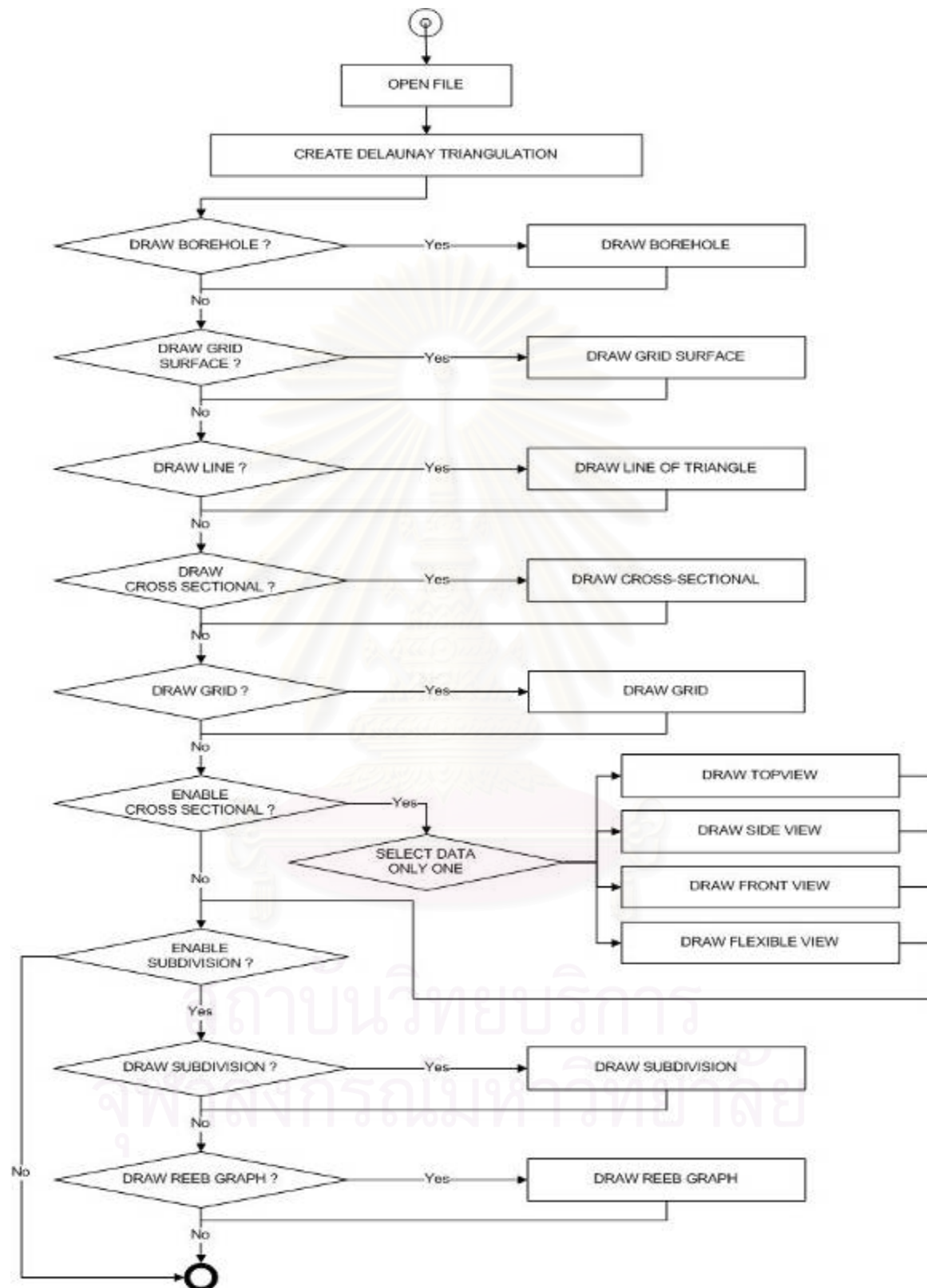


Figure 4.3: Flowchart of Process for 3D Modeling Hydrogeological Information

4.1.3.2 Creating the surface plane of soil layers

We create the surface plane of each soil layer by estimating the value in the range from the coordinates of soil layer, and the depth of each category of soil layer obtained in the first step. The research creates the surface plane of geographical data with Delaunay Triangulation. This method is used to create the surface plane of hydrological and geological information for further smoothness and detail to the surface plane of the geological data.

Calculating and creating the surface plane of geological data with the Delaunay Triangulation method will be considered according to the surface plane of each type of soil layer.

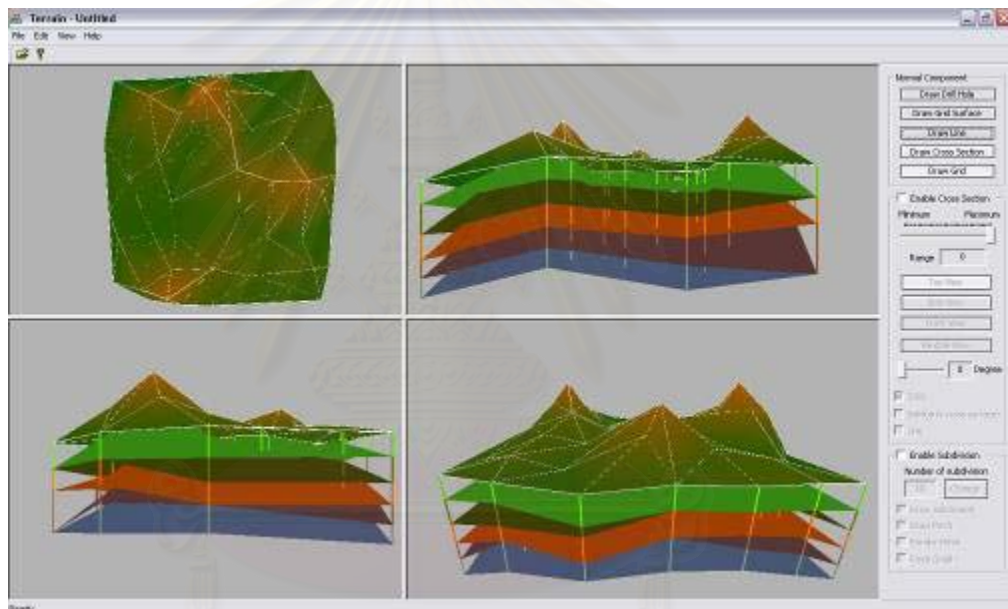


Figure 4.5: Geographical surface model according to the category of soil layer

In creating the surface plane with Delaunay Triangulation, we create the surface according to each category of soil layer, in other words, we create the surface plane for each layer in order of soil layer category. Creating the first layer's surface plane, we first take the reference axes coordinate data to calculate and create the surface, namely the x , y , z coordinates of the soil layer in 3D. Next we find the first coordinate points, which is obtained from receiving the first set of data from the file as x , y , z , coordinate data. We then take first position to find two next closest coordinates to create a triangle by connecting the three positions with lines. Next, we take the two coordinates we have found to find the next closest

coordinates with the aforementioned steps, with those coordinates not having been used to create earlier triangles, to use in creating more triangles, expanding until no more can be created.

In creating the surface planes of the subsequent layers, the method is the same as creating the first layer, except for the depth of each category of soil layer, where the position changes according to the height of the soil layer, i.e., the z -axis. The z value changes according to the height of soil layer category in each layer, as in Figure 4.4.

4.1.3.3 Calculation the cross section of each soil layer

We define the manifold M here by representing it with a smoothed geological surface plane. This surface plane will be continuous. The height function of a given x, y, z coordinate returns a z value, which represents the height of soil layer, while the contour at height h of soil layer is the set of points on the surface plane; when entered in the height formula it returns a value of h as in Figure 4.5.

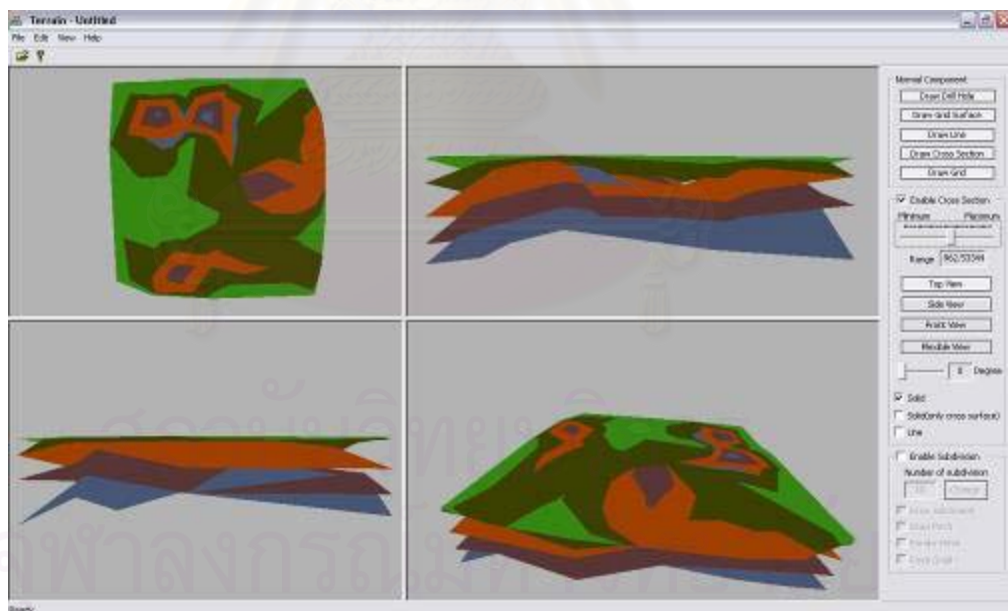


Figure 4.6: Cross section of soil layers in each category

4.1.3.4 Creating the Reeb graph

We create the Reeb Graph from the contours of Section 4.1.3.3. We specify the node of the graph as the center of each contour, and the edges as lines connecting each node according to height order.



Figure 4.7: Surface reconstruction by creating the Reeb graph

4.1.3.5 Creating the surface and complete internal structure of geographical information

From the enhanced Reeb graph obtained in Section 4.1.3.4 and the contours obtained in Section 4.1.3.3, we create the surface of each soil layer. Creating the surface and complete internal structure begins with matching appropriate nodes between contours on adjacent layers. After that, we approximate contours in the area between contours to make a more detailed surface plane. We then connected the points on adjacent contours to create into triangles as in Figure 4.7.

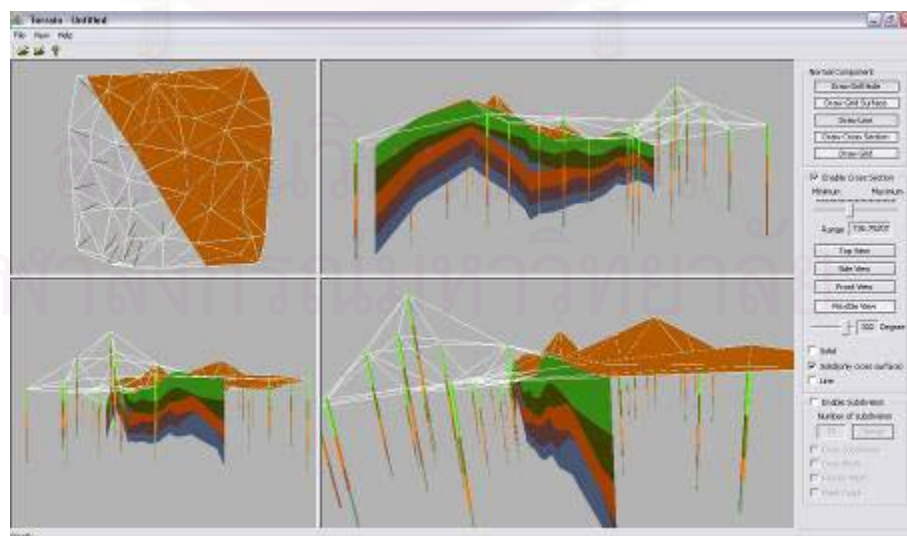


Figure 4.8: Model of the surface and internal structure of geographical information

4.1.4 Result Testing

This research evaluated the data calculated from the model with the actual data by comparing depth at the same planar coordinate. We conduct a comparison between the survey data set containing 52, 104 and 203 drill holes and the depth calculated, after randomly removing two, five and ten drill holes at a time from the original data set consequently. Then we approximate the depth at those coordinates using the proposed model, and compare the obtained depth. We repeat the process until the size of sample is over 30 percent of the original boreholes.

4.1.4.1 Using the Z-test to test statistical hypotheses for our research problem

Research Problem: We randomly delete 5 percents of boreholes from the data set and recalculate them by the proposed interpolation model. We repeat this process until the subject's size is over than 30 percents of each original data set as shown in Table 4.2, 4.3 and 4.4. The research question for this experiment is “Does the depths of each interpolated boreholes significantly different from the depths of the original boreholes at the same coordinate?” We will use the six-step process to test statistical hypotheses for this research problem.

1. With every recalculated mean depth μ_1 and mean depth μ_2 at each soil layer and standard deviation S_1 and S_2 consequently shown in Table 4.2, 4.3 and 4.4., we state null hypothesis and alternative hypothesis

$$\begin{array}{ll} H_0 : \mu_1 - \mu_2 = 0 & \text{if } d_0 = 0 \text{ assumption } H_0 : \mu_1 = \mu_2 \\ H_1 : \mu_1 - \mu_2 \neq 0 & H_1 : \mu_1 \neq \mu_2 \end{array}$$

2. Set the alpha level: $\alpha = 0.05$
3. Calculate the value of the proper statistic:

Since this problem involves comparing a single group's mean with the population mean and the standard deviation for the population is known, the proper statistical test to use is the Z-test.

$$Z = \frac{(\bar{X}_1 - \bar{X}_2) - d_0}{\sqrt{(S_1^2 / n_1) + (S_2^2 / n_2)}}$$

The Z values are shown in the Table 4.2, 4.3 and 4.4

4. State the rule for rejecting the null hypothesis:

We need to find the value of Z that will only be exceeded 5% of the time since we have set our alpha level at 0.05. Since the $Z_{0.05}$ - score is normally distributed (or has the Z distribution), The associated $Z_{0.975}$ - score would be 1.96.

Our rejection rule then would be: Reject H_0 if. $|Z| > 1.96$

5. Decision: Reject H_1 , $|Z| \leq 1.96$, two-tailed.

Our decision rule said reject H_1 if the $|Z|$ value is not greater than 1.96. From the Table 4.2, 4.3 and 4.4, every of our Z values except the Z for borehole no.5 in Table 4.3 and borehole no.5 in Table 4.4 is greater than 1.96 so we reject H_1 of every pair of depths except the borhole no.5 in Table 4.3 and borehole no.5 in Table 4.4.

6. Statement of results: The results of testing state that the 90 % of differences between the real data and the data generated by the enhanced Reeb model show no significant differences with statistical Z - test . Therefore we conclude that the 3D geographical information model displays internal structures appropriately for accurate data analysis, by processing cross sections to find the limit of the research area in the geological model accurately, as well as approximating the soil layer heights correctly, and categorizing soil layers correctly as well, to create proper relations between soil layers and drill holes.

Table 4.2: Result of compare from example one with Z-test

Sample_1		Layer 1		Layer 2		Layer 3		Layer 4		Layer 5		Layer 6	
X	Y	Depth 1	Depth 2	Depth 1	Depth 2	Depth 1	Depth 2	Depth 1	Depth 2	Depth 1	Depth 2	Depth 1	Depth 2
-155	-22.5	51.3948	49.50737	52.04788	40.73864	0	11.78851	52.65265	52.37867	41.80584	38.40042	36.36157	35.555
70	-72.5	55.37138	46.49345	45.75968	57.99931	0	0	0	25.31123	60.58506	47.13757	30.90365	33.03824
-105	115	40.65987	49.9874	41.04004	44.80709	0	10.60261	51.14393	53.78613	41.00604	37.30718	36.40396	42.50364
57.5	77.5	44.18732	49.3705	72.97251	42.2906	0	0	0	27.09419	60.87439	46.8964	32.03487	34.52068
20	352.5	40.2733	47.8109	48.22603	39.1961	0	0	41.02621	42.41733	43.08557	35.28707	31.62647	40.17003
-30	202.5	44.53484	48.8013	40.06006	38.47902	0	12.55572	53.48008	53.84938	31.99863	34.76559	45.64749	41.09573
157.5	-135	43.83072	49.48459	56.17483	44.20699	0	0	43.95358	18.76747	35.58185	51.08326	36.46592	35.41643
282.5	-147.5	38.6031	44.8887	48.50264	46.2526	0	0	37.03754	48.52197	41.49533	37.62269	46.58272	37.80685
20	302.5	53.21579	42.85648	39.6129	44.90956	0	0	36.85648	44.35817	33.56873	40.37904	37.28146	33.01387
45	390	44.90012	46.90789	38.01799	49.09689	0	0	47.27663	44.52212	36.42554	46.03875	41.86197	35.47696
20	302.5	53.21579	42.85648	39.6129	44.90956	0	0	36.85648	44.35817	33.56873	40.37904	37.28146	33.01387
45	415	50.95647	51.38591	49.68725	45.66258	0	0	47.01685	42.9911	48.22347	43.06194	37.93039	37.51709
157.5	40	36.90449	51.91985	61.11545	58.87231	0	0	0	26.60266	60.25994	47.97664	47.55134	30.93935
282.5	-147.5	38.6031	48.18964	48.50264	39.54898	0	0	37.03754	49.43662	41.49533	23.50083	46.58272	39.23856
107.5	215	39.88676	43.37868	37.78405	41.19494	40.00215	0	41.33024	50.84152	48.3563	34.74624	45.84436	36.48163
195	340	42.18156	44.01965	47.82794	43.5286	0	0	38.05547	47.18103	39.72579	37.51043	31.59209	37.53716
32.5	202.5	46.47219	42.38118	36.69643	39.79004	0	16.45658	52.73171	46.78932	33.99262	39.62239	35.43713	45.78875
57.5	77.5	44.18732	38.74067	72.97251	52.9172	0	0	0	20.87264	60.87439	51.7359	32.03487	43.80132
-17.5	-222.5	53.20295	54.68021	37.66183	23.26462	0	0	40.78426	37.39648	40.48782	28.94419	30.38435	51.82787
-117.5	-322.5	42.86835	53.401	45.12829	37.92905	0	0	43.32227	49.7525	48.70776	25.52248	39.79879	53.8987
45	415	50.95647	51.38591	49.68725	45.66258	0	0	47.01685	42.9911	48.22347	43.06194	37.93039	37.51709
-92.5	202.5	51.13041	41.05846	40.26161	42.39486	25.11142	10.52887	54.96707	50.98924	35.53856	38.79184	46.75435	38.84097
-205	290	54.18506	42.47886	0	46.03695	0	7.255872	25	47.9022	40	40.78814	30	38.03209
245	40	56.37865	38.70738	52.28149	47.7046	0	0	50.63086	31.81509	36.3924	41.03342	30.20529	48.03179
195	340	42.18156	44.01965	47.82794	43.5286	0	0	38.05547	47.18103	39.72579	37.51043	31.59209	37.53716
20	302.5	53.21579	42.85648	39.6129	44.90956	0	0	36.85648	44.35817	33.56873	40.37904	37.28146	33.01387
107.5	-260	54.86822	51.41132	0	40.22644	0	0	42.41947	33.97087	0	22.96063	70	32.4038
-217.5	-135	55.24107	46.6363	54.61775	47.45622	0	0	46.08606	47.00763	47.5264	35.88902	43.18688	34.43759
157.5	-135	43.83072	49.48459	56.17483	44.20699	0	0	43.95358	18.76747	35.58185	51.08326	36.46592	35.41643
282.5	-147.5	38.6031	44.8887	48.50264	46.2526	0	0	37.03754	48.52197	41.49533	37.62269	46.58272	37.80685
AVERAGE		46.86804	46.66632	44.94568	44.13247	2.170452	2.306272	37.41951	41.35778	41.33906	39.23462	38.98689	38.38931
SD		6.216499	4.246733	15.31333	6.344813	8.488186	4.855809	16.28828	10.74609	11.62528	7.448491	8.291663	5.587376
$(SD)^2$		38.64486	18.03474	234.4981	40.25665	72.04929	23.57888	265.3081	115.4784	135.1472	55.48002	68.75168	31.21878
Z		0.146761		0.268713		-0.07607		-1.10542		0.834843		0.327355	

Table 4.3: Result of compare from example two with Z-test

Sample 2		Layer 1		Layer 2		Layer 3		Layer 4		Layer 5		Layer 6	
X	Y	Depth 1	Depth 2	Depth 1	Depth 2	Depth 1	Depth 2	Depth 1	Depth 2	Depth 1	Depth 2	Depth 1	Depth 2
70	-72.5	55.37138	49.05627	45.75968	52.74947	0	0	0	41.98352	60.58506	42.04396	30.90365	35.64042
57.5	77.5	44.18732	44.62867	72.97251	50.98073	0	14.5005	0	23.76702	60.87439	50.27226	32.03487	42.54244
45	390	44.90012	46.68318	38.01799	49.10279	0	0	47.27663	44.62061	36.42554	46.16826	41.86197	35.40885
15	402.5	36.69156	46.72873	43.10695	48.31092	0	0	44.53475	45.59731	37.7572	45.56855	45.43108	38.1802
15	115	40.65987	47.89512	41.04004	44.48215	0	17.28303	51.14393	38.16148	41.00604	43.45721	36.40396	39.32213
190	-72.5	55.37138	48.31212	45.75968	54.78435	0	0	0	46.33833	60.58506	35.87133	30.90365	34.22998
45	415	50.95647	50.3832	49.68725	46.22443	0	0	47.01685	43.41557	48.22347	43.57785	37.93039	38.04255
-30	202.5	44.53484	48.80131	40.06006	38.47902	0	12.55571	53.48008	53.84939	31.99863	34.76559	45.64749	41.09575
165	415	50.95647	52.43643	49.68725	45.07398	0	0	47.01685	42.54632	48.22347	42.52158	37.93039	36.96652
27.5	202.5	51.13041	46.65854	40.26161	36.83903	25.11142	1.004461	54.96707	52.82112	35.53856	34.05447	46.75435	35.88982
-35	-22.5	51.3948	51.639	52.04788	40.9469	0	14.96556	52.65265	47.51911	41.80584	40.28482	36.36157	35.16774
-110	-285	55.18623	45.7177	54.19158	50.98679	0	0	41.24541	52.76963	32.02509	44.82726	31.09666	47.38069
-155	-22.5	51.3948	52.95259	52.04788	44.85137	0	0	52.65265	51.99447	41.80584	40.79287	36.36157	37.7752
-85	290	54.18506	43.83661	0	46.69123	0	7.79337	25	43.73238	40	41.50397	30	38.04871
-172.5	165	38.44199	47.78823	46.18955	40.88174	0	26.49903	50.59038	50.22433	33.70782	39.16122	37.92737	36.3012
2.5	-322.5	42.86835	54.81417	45.12829	49.22934	0	0	43.32227	48.51542	48.70776	18.65732	39.79879	52.37363
-210	-147.5	43.92182	55.14973	54.95108	52.91203	0	0	38.49907	45.45598	32.65571	47.10252	33.79747	42.66513
152.5	202.5	46.47219	39.11741	36.69643	41.77868	0	30.00162	52.73171	41.2286	33.99262	45.01037	35.43713	46.19001
90	202.5	44.53484	40.59073	40.06006	38.05115	0	31.72585	53.48008	43.50925	31.99863	46.17912	45.64749	43.80069
195	340	42.18156	41.83984	47.82794	42.87016	0	0	38.05547	47.36876	39.72579	37.35254	31.59209	38.05489
-105	115	40.65987	54.67863	41.04004	38.94892	0	35.11472	51.14393	52.42408	41.00604	38.62931	36.40396	36.60035
-230	-285	55.18623	50.41438	54.19158	16.51174	0	0	41.24541	46.42956	32.02509	36.93982	31.09666	49.24202
227.5	215	39.88676	38.08095	37.78405	49.74182	40.00215	0	41.33024	45.95345	48.3563	35.65256	45.84436	40.65509
-235	-297.5	56.45795	51.14547	0	12.68102	0	0	47.61565	47.16253	90	38.68979	0	49.33788
165	390	44.90012	47.35734	38.01799	49.08516	0	0	47.27663	44.32515	36.42554	45.77958	41.86197	35.61329
15	115	40.65987	47.89512	41.04004	44.48215	0	17.28303	51.14393	38.16148	41.00604	43.45721	36.40396	39.32213
157.5	-135	43.83072	54.12819	56.17483	42.82591	0	0	43.95358	17.85435	35.58185	51.6802	36.46592	30.87181
57.5	77.5	44.18732	44.62867	72.97251	50.98073	0	14.5005	0	23.76702	60.87439	50.27226	32.03487	42.54244
-30	202.5	44.53484	51.13041	40.06006	40.26161	0	25.11142	53.48008	54.96706	31.99863	35.53856	45.64749	46.75435
-105	402.5	36.69156	48.14915	43.10695	43.45791	0	0	44.53475	42.7177	37.7572	44.46097	45.43108	38.4235
AVERAGE		46.41122	48.08793	43.99606	43.50677	2.170452	8.27796	40.513	43.9727	43.08912	41.34244	36.50041	40.14798
SD		6.022311	4.514526	14.97102	9.241281	8.488186	11.56393	17.31485	8.723237	12.79433	6.426748	8.799555	5.163856
(SD) ²		36.26823	20.38094	224.1315	85.40128	72.04929	133.7244	299.8041	76.09486	163.6948	41.30309	77.43216	26.66541
Z		-1.22017		0.152324		-2.33201		-0.97738		0.668188		-1.95814	

Table 4.4: Result of compare from example three with Z-test

Sample 3		Layer 1		Layer 2		Layer 3		Layer 4		Layer 5		Layer 6		Layer 7	
X	Y	Depth 1	Depth 2	Depth 1	Depth 2	Depth 1	Depth 2	Depth 1	Depth 2	Depth 1	Depth 2	Depth 1	Depth 2	Depth 1	Depth 2
-239	343	40	39.5081	14	21.8521	0	0	30	13.7965	0	4.53436	18	16.0861	27	26.0286
-217	-135	26	30.9564	39	15.7084	15	8.1767	27	31.0047	0	0	14	5.91918	23	41.5586
-192	115	39	27.0591	24	22.5651	0	0	10	23.2859	0	0	19	13.6993	53	33.898
-155	-22	45	36.7317	30	14.2893	0	0	34	20.1568	0	0	1	15.3824	33	21.4689
-112	232	37	35.6429	41	22.9286	0	0	30	27.5714	0	0	1	13.2143	30	48.0714
-89	-233	24	37.2515	30	19.0729	10	10.3696	28	22.6725	0	0	10	24.7988	46	31.3337
-17	-360	42	36.457	17	36.5197	0	0	25	28.2332	0	0	13	19.7488	29	40.0254
32	202	40	43.5069	31	20.3823	0	0	16	25.9112	0	0.61142	18	21.1014	30	21.2518
57	77	26	36.6638	35	40.1601	0	0	27	34.7272	12	7.05973	5	7.96	25	28.036
115	355	48	33.8285	23	41	0	5.06431	26	23.4017	0	0	8	17.7251	32	38.0969
-332	143	47	45.2812	40	17.0388	0	0	30	30.696	0	0	6	14.443	36	36.8473
-329	-48	24	31.6622	11	31.2095	0	0	29	19.8243	0	0	4	9.27703	43	34.7703
-220	-333	24	42.9985	17	13.8662	0	0	30	32.058	0	0	10	11.055	39	21.4282
-186	-65	41	36.218	32	16.1664	0	0	11	29.416	0	0	29	8.39933	34	29.7754
-149	-230	45	41.2368	11	13.6283	29	23.0021	16	20.6883	0	0	14	17.0715	20	47.0974
-97	204	42	36.3232	15	33.1017	0	0	21	23.4241	0	0.18697	15	7.20198	18	45.2756
-58	-214	43	32.1267	15	38.5903	0	3.36039	19	28.5295	0	0	29	16.8672	17	38.2931
-47	147	31	23.888	15	32.9227	0	0	19	15.0943	0	0.82216	10	8.96259	27	35.6907
13	-245	23	44.7482	46	27.108	0	0	18	28.4907	0	0	3	24.3748	22	27.8971
45	415	41	39.7058	0	-7E-06	0	0	39	23.2942	0	0	29	17.2458	26	47.4153
-42	277	35	40.9134	41	17.9852	0	6.43395	29	29.8257	0	0	22	20.6905	33	26.101
8	53	32	28.9173	38	33.6124	0	0	33	24.7787	15	15.0719	2	16.4541	35	38.8344
47	32	30	35.2179	45	40.1295	0	0	34	20.9504	7	15.2756	2	6.92323	46	38.4966
83	383	36	29.5527	25	39.4394	0	0	10	20.4394	0	0	27	8.7665	44	44.5695
130	175	33	29.5618	48	36.9154	0	0	31	22.0106	0	0	2	25.8562	24	33.2126
157	-135	41	44.9266	11	45.3977	0	0	20	23.4379	0	0	1	21.9211	16	39.3247
195	340	37	41.7488	41	20.564	0	0	10	27.4105	0	0	8	9.8872	49	33.7628
231	-90	40	36.9093	17	29.3319	0	0	39	17.5803	0	7.94624	28	16.2114	53	40.0497
254	94	28	35.3167	24	20.7734	0	0.14308	20	20.5341	0	0	2	27.004	40	49.5794
277	-121	22	34.2665	27	23.6352	0	0.19616	24	19.8981	20	14.5407	4	18.9955	23	44.9178
-327	-257	49	28.6708	11	10.7163	0	0	12	24.8873	0	0	7	14.8566	26	40.9634
-290	320	32	37.4854	44	39.5713	0	0	21	21.1217	0	3.98685	10	18.7349	21	33.215
-186	-65	41	36.218	32	16.1664	0	0	11	29.416	0	0	29	8.39933	34	29.7754
-106	-30	45	39.2049	14	21.99	0	0	22	32.6164	0	2.46716	9	13.8965	18	34.5254

Sample_3		Layer 1		Layer 2		Layer 3		Layer 4		Layer 5		Layer 6		Layer 7	
X	Y	Depth 1	Depth 2	Depth 1	Depth 2	Depth 1	Depth 2	Depth 1	Depth 2	Depth 1	Depth 2	Depth 1	Depth 2	Depth 1	Depth 2
8	53	32	27.0014	38	35.4007	0	0	33	29.5703	15	12.0333	2	14.6464	35	41.5895
42	99	43	28.1295	36	32.2043	0	0	35	24.8473	9	9.26613	7	7.01947	23	25.7868
127	307	41	37.588	47	29.1919	11	0	30	22.1127	0	0	19	14.1431	33	31.8664
209	-306	29	22.3037	27	20.4635	0	0	26	25.7278	0	0	7	25.856	32	35.3728
254	94	28	35.3167	24	20.7734	0	0.14308	20	20.5341	0	0	2	27.004	40	49.5794
318	308	27	33.6888	27	10.2535	0	0	34	29.5489	0	0	9	17.3139	32	30.7437
-319	292	36	29.5033	26	38.3818	0	0	14	20.0202	0	0	14	13.1687	27	30.9033
-278	353	42	42.0261	15	36.5505	0	0	13	19.3411	0	0	23	22.8229	42	30.0496
-206	241	41	34.6784	19	27.6907	0	0	10	14.0166	15	11.5477	27	8.96246	37	31.5866
-142	-135	49	33.9432	23	15.4498	0	7.9476	28	28.8428	0	0	2	11.4673	32	43.0699
-105	115	28	29.2955	21	33.2639	0	0	12	16.1525	0	0	22	14.1139	19	34.9092
-46	362	29	29.5558	44	16.8591	0	2.66066	36	23.9019	0	0	2	20.4983	46	30.3337
43	-209	26	38.5142	42	31.9666	0	0	11	26.4137	0	0	27	15.043	34	37.4046
130	75	25	34.8205	47	28.9407	0	0	35	18.6647	0	2.61694	22	23.25	15	42.2023
215	-308	22	29.1583	19	26.9943	0	0	36	25.8976	0	0	25	7.10806	30	30.4682
321	37	39	42.028	14	24.7248	20	12.8774	25	11.9721	0	0	20	13.6636	30	26.3238
-174	142	23	30.4551	23	39.1685	0	0	20	16.573	0	1.16291	0	15.8146	27	42.9045
-99	41	22	43.4396	30	22.5891	0	0	26	21.2251	0	0	20	16.0181	52	27.3688
-66	141	21	33.9583	33	17.9667	0	0	10	19.2583	0	0	8	15.9333	36	29.1833
19	213	25	41.6127	48	20.5959	0	0	25	25.3175	0	0	7	21.9913	18	23.7582
83	383	36	29.5527	25	39.4394	0	0	10	20.4394	0	0	27	8.7665	44	44.5695
141	-3	23	42.5316	36	42.2957	0	0	24	24.5224	0	0	13	11.8635	15	28.3949
194	45	43	36.4786	17	38.9746	0	0	36	32.8707	0	0	27	6.66843	36	28.1081
261	-344	40	24.4124	37	25.8433	0	0	20	32.0395	0	0	3	10.3669	18	35.8969
326	-209	29	36.0344	48	38.1137	0	0	17	27.2523	10	8.6231	17	7.5438	52	34.522
295	225	36	37.9065	14	38.2537	0	0	10	17.6837	0	0	22	12.2113	16	25.8958
AVERAGE		34.4	35.244	28.0667	27.1115	1.41667	1.33958	23.2833	23.8655	1.71667	1.96255	13.05	15.0398	31.55	34.9063
SD		8.24868	5.62505	12.2085	10.1336	5.15289	3.92795	8.87978	5.27561	4.64354	4.20658	9.54104	5.82974	10.5162	7.45652
(SD) ²		68.0407	31.6412	149.046	102.691	26.5523	15.4288	78.8506	27.8321	21.5624	17.6953	91.0314	33.9859	110.591	55.5997
Z		-0.65477		0.46633		0.09215		-0.43659		-0.30398		-1.3785		-2.01666	

Table 4.5: Conclusion of compare from example one, two and three with Z-test

Sample1 data	Layer 1		Layer 2		Layer 3		Layer 4		Layer 5		Layer 6		Layer 7	
Z-TEST	Depth 1	Depth 2	Depth 1	Depth 2	Depth 1	Depth 2	Depth 1	Depth 2	Depth 1	Depth 2	Depth 1	Depth 2	Depth 1	Depth 2
Average	46.868	46.666	44.946	44.132	2.1705	2.3063	37.42	41.358	0	0	41.339	39.235	38.987	38.389
SD	6.2165	4.2467	15.313	6.3448	8.4882	4.8558	16.288	10.746	0	0	11.625	7.4485	8.2917	5.5874
$(SD)^2$	38.645	18.035	234.5	40.257	72.049	23.579	265.31	115.48	0	0	135.15	55.48	68.752	31.219
Z	0.1468		0.2687		-0.076		-1.105		0		0.8348		0.3274	
Absolute Z	0.1468		0.2687		0.0761		1.1054				0.8348		0.3274	
Sample2 data	Layer 1		Layer 2		Layer 3		Layer 4		Layer 5		Layer 6		Layer 7	
Z-TEST	Depth 1	Depth 2	Depth 1	Depth 2	Depth 1	Depth 2	Depth 1	Depth 2	Depth 1	Depth 2	Depth 1	Depth 2	Depth 1	Depth 2
Average	46.411	48.088	43.996	43.507	2.1705	8.278	40.513	43.973	0	0	43.089	41.342	36.5	40.148
SD	6.0223	4.5145	14.971	9.2413	8.4882	11.564	17.315	8.7232	0	0	12.794	6.4267	8.7996	5.1639
$(SD)^2$	36.268	20.381	224.13	85.401	72.049	133.72	299.8	76.095	0	0	163.69	41.303	77.432	26.665
Z	-1.22		0.1523		-2.332		-0.977		0		0.6682		-1.958	
Absolute Z	1.2202		0.1523		2.332		0.9774		0		0.6682		1.9581	
Sample3 data	Layer 1		Layer 2		Layer 3		Layer 4		Layer 5		Layer 6		Layer 7	
Z-TEST	Depth 1	Depth 2	Depth 1	Depth 2	Depth 1	Depth 2	Depth 1	Depth 2	Depth 1	Depth 2	Depth 1	Depth 2	Depth 1	Depth 2
Average	34.4	35.244	28.067	27.111	1.4167	1.3396	23.283	23.865	1.7167	1.9626	13.05	15.04	31.55	34.906
SD	8.2487	5.625	12.208	10.134	5.1529	3.9279	8.8798	5.2756	4.6435	4.2066	9.541	5.8297	10.516	7.4565
$(SD)^2$	68.041	31.641	149.05	102.69	26.552	15.429	78.851	27.832	21.562	17.695	91.031	33.986	110.59	55.6
Z	-0.655		0.4663		0.0922		-0.437		-0.304		-1.378		-2.017	
Absolute Z	0.6548		0.4663		0.0922		0.4366		0.304		1.3785		2.0167	

สถาบันวิทยบริการ
จุฬาลงกรณ์มหาวิทยาลัย

4.1.4.2 Confidence intervals of difference between the interpolated depths and the original depth using 30 percent sample size

Consider a normally distributed population. To estimate the interpolation's variance by our proposed model, we take a three sample of size 52,104 and 203 boreholes and calculate the sample's variance. The random sample of boreholes has different depth shown in the Table 4.6-4.11.

Calculate a 95% confidence interval for the difference's mean weight.

The sample's different depth mean weight is as the Table 4.6-4.11 with standard deviation as the Table 4.6-4.11. The t distribution tells us that, for ∞ degree of freedom, the probability that $t > 1.96$ is 0.975. Also, the probability that $t < -1.96$ is 0.975. Using the formula for t with $t = \pm 1.96$ at 95% confidence interval for the populations mean may be found by making μ the subject of the equation. We random sample of boreholes has different depth shown in the Table 4.6-4.11.

$$\bar{d} - t_{0.975} \frac{S_d}{\sqrt{n}} < \mu_d < \bar{d} + t_{0.975} \frac{S_d}{\sqrt{n}}$$

That is the difference between the interpolated depth from our model and the original survey depth as the Table 4.6-4.11 with 95 % confidence.

Table 4.6: Difference between the interpolated depth from our model and the original survey depth from example one with each soil layer

Sample_1		Layer 1				Layer 2				Layer 3				Layer 4				Layer 5				Layer 6				
X	Y	Depth 1	Depth 2	D 2-1	Square	Depth 1	Depth 2	D 2-1	Square	Depth 1	Depth 2	D2-1	Square	Depth 1	Depth 2	D 2-1	Square	Depth 1	Depth 2	D 2-1	Square	Depth 1	Depth 2	D 2-1	Square	
-155	-22.5	51.395	49.507	1.8874	3.5624	52.048	40.739	11.309	127.9	0	11.789	-11.79	138.97	52.653	52.379	0.274	0.0751	41.806	38.4	3.4054	11.597	36.362	35.555	0.8066	0.6506	
70	-72.5	55.371	46.493	8.8779	78.818	45.76	57.999	-12.24	149.81	0	0	0	0	0	25.311	-25.31	640.66	60.585	47.138	13.447	180.83	30.904	33.038	-2.135	4.5565	
-105	115	40.66	49.987	-9.328	87.003	41.04	44.807	-3.767	14.191	0	10.603	-10.6	112.42	51.144	53.786	-2.642	6.9812	41.006	37.307	3.6989	13.682	36.404	42.504	-6.1	37.206	
57.5	77.5	44.187	49.37	-5.183	26.865	72.973	42.291	30.682	941.38	0	0	0	0	0	27.094	-27.09	734.1	60.874	46.896	13.978	195.38	32.035	34.521	-2.486	6.1792	
20	352.5	40.273	47.811	-7.538	56.815	48.226	39.196	9.0299	81.54	0	0	0	0	41.026	42.417	-1.391	1.9352	43.086	35.287	7.7985	60.817	31.626	40.17	-8.544	72.992	
-30	202.5	44.535	48.801	-4.266	18.203	40.06	38.479	1.581	2.4997	0	12.556	-12.56	157.65	53.48	53.849	-0.369	0.1364	31.999	34.766	-2.767	7.6561	45.647	41.096	4.5518	20.718	
157.5	-135	43.831	49.485	-5.654	31.966	56.175	44.207	11.968	143.23	0	0	0	0	43.954	18.767	25.186	634.34	35.582	51.083	-15.5	240.29	36.466	35.416	1.0495	1.1014	
282.5	-147.5	38.603	44.889	-6.286	39.509	48.503	46.253	2.25	5.0627	0	0	0	0	37.038	48.522	-11.48	131.89	41.495	37.623	3.8726	14.997	46.583	37.807	8.7759	77.016	
20	302.5	53.216	42.856	10.359	107.32	39.613	44.91	-5.297	28.055	0	0	0	0	36.856	44.358	-7.502	56.275	33.569	40.379	-6.81	46.38	37.281	33.014	4.2676	18.212	
45	390	44.9	46.908	-2.008	4.0311	38.018	49.097	-11.08	122.74	0	0	0	0	47.277	44.522	2.7545	7.5873	36.426	46.039	-9.613	92.414	41.862	35.477	6.385	40.768	
20	302.5	53.216	42.856	10.359	107.32	39.613	44.91	-5.297	28.055	0	0	0	0	36.856	44.358	-7.502	56.275	33.569	40.379	-6.81	46.38	37.281	33.014	4.2676	18.212	
45	415	50.956	51.386	-0.429	0.1844	49.687	45.663	4.0247	16.198	0	0	0	0	47.017	42.991	4.0258	16.207	48.223	43.062	5.1615	26.641	37.93	37.517	0.4133	0.1708	
157.5	40	36.904	51.92	-15.02	225.46	61.115	58.872	2.2431	5.0316	0	0	0	0	0	26.603	-26.6	707.7	60.26	47.977	12.283	150.88	47.551	30.939	16.612	275.96	
282.5	-147.5	38.603	48.19	-9.587	91.902	48.503	39.549	8.9537	80.168	0	0	0	0	37.038	49.437	-12.4	153.74	41.495	23.501	17.995	323.8	46.583	39.239	7.3442	53.937	
107.5	215	39.887	43.379	-3.492	12.194	37.784	41.195	-3.411	11.634	40.002	0	40.002	1600.2	41.33	50.842	-9.511	90.464	48.356	34.746	13.61	185.23	45.844	36.482	9.3627	87.661	
195	340	42.182	44.02	-1.838	3.3786	47.828	43.529	4.2993	18.484	0	0	0	0	38.055	47.181	-9.126	83.276	39.726	37.51	2.2154	4.9078	31.592	37.537	-5.945	35.344	
32.5	202.5	46.472	42.381	4.091	16.736	36.696	39.79	-3.094	9.5704	0	16.457	-16.46	270.82	52.732	46.789	5.9424	35.312	33.993	39.622	-5.63	31.694	35.437	45.789	-10.35	107.16	
57.5	77.5	44.187	38.741	5.4467	29.666	72.973	52.917	20.055	402.22	0	0	0	0	0	20.873	-20.87	435.67	60.874	51.736	9.1385	83.512	32.035	43.801	-11.77	138.45	
-17.5	-222.5	53.203	54.68	-1.477	2.1823	37.662	23.265	14.397	207.28	0	0	0	0	40.784	37.396	3.3878	11.477	40.488	28.944	11.544	133.26	30.384	51.828	-21.44	459.82	
-117.5	-322.5	42.868	53.401	-10.53	110.94	45.128	37.929	7.1992	51.829	0	0	0	0	43.322	49.752	-6.43	41.348	48.708	25.522	23.185	537.56	39.799	53.899	-14.1	198.81	
45	415	50.956	51.386	-0.429	0.1844	49.687	45.663	4.0247	16.198	0	0	0	0	47.017	42.991	4.0258	16.207	48.223	43.062	5.1615	26.641	37.93	37.517	0.4133	0.1708	
-92.5	202.5	51.13	41.058	10.072	101.44	40.262	42.395	-2.133	4.5507	25.111	10.529	14.583	212.65	54.967	50.989	3.9778	15.823	35.539	38.792	-3.253	10.584	46.754	38.841	7.9134	62.622	
-205	290	54.185	42.479	11.706	137.04	0	46.037	-46.04	2119.4	0	7.2559	-7.256	52.648	25	47.902	-22.9	524.51	40	40.788	-0.788	0.6212	30	38.032	-8.032	64.515	
245	40	56.379	38.707	17.671	312.27	52.281	47.705	4.5769	20.948	0	0	0	0	50.631	31.815	18.816	354.03	36.392	41.033	-4.641	21.539	30.205	48.032	-17.83	317.78	
195	340	42.182	44.02	-1.838	3.3786	47.828	43.529	4.2993	18.484	0	0	0	0	38.055	47.181	-9.126	83.276	39.726	37.51	2.2154	4.9078	31.592	37.537	-5.945	35.344	
20	302.5	53.216	42.856	10.359	107.32	39.613	44.91	-5.297	28.055	0	0	0	0	36.856	44.358	-7.502	56.275	33.569	40.379	-6.81	46.38	37.281	33.014	4.2676	18.212	
107.5	-260	54.868	51.411	3.4569	11.95	0	40.226	-40.23	1618.2	0	0	0	0	42.419	33.971	8.4486	71.379	0	22.961	-22.96	527.19	70	32.404	37.596	1413.5	
-217.5	-135	55.241	46.636	8.6048	74.042	54.618	47.456	7.1615	51.288	0	0	0	0	46.086	47.008	-0.922	0.8493	47.526	35.889	11.637	135.43	43.187	34.438	8.7493	76.55	
157.5	-135	43.831	49.485	-5.654	31.966	56.175	44.207	11.968	143.23	0	0	0	0	43.954	18.767	25.186	634.34	35.582	51.083	-15.5	240.29	36.466	35.416	1.0495	1.1014	
282.5	-147.5	38.603	44.889	-6.286	39.509	48.503	46.253	2.25	5.0627	0	0	0	0	37.038	48.522	-11.48	131.89	41.495	37.623	3.8726	14.997	46.583	37.807	8.7759	77.016	
$\sum d$, $\sum d^2$				6.0518	1873.1			24.396	6472.3				-4.075	2545.3			-118.1	5734			63.133	3416.5			17.927	3721.7
$(\sum d)^2$				36.624				595.18					16.602				13959			3985.8					321.39	
\bar{d}				0.2017				0.8132					-0.136				-3.938			2.1044					0.5976	
S^2				64.549				222.5					87.751				181.68			113.23					127.97	
S				8.0342				14.916					9.3675				13.479			10.641					11.312	
t(0.975)	2.04					2.04				2.04				2.04					2.04				2.04			
Left value				-2.791				-4.742					-3.625				-8.958			-1.859					-3.816	
Right value				3.1941				6.3688					3.3531				1.082			6.0677					4.8108	

Table 4.7: Difference between the interpolated depth from our model and the original survey depth from example one with all soil layer

Sample_1		Layer 1				Layer 2				Layer 3				Layer 4				Layer 5				Layer 6				
X	Y	Depth 1	Depth 2	D 2-1	Square	Depth 1	Depth 2	D 2-1	Square	Depth 1	Depth 2	D 2-1	Square	Depth 1	Depth 2	D 2-1	Square	Depth 1	Depth 2	D 2-1	Square	Depth 1	Depth 2	D 2-1	Square	
-155	-22.5	51.395	49.507	1.8874	3.5624	52.048	40.739	11.309	127.9	0	11.789	-11.79	138.97	52.653	52.379	0.274	0.0751	41.806	38.4	3.4054	11.597	36.362	35.555	0.8066	0.6506	
70	-72.5	55.371	46.493	8.8779	78.818	45.76	57.999	-12.24	149.81	0	0	0	0	25.311	-25.31	640.66	60.585	47.138	13.447	180.83	30.904	33.038	-2.135	4.5565		
-105	115	40.66	49.987	-9.328	87.003	41.04	44.807	-3.767	14.191	0	10.603	-10.6	112.42	51.144	53.786	-2.642	6.9812	41.006	37.307	3.6989	13.682	36.404	42.504	-6.1	37.206	
57.5	77.5	44.187	49.37	-5.183	26.865	72.973	42.291	30.682	941.38	0	0	0	0	27.094	-27.09	734.1	60.874	46.896	13.978	195.38	32.035	34.521	-2.486	6.1792		
20	352.5	40.273	47.811	-7.538	56.815	48.226	39.196	9.0299	81.54	0	0	0	0	41.026	42.417	-1.391	1.9352	43.086	35.287	7.7985	60.817	31.626	40.17	-8.544	72.992	
-30	202.5	44.535	48.801	-4.266	18.203	40.06	38.479	1.581	2.4997	0	12.556	-12.56	157.65	53.48	53.849	-0.369	0.1364	31.999	34.766	-2.767	7.6561	45.647	41.096	4.5518	20.718	
157.5	-135	43.831	49.485	-5.654	31.966	56.175	44.207	11.968	143.23	0	0	0	0	43.954	18.767	25.186	634.34	35.582	51.083	-15.5	240.29	36.466	35.416	1.0495	1.1014	
282.5	-147.5	38.603	44.889	-6.286	39.509	48.503	46.253	2.25	5.0627	0	0	0	0	37.038	48.522	-11.48	131.89	41.495	37.623	3.8726	14.997	46.583	37.807	8.7759	77.016	
20	302.5	53.216	42.856	10.359	107.32	39.613	44.91	-5.297	28.055	0	0	0	0	36.856	44.358	-7.502	56.275	33.569	40.379	-6.81	46.38	37.281	33.014	4.2676	18.212	
45	390	44.9	46.908	-2.008	4.0311	38.018	49.097	-11.08	122.74	0	0	0	0	47.277	44.522	2.7545	7.5873	36.426	46.039	-9.613	92.414	41.862	35.477	6.385	40.768	
20	302.5	53.216	42.856	10.359	107.32	39.613	44.91	-5.297	28.055	0	0	0	0	36.856	44.358	-7.502	56.275	33.569	40.379	-6.81	46.38	37.281	33.014	4.2676	18.212	
45	415	50.956	51.386	-0.429	0.1844	49.687	45.663	4.0247	16.198	0	0	0	0	47.017	42.991	4.0258	16.207	48.223	43.062	5.1615	26.641	37.93	37.517	0.4133	0.1708	
157.5	40	36.904	51.92	-15.02	225.46	61.115	58.872	2.2431	5.0316	0	0	0	0	26.603	-26.6	707.7	60.26	47.977	12.283	150.88	47.551	30.939	16.612	275.96		
282.5	-147.5	38.603	48.19	-9.587	91.902	48.503	39.549	8.9537	80.168	0	0	0	0	37.038	49.437	-12.4	153.74	41.495	23.501	17.995	323.8	46.583	39.239	7.3442	53.937	
107.5	215	39.887	43.379	-3.492	12.194	37.784	41.195	-3.411	11.634	40.002	0	40.002	1600.2	41.33	50.842	-9.511	90.464	48.356	34.746	13.61	185.23	45.844	36.482	9.3627	87.661	
195	340	42.182	44.02	-1.838	3.3786	47.828	43.529	4.2993	18.484	0	0	0	0	38.055	47.181	-9.126	83.276	39.726	37.51	2.2154	4.9078	31.592	37.537	-5.945	35.344	
32.5	202.5	46.472	42.381	4.091	16.736	36.696	39.79	-3.094	9.5704	0	16.457	-16.46	270.82	52.732	46.789	5.9424	35.312	33.993	39.622	-5.63	31.694	35.437	45.789	-10.35	107.16	
57.5	77.5	44.187	38.741	5.4467	29.666	72.973	52.917	20.055	402.22	0	0	0	0	20.873	-20.87	435.67	60.874	51.736	9.1385	83.512	32.035	43.801	-11.77	138.45		
-17.5	-222.5	53.203	54.68	-1.477	2.1823	37.662	23.265	14.397	207.28	0	0	0	0	40.784	37.396	3.3878	11.477	40.488	28.944	11.544	133.26	30.384	51.828	-21.44	459.82	
-117.5	-322.5	42.868	53.401	-10.53	110.94	45.128	37.929	7.1992	51.829	0	0	0	0	43.322	49.752	-6.43	41.348	48.708	25.522	23.185	537.56	39.799	53.899	-14.1	198.81	
45	415	50.956	51.386	-0.429	0.1844	49.687	45.663	4.0247	16.198	0	0	0	0	47.017	42.991	4.0258	16.207	48.223	43.062	5.1615	26.641	37.93	37.517	0.4133	0.1708	
-92.5	202.5	51.13	41.058	10.072	101.44	40.262	42.395	-2.133	4.5507	25.111	10.529	14.583	212.65	54.967	50.989	3.9778	15.823	35.539	38.792	-3.253	10.584	46.754	38.841	7.9134	62.622	
-205	290	54.185	42.479	11.706	137.04	0	46.037	-46.04	2119.4	0	7.2559	-7.256	52.648	25	47.902	-22.9	524.51	40	40.788	-0.788	0.6212	30	38.032	-8.032	64.515	
245	40	56.379	38.707	17.671	312.27	52.281	47.705	4.5769	20.948	0	0	0	0	50.631	31.815	18.816	354.03	36.392	41.033	-4.641	21.539	30.205	48.032	-17.83	317.78	
195	340	42.182	44.02	-1.838	3.3786	47.828	43.529	4.2993	18.484	0	0	0	0	38.055	47.181	-9.126	83.276	39.726	37.51	2.2154	4.9078	31.592	37.537	-5.945	35.344	
20	302.5	53.216	42.856	10.359	107.32	39.613	44.91	-5.297	28.055	0	0	0	0	36.856	44.358	-7.502	56.275	33.569	40.379	-6.81	46.38	37.281	33.014	4.2676	18.212	
107.5	-260	54.868	51.411	3.4569	11.95	0	40.226	-40.23	1618.2	0	0	0	0	42.419	33.971	8.4486	71.379	0	22.961	-22.96	527.19	70	32.404	37.596	1413.5	
-217.5	-135	55.241	46.636	8.6048	74.042	54.618	47.456	7.1615	51.288	0	0	0	0	46.086	47.008	-0.922	0.8493	47.526	35.889	11.637	135.43	43.187	34.438	8.7493	76.55	
157.5	-135	43.831	49.485	-5.654	31.966	56.175	44.207	11.968	143.23	0	0	0	0	43.954	18.767	25.186	634.34	35.582	51.083	-15.5	240.29	36.466	35.416	1.0495	1.1014	
282.5	-147.5	38.603	44.889	-6.286	39.509	48.503	46.253	2.25	5.0627	0	0	0	0	37.038	48.522	-11.48	131.89	41.495	37.623	3.8726	14.997	46.583	37.807	8.7759	77.016	
$\sum d$		-10.71	$\sum d^2$		23763	$(\sum d)^2$		114.79	\bar{d}		-0.06	S^2		132.75	\bar{S}		11.522	t(0.975)		1.96	Left value		-1.743	Right value		1.6237

Table 4.8: Difference between the interpolated depth from our model and the original survey depth from example two with each soil layer

Sample_2		Layer 1				Layer 2				Layer 3				Layer 4				Layer 5				Layer 6				
X	Y	Depth 1	Depth 2	D 2-1	Square	Depth 1	Depth 2	D 2-1	Square	Depth 1	Depth 2	D2-1	Square	Depth 1	Depth 2	D 2-1	Square	Depth 1	Depth 2	D 2-1	Square	Depth 1	Depth 2	D 2-1	Square	
70	-72.5	55.371	49.056	6.3151	39.881	45.76	52.749	-6.99	48.857	0	0	0	0	0	41.984	-41.98	1762.6	60.585	42.044	18.541	343.77	30.904	35.64	-4.737	22.437	
57.5	77.5	44.187	44.629	-0.441	0.1948	72.973	50.981	21.992	483.64	0	14.5	-14.5	210.26	0	23.767	-23.77	564.87	60.874	50.272	10.602	112.4	32.035	42.542	-10.51	110.41	
45	390	44.9	46.683	-1.783	3.1793	38.018	49.103	-11.08	122.87	0	0	0	0	47.277	44.621	2.656	7.0545	36.426	46.168	-9.743	94.921	41.862	35.409	6.4531	41.643	
15	402.5	36.692	46.729	-10.04	100.74	43.107	48.311	-5.204	27.081	0	0	0	0	44.535	45.597	-1.063	1.129	37.757	45.569	-7.811	61.017	45.431	38.18	7.2509	52.575	
15	115	40.66	47.895	-7.235	52.349	41.04	44.482	-3.442	11.848	0	17.283	-17.28	298.7	51.144	38.161	12.982	168.54	41.006	43.457	-2.451	6.0082	36.404	39.322	-2.918	8.5157	
190	-72.5	55.371	48.312	7.0593	49.833	45.76	54.784	-9.025	81.445	0	0	0	0	46.338	-46.34	2147.2	60.585	35.871	24.714	610.77	30.904	34.23	-3.326	11.064		
45	415	50.956	50.383	0.5733	0.3286	49.687	46.224	3.4628	11.991	0	0	0	0	47.017	43.416	3.6013	12.969	48.223	43.578	4.6456	21.582	37.93	38.043	-0.112	0.0126	
-30	202.5	44.535	48.801	-4.266	18.203	40.06	38.479	1.581	2.4997	0	12.556	-12.56	157.65	53.48	53.849	-0.369	0.1364	31.999	34.766	-2.767	7.6561	45.647	41.096	4.5517	20.718	
165	415	50.956	52.436	-1.48	2.1903	49.687	45.074	4.6133	21.282	0	0	0	0	47.017	42.546	4.4705	19.986	48.223	42.522	5.7019	32.512	37.93	36.967	0.9639	0.9291	
27.5	202.5	51.13	46.659	4.4719	19.998	40.262	36.839	3.4226	11.714	25.111	1.0045	24.107	581.15	54.967	52.821	2.1459	4.6051	35.539	34.054	1.4841	2.2025	46.754	35.89	10.865	118.04	
-35	-22.5	51.395	51.639	-0.244	0.0596	52.048	40.947	11.101	123.23	0	14.966	-14.97	223.97	52.653	47.519	5.1335	26.353	41.806	40.285	1.521	2.3135	36.362	35.168	1.1938	1.4252	
-110	-285	55.186	45.718	9.4685	89.653	54.192	50.987	3.2048	10.271	0	0	0	0	41.245	52.77	-11.52	132.81	32.025	44.827	-12.8	163.9	31.097	47.381	-16.28	265.17	
-155	-22.5	51.395	52.953	-1.558	2.4267	52.048	44.851	7.1965	51.79	0	0	0	0	52.653	51.994	0.6582	0.4332	41.806	40.793	1.013	1.0261	36.362	37.775	-1.414	1.9983	
-85	290	54.185	43.837	10.348	107.09	0	46.691	-46.69	2180.1	0	7.7934	-7.793	60.737	25	43.732	-18.73	350.9	40	41.504	-1.504	2.2619	30	38.049	-8.049	64.782	
-172.5	165	38.442	47.788	-9.346	87.352	46.19	40.882	5.3078	28.173	0	26.499	-26.5	702.2	50.59	50.224	0.366	0.134	33.708	39.161	-5.453	29.74	37.927	36.301	1.6262	2.6444	
2.5	-322.5	42.868	54.814	-11.95	142.7	45.128	49.229	-4.101	16.819	0	0	0	0	43.322	48.515	-5.193	26.969	48.708	18.657	30.05	903.03	39.799	52.374	-12.57	158.13	
-210	-147.5	43.922	55.15	-11.23	126.07	54.951	52.912	2.0391	4.1577	0	0	0	0	38.499	45.456	-6.957	48.399	32.656	47.103	-14.45	208.71	33.797	42.665	-8.868	78.635	
152.5	202.5	46.472	39.117	7.3548	54.093	36.696	41.779	-5.082	25.829	0	30.002	-30	900.1	52.732	41.229	11.503	132.32	33.993	45.01	-11.02	121.39	35.437	46.19	-10.75	115.62	
90	202.5	44.535	40.591	3.9441	15.556	40.06	38.051	2.0089	4.0357	0	31.726	-31.73	1006.5	53.48	43.509	9.9708	99.417	31.999	46.179	-14.18	201.09	45.647	43.801	1.8468	3.4107	
195	340	42.182	41.84	0.3417	0.1168	47.828	42.87	4.9578	24.58	0	0	0	0	38.055	47.369	-9.313	86.737	39.726	37.353	2.3733	5.6324	31.592	38.055	-6.463	41.768	
-105	115	40.66	54.679	-14.02	196.53	41.04	38.949	2.0911	4.3728	0	35.115	-35.11	1233	51.144	52.424	-1.28	1.6388	41.006	38.629	2.3767	5.6488	36.404	36.6	-0.196	0.0386	
-230	-285	55.186	50.414	4.7719	22.771	54.192	16.512	37.68	1419.8	0	0	0	0	41.245	46.43	-5.184	26.875	32.025	36.94	-4.915	24.155	31.097	49.242	-18.15	329.25	
227.5	215	39.887	38.081	1.8058	3.2609	37.784	49.742	-11.96	142.99	40.002	0	40.002	1600.2	41.33	45.953	-4.623	21.374	48.356	35.653	12.704	161.39	45.844	40.655	5.1893	26.929	
-235	-297.5	56.458	51.145	5.3125	28.222	0	12.681	-12.68	160.81	0	0	0	0	47.616	47.163	0.4531	0.2053	90	38.69	51.31	2632.7	0	49.338	-49.34	2434.2	
165	390	44.9	47.357	-2.457	6.0379	38.018	49.085	-11.07	122.48	0	0	0	0	47.277	44.325	2.9515	8.7112	36.426	45.78	-9.354	87.498	41.862	35.613	6.2487	39.046	
15	115	40.66	47.895	-7.235	52.349	41.04	44.482	-3.442	11.848	0	17.283	-17.28	298.7	51.144	38.161	12.982	168.54	41.006	43.457	-2.451	6.0082	36.404	39.322	-2.918	8.5157	
157.5	-135	43.831	54.128	-10.3	106.04	56.175	42.826	13.349	178.19	0	0	0	0	43.954	17.854	26.099	681.17	35.582	51.68	-16.1	259.16	36.466	30.872	5.5941	31.294	
57.5	77.5	44.187	44.629	-0.441	0.1948	72.973	50.981	21.992	483.64	0	14.5	-14.5	210.26	0	23.767	-23.77	564.87	60.874	50.272	10.602	112.4	32.035	42.542	-10.51	110.41	
-30	202.5	44.535	51.13	-6.596	43.501	40.06	40.262	-0.202	0.0406	0	25.111	-25.11	630.58	53.48	54.967	-1.487	2.2111	31.999	35.539	-3.54	12.531	45.647	46.754	-1.107	1.2251	
-105	402.5	36.692	48.149	-11.46	131.28	43.107	43.458	-0.351	0.1232	0	0	0	0	44.535	42.718	1.8171	3.3017	37.757	44.461	-6.704	44.941	45.431	38.423	7.0076	49.106	
$\sum d, \sum d^2$				-50.3	1502.2			14.679	5816.5				-183.2	8114.1			-103.8	7072.5			52.4	6278.4			-109.4	4150
$(\sum d)^2$				2530.2				215.46					33571				10773				2745.8				11974	
\bar{d}				-1.677				0.4893					-6.108				-3.46				1.7467				-3.648	
S^2				48.892				200.32					241.21				231.5				213.34				129.34	
S				6.9922				14.153					15.531				15.215				14.606				11.373	
t(0.975)	2.04				2.04					2.04				2.04					2.04				2.04			
Left value				-4.281				-4.782					-11.89				-9.127				-3.693				-7.883	
Right value				0.9276				5.7607					-0.323				2.2072				7.1868				0.5882	

Table 4.9: Difference between the interpolated depth from our model and the original survey depth from example two with all soil layer

Sample_2		Layer 1				Layer 2				Layer 3				Layer 4				Layer 5				Layer 6			
X	Y	Depth 1	Depth 2	D 2-1	Square	Depth 1	Depth 2	D 2-1	Square	Depth 1	Depth 2	D 2-1	Square	Depth 1	Depth 2	D 2-1	Square	Depth 1	Depth 2	D 2-1	Square	Depth 1	Depth 2	D 2-1	Square
70	-72.5	55.371	49.056	6.3151	39.881	45.76	52.749	-6.99	48.857	0	0	0	0	0	41.984	-41.98	1762.6	60.585	42.044	18.541	343.77	30.904	35.64	-4.737	22.437
57.5	77.5	44.187	44.629	-0.441	0.1948	72.973	50.981	21.992	483.64	0	14.5	-14.5	210.26	0	23.767	-23.77	564.87	60.874	50.272	10.602	112.4	32.035	42.542	-10.51	110.41
45	390	44.9	46.683	-1.783	3.1793	38.018	49.103	-11.08	122.87	0	0	0	0	47.277	44.621	2.656	7.0545	36.426	46.168	-9.743	94.921	41.862	35.409	6.4531	41.643
15	402.5	36.692	46.729	-10.04	100.74	43.107	48.311	-5.204	27.081	0	0	0	0	44.535	45.597	-1.063	1.129	37.757	45.569	-7.811	61.017	45.431	38.18	7.2509	52.575
15	115	40.66	47.895	-7.235	52.349	41.04	44.482	-3.442	11.848	0	17.283	-17.28	298.7	51.144	38.161	12.982	168.54	41.006	43.457	-2.451	6.0082	36.404	39.322	-2.918	8.5157
190	-72.5	55.371	48.312	7.0593	49.833	45.76	54.784	-9.025	81.445	0	0	0	0	46.338	-46.34	2147.2	60.585	35.871	24.714	610.77	30.904	34.23	-3.326	11.064	
45	415	50.956	50.383	0.5733	0.3286	49.687	46.224	3.4628	11.991	0	0	0	0	47.017	43.416	3.6013	12.969	48.223	43.578	4.6456	21.582	37.93	38.043	-0.112	0.0126
-30	202.5	44.535	48.801	-4.266	18.203	40.06	38.479	1.581	2.4997	0	12.556	-12.56	157.65	53.48	53.849	-0.369	0.1364	31.999	34.766	-2.767	7.6561	45.647	41.096	4.5517	20.718
165	415	50.956	52.436	-1.48	2.1903	49.687	45.074	4.6133	21.282	0	0	0	0	47.017	42.546	4.4705	19.986	48.223	42.522	5.7019	32.512	37.93	36.967	0.9639	0.9291
27.5	202.5	51.13	46.659	4.4719	19.998	40.262	36.839	3.4226	11.714	25.111	1.0045	24.107	581.15	54.967	52.821	2.1459	4.6051	35.539	34.054	1.4841	2.2025	46.754	35.89	10.865	118.04
-35	-22.5	51.395	51.639	-0.244	0.0596	52.048	40.947	11.101	123.23	0	14.966	-14.97	223.97	52.653	47.519	5.1335	26.353	41.806	40.285	1.521	2.3135	36.362	35.168	1.1938	1.4252
-110	-285	55.186	45.718	9.4685	89.653	54.192	50.987	3.2048	10.271	0	0	0	0	41.245	52.77	-11.52	132.81	32.025	44.827	-12.8	163.9	31.097	47.381	-16.28	265.17
-155	-22.5	51.395	52.953	-1.558	2.4267	52.048	44.851	7.1965	51.79	0	0	0	0	52.653	51.994	0.6582	0.4332	41.806	40.793	1.013	1.0261	36.362	37.775	-1.414	1.9983
-85	290	54.185	43.837	10.348	107.09	0	46.691	-46.69	2180.1	0	7.7934	-7.793	60.737	25	43.732	-18.73	350.9	40	41.504	-1.504	2.2619	30	38.049	-8.049	64.782
-172.5	165	38.442	47.788	-9.346	87.352	46.19	40.882	5.3078	28.173	0	26.499	-26.5	702.2	50.59	50.224	0.366	0.134	33.708	39.161	-5.453	29.74	37.927	36.301	1.6262	2.6444
2.5	-322.5	42.868	54.814	-11.95	142.7	45.128	49.229	-4.101	16.819	0	0	0	0	43.322	48.515	-5.193	26.969	48.708	18.657	30.05	903.03	39.799	52.374	-12.57	158.13
-210	-147.5	43.922	55.15	-11.23	126.07	54.951	52.912	2.0391	4.1577	0	0	0	0	38.499	45.456	-6.957	48.399	32.656	47.103	-14.45	208.71	33.797	42.665	-8.868	78.635
152.5	202.5	46.472	39.117	7.3548	54.093	36.696	41.779	-5.082	25.829	0	30.002	-30	900.1	52.732	41.229	11.503	132.32	33.993	45.01	-11.02	121.39	35.437	46.19	-10.75	115.62
90	202.5	44.535	40.591	3.9441	15.556	40.06	38.051	2.0089	4.0357	0	31.726	-31.73	1006.5	53.48	43.509	9.9708	99.417	31.999	46.179	-14.18	201.09	45.647	43.801	1.8468	3.4107
195	340	42.182	41.84	0.3417	0.1168	47.828	42.87	4.9578	24.58	0	0	0	0	38.055	47.369	-9.313	86.737	39.726	37.353	2.3733	5.6324	31.592	38.055	-6.463	41.768
-105	115	40.66	54.679	-14.02	196.53	41.04	38.949	2.0911	4.3728	0	35.115	-35.11	1233	51.144	52.424	-1.28	1.6388	41.006	38.629	2.3767	5.6488	36.404	36.6	-0.196	0.0386
-230	-285	55.186	50.414	4.7719	22.771	54.192	16.512	37.68	1419.8	0	0	0	0	41.245	46.43	-5.184	26.875	32.025	36.94	-4.915	24.155	31.097	49.242	-18.15	329.25
227.5	215	39.887	38.081	1.8058	3.2609	37.784	49.742	-11.96	142.99	40.002	0	40.002	1600.2	41.33	45.953	-4.623	21.374	48.356	35.653	12.704	161.39	45.844	40.655	5.1893	26.929
-235	-297.5	56.458	51.145	5.3125	28.222	0	12.681	-12.68	160.81	0	0	0	0	47.616	47.163	0.4531	0.2053	90	38.69	51.31	2632.7	0	49.338	-49.34	2434.2
165	390	44.9	47.357	-2.457	6.0379	38.018	49.085	-11.07	122.48	0	0	0	0	47.277	44.325	2.9515	8.7112	36.426	45.78	-9.354	87.498	41.862	35.613	6.2487	39.046
15	115	40.66	47.895	-7.235	52.349	41.04	44.482	-3.442	11.848	0	17.283	-17.28	298.7	51.144	38.161	12.982	168.54	41.006	43.457	-2.451	6.0082	36.404	39.322	-2.918	8.5157
157.5	-135	43.831	54.128	-10.3	106.04	56.175	42.826	13.349	178.19	0	0	0	0	43.954	17.854	26.099	681.17	35.582	51.68	-16.1	259.16	36.466	30.872	5.5941	31.294
57.5	77.5	44.187	44.629	-0.441	0.1948	72.973	50.981	21.992	483.64	0	14.5	-14.5	210.26	0	23.767	-23.77	564.87	60.874	50.272	10.602	112.4	32.035	42.542	-10.51	110.41
-30	202.5	44.535	51.13	-6.596	43.501	40.06	40.262	-0.202	0.0406	0	25.111	-25.11	630.58	53.48	54.967	-1.487	2.2111	31.999	35.539	-3.54	12.531	45.647	46.754	-1.107	1.2251
-105	402.5	36.692	48.149	-11.46	131.28	43.107	43.458	-0.351	0.1232	0	0	0	0	44.535	42.718	1.8171	3.3017	37.757	44.461	-6.704	44.941	45.431	38.423	7.0076	49.106
$\sum d$		-379.7		$\sum d^2$	32934	$(\sum d)^2$		144146	\bar{d}		-2.109		S^2	179.51	S		13.398	t(0.975)	1.96		Left value		Right value		-0.152

Table 4.10: Difference between the interpolated depth from our model and the original survey depth from example three with each soil layer

Sample_3		Layer 1				Layer 2				Layer 3				Layer 4				Layer 5				Layer 6				Layer 7			
X	Y	D 1	D 2	D (2-1)	Sqr	D 1	D 2	D (2-1)	Sqr	D 1	D 2	D (2-1)	Sqr	D 1	D 2	D (2-1)	Sqr	D 1	D 2	D (2-1)	Sqr	D 1	D 2	D (2-1)	Sqr	D 1	D 2	D (2-1)	Sqr
-239	343	40	39.5	0.49	0.24	14	21.9	-7.85	61.7	0	0	0	0	30	13.8	16.2	263	0	4.53	-4.53	20.6	18	16.1	1.91	3.66	27	26	0.97	0.94
-217	-135	26	31	-4.96	24.6	39	15.7	23.3	542	15	8.18	6.82	46.6	27	31	-4	16	0	0	0	0	14	5.92	8.08	65.3	23	41.6	-18.6	344
-192	115	39	27.1	11.9	143	24	22.6	1.43	2.06	0	0	0	0	10	23.3	-13.3	177	0	0	0	0	19	13.7	5.3	28.1	53	33.9	19.1	365
-155	-22	45	36.7	8.27	68.4	30	14.3	15.7	247	0	0	0	0	34	20.2	13.8	192	0	0	0	0	1	15.4	-14.4	207	33	21.5	11.5	133
-112	232	37	35.6	1.36	1.84	41	22.9	18.1	327	0	0	0	0	30	27.6	2.43	5.9	0	0	0	0	1	13.2	-12.2	149	30	48.1	-18.1	327
-89	-233	24	37.3	-13.3	176	30	19.1	10.9	119	10	10.4	-0.37	0.14	28	22.7	5.33	28.4	0	0	0	0	10	24.8	-14.8	219	46	31.3	14.7	215
-17	-360	42	36.5	5.54	30.7	17	36.5	-19.5	381	0	0	0	0	25	28.2	-3.23	10.5	0	0	0	0	13	19.7	-6.75	45.5	29	40	-11	122
32	202	40	43.5	-3.51	12.3	31	20.4	10.6	113	0	0	0	0	16	25.9	-9.91	98.2	0	0.61	-0.61	0.37	18	21.1	-3.1	9.62	30	21.3	8.75	76.5
57	77	26	36.7	-10.7	114	35	40.2	-5.16	26.6	0	0	0	0	27	34.7	-7.73	59.7	12	7.06	4.94	24.4	5	7.96	-2.96	8.76	25	28	-3.04	9.22
115	355	48	33.8	14.2	201	23	41	-18	324	0	5.06	-5.06	25.6	26	23.4	2.6	6.75	0	0	0	0	8	17.7	-9.73	94.6	32	38.1	-6.1	37.2
-332	143	47	45.3	1.72	2.95	40	17	23	527	0	0	0	0	30	30.7	-0.7	0.48	0	0	0	0	6	14.4	-8.44	71.3	36	36.8	-0.85	0.72
-329	-48	24	31.7	-7.66	58.7	11	31.2	-20.2	408	0	0	0	0	29	19.8	9.18	84.2	0	0	0	0	4	9.28	-5.28	27.8	43	34.8	8.23	67.7
-220	-333	24	43	-1.9	36.1	17	13.9	3.13	9.82	0	0	0	0	30	32.1	-2.06	4.24	0	0	0	0	10	11.1	-1.06	1.11	39	21.4	17.6	309
-186	-65	41	36.2	4.78	22.9	32	16.2	15.8	251	0	0	0	0	11	29.4	-18.4	339	0	0	0	0	29	8.4	20.6	424	34	29.8	4.22	17.8
-149	-230	45	41.2	3.76	14.2	11	13.6	-2.63	6.91	29	23	6	36	16	20.7	-4.69	22	0	0	0	0	14	17.1	-3.07	9.43	20	47.1	-27.1	734
-97	204	42	36.3	5.68	32.2	15	33.1	-18.1	328	0	0	0	0	21	23.4	-2.42	5.88	0	0.19	-0.19	0.03	15	7.2	7.8	60.8	18	45.3	-27.3	744
-58	-214	43	32.1	10.9	118	15	38.6	-23.6	556	0	3.36	-3.36	11.3	19	28.5	-9.53	90.8	0	0	0	0	29	16.9	12.1	147	17	38.3	-21.3	453
-47	147	31	23.9	7.11	50.6	15	32.9	-17.9	321	0	0	0	0	19	15.1	3.91	15.3	0	0.82	-0.82	0.68	10	8.96	1.04	1.08	27	35.7	-8.69	75.5
13	-245	23	44.7	-21.7	473	46	27.1	18.9	357	0	0	0	0	18	28.5	-10.5	110	0	0	0	0	3	24.4	-21.4	457	22	27.9	-5.9	34.8
45	415	41	39.7	1.29	1.68	0	-0	0	0	0	0	0	0	39	23.3	15.7	247	0	0	0	0	29	17.2	11.8	138	26	47.4	-21.4	459
-42	277	35	40.9	-5.91	35	41	18	23	530	0	6.43	-6.43	41.4	29	29.8	-0.83	0.68	0	0	0	0	22	20.7	1.31	1.71	33	26.1	6.9	47.6
8	53	32	28.9	3.08	9.5	38	33.6	4.39	19.3	0	0	0	0	33	24.8	8.22	67.6	15	15.1	-0.07	0.01	2	16.5	-14.5	209	35	38.8	-3.83	14.7
47	32	30	35.2	-5.22	27.2	45	40.1	4.87	23.7	0	0	0	0	34	21	13	170	7	15.3	-8.28	68.5	2	6.92	-4.92	24.2	46	38.5	7.5	56.3
83	383	36	29.6	6.45	41.6	25	39.4	-14.4	208	0	0	0	0	10	20.4	-10.4	109	0	0	0	0	27	8.77	18.2	332	44	44.6	-0.57	0.32
130	175	33	29.6	3.44	11.8	48	36.9	11.1	123	0	0	0	0	31	22	8.99	80.8	0	0	0	0	2	25.9	-23.9	569	24	33.2	-9.21	84.9
157	-135	41	44.9	-3.93	15.4	11	45.4	-34.4	1183	0	0	0	0	20	23.4	-3.44	11.8	0	0	0	0	1	21.9	-20.9	438	16	39.3	-23.3	544
195	340	37	41.7	-4.75	22.6	41	20.6	20.4	418	0	0	0	0	10	27.4	-17.4	303	0	0	0	0	8	9.89	-1.89	3.56	49	33.8	15.2	232
231	-90	40	36.9	3.09	9.55	17	29.3	-12.3	152	0	0	0	0	39	17.6	21.4	459	0	7.95	-7.95	63.1	28	16.2	11.8	139	53	40	13	168
254	94	28	35.3	-7.32	53.5	24	20.8	3.23	10.4	0	0.14	-0.14	0.02	20	20.5	-0.53	0.29	0	0	0	0	2	27	-25	625	40	49.6	-9.58	91.8
277	-121	22	34.3	-12.3	150	27	23.6	3.36	11.3	0	0.2	-0.2	0.04	24	19.9	4.1	16.8	20	14.5	5.46	29.8	4	19	-15	225	23	44.9	-21.9	480
-327	-257	49	28.7	20.3	413	11	10.7	0.28	0.08	0	0	0	0	12	24.9	-12.9	166	0	0	0	0	7	14.9	-7.86	61.7	26	41	-15	224
-290	320	32	37.5	-5.49	30.1	44	39.6	4.43	19.6	0	0	0	0	21	21.1	-0.12	0.01	0	3.99	-3.99	15.9	10	18.7	-8.73	76.3	21	33.2	-12.2	149
-186	-65	41	36.2	4.78	22.9	32	16.2	15.8	251	0	0	0	0	11	29.4	-18.4	339	0	0	0	0	29	8.4	20.6	424	34	29.8	4.22	17.8
-106	-30	45	39.2	5.8	33.6	14	22	-7.99	63.8	0	0	0	0	22	32.6	-10.6	113	0	2.47	-2.47	6.09	9	13.9	-4.9	24	18	34.5	-16.5	273
8	53	32	27	5	25	38	35.4	2.6	6.76	0	0	0	0	33	29.6	3.43	11.8	15	12	2.97	8.8	2	14.6	-12.6	160	35	41.6	-6.59	43.4
42	99	43	28.1	14.9	221	36	32.2	3.8	14.4	0	0	0	0	35	24.8	10.2	103	9	9.27	-0.27	0.07	7	7.02	-0.02	0	23	25.8	-2.79	7.76
127	307	41	37.6	3.41	11.6	47	29.2	17.8	317	11	0	11	121	30	22.1	7.89	62.2	0	0	0	0	19	14.1	4.86	23.6	33	31.9	1.13	1.29

Sample_3		Layer 1				Layer 2				Layer 3				Layer 4				Layer 5				Layer 6				Layer 7				
X	Y	D 1	D 2	D (2-1)	Sqr	D 1	D 2	D (2-1)	Sqr	D 1	D 2	D (2-1)	Sqr	D 1	D 2	D (2-1)	Sqr	D 1	D 2	D (2-1)	Sqr	D 1	D 2	D (2-1)	Sqr	D 1	D 2	D (2-1)	Sqr	
209	-306	29	22.3	6.7	44.8	27	20.5	6.54	42.7	0	0	0	0	26	25.7	0.27	0.07	0	0	0	0	7	25.9	-18.9	356	32	35.4	-3.37	11.4	
254	94	28	35.3	-7.32	53.5	24	20.8	3.23	10.4	0	0.14	-0.14	0.02	20	20.5	-0.53	0.29	0	0	0	0	2	27	-25	625	40	49.6	-9.58	91.8	
318	308	27	33.7	-6.69	44.7	27	10.3	16.7	280	0	0	0	0	34	29.5	4.45	19.8	0	0	0	0	9	17.3	-8.31	69.1	32	30.7	1.26	1.58	
-319	292	36	29.5	6.5	42.2	26	38.4	-12.4	153	0	0	0	0	14	20	-6.02	36.2	0	0	0	0	14	13.2	0.83	0.69	27	30.9	-3.9	15.2	
-278	353	42	42	-0.03	0	15	36.6	-21.6	464	0	0	0	0	13	19.3	-6.34	40.2	0	0	0	0	23	22.8	0.18	0.03	42	30	12	143	
-206	241	41	34.7	6.32	40	19	27.7	-8.69	75.5	0	0	0	0	10	14	-4.02	16.1	15	11.5	3.45	11.9	27	8.96	18	325	37	31.6	5.41	29.3	
-142	-135	49	33.9	15.1	227	23	15.4	7.55	57	0	7.95	-7.95	63.2	28	28.8	-0.84	0.71	0	0	0	0	2	11.5	-9.47	89.6	32	43.1	-11.1	123	
-105	115	28	29.3	-1.3	1.68	21	33.3	-12.3	150	0	0	0	0	12	16.2	-4.15	17.2	0	0	0	0	22	14.1	7.89	62.2	19	34.9	-15.9	253	
-46	362	29	29.6	-0.56	0.31	44	16.9	27.1	737	0	2.66	-2.66	7.08	36	23.9	12.1	146	0	0	0	0	2	20.5	-18.5	342	46	30.3	15.7	245	
43	-209	26	38.5	-12.5	157	42	32	10	101	0	0	0	0	11	26.4	-15.4	238	0	0	0	0	27	15	12	143	34	37.4	-3.4	11.6	
130	75	25	34.8	-9.82	96.4	47	28.9	18.1	326	0	0	0	0	35	18.7	16.3	267	0	2.62	-2.62	6.85	22	23.3	-1.25	1.56	15	42.2	-27.2	740	
215	-308	22	29.2	-7.16	51.2	19	27	-7.99	63.9	0	0	0	0	36	25.9	10.1	102	0	0	0	0	25	7.11	17.9	320	30	30.5	-0.47	0.22	
321	37	39	42	-3.03	9.17	14	24.7	-10.7	115	20	12.9	7.12	50.7	25	12	13	170	0	0	0	0	20	13.7	6.34	40.1	30	26.3	3.68	13.5	
-174	142	23	30.5	-7.46	55.6	23	39.2	-16.2	261	0	0	0	0	20	16.6	3.43	11.7	0	1.16	-1.16	1.35	0	15.8	-15.8	250	27	42.9	-15.9	253	
-99	41	22	43.4	-21.4	460	30	22.6	7.41	54.9	0	0	0	0	26	21.2	4.77	22.8	0	0	0	0	20	16	3.98	15.9	52	27.4	24.6	607	
-66	141	21	34	-13	168	33	18	15	226	0	0	0	0	10	19.3	-9.26	85.7	0	0	0	0	8	15.9	-7.93	62.9	36	29.2	6.82	46.5	
19	213	25	41.6	-16.6	276	48	20.6	27.4	751	0	0	0	0	25	25.3	-0.32	0.1	0	0	0	0	7	22	-15	225	18	23.8	-5.76	33.2	
83	383	36	29.6	6.45	41.6	25	39.4	-14.4	208	0	0	0	0	10	20.4	-10.4	109	0	0	0	0	27	8.77	18.2	332	44	44.6	-0.57	0.32	
141	-3	23	42.5	-19.5	381	36	42.3	-6.3	39.6	0	0	0	0	24	24.5	-0.52	0.27	0	0	0	0	13	11.9	1.14	1.29	15	28.4	-13.4	179	
194	45	43	36.5	6.52	42.5	17	39	-22	483	0	0	0	0	36	32.9	3.13	9.79	0	0	0	0	27	6.67	20.3	413	36	28.1	7.89	62.3	
261	-344	40	24.4	15.6	243	37	25.8	11.2	124	0	0	0	0	20	32	-12	145	0	0	0	0	3	10.4	-7.37	54.3	18	35.9	-17.9	320	
326	-209	29	36	-7.03	49.5	48	38.1	9.89	97.7	0	0	0	0	17	27.3	-10.3	105	10	8.62	1.38	1.9	17	7.54	9.46	89.4	52	34.5	17.5	305	
295	225	36	37.9	-1.91	3.63	14	38.3	-24.3	588	0	0	0	0	10	17.7	-7.68	59	0	0	0	0	22	12.2	9.79	95.8	16	25.9	-9.9	97.9	
$\sum d$	$\sum d^2$	-50.63785	5528.53338		57.311663	13671.3902	4.62505	403.059195	-34.92955	5390.88032	-14.753218	260.356888	-119.38965	9420.48813	-201.3781	10544.8219														
$(\sum d)^2$			2564.19185			3284.62672		21.3910875		1220.07346		217.657441		14253.8876		40553.1384														
\bar{d}			-0.8439642			0.95519438		0.07708417		-0.5821592		-0.245887		-1.9898274		-3.3563016														
S^2			92.9796076			230.790617		6.82546909		91.0261994		4.35134346		155.642768		167.270106														
S			9.64259341			15.1917944		2.61255987		9.54076514		2.08598741		12.4756871		12.9332945														
t(0.975)		1.96				1.96				1.96				1.96								1.96					1.96			
Left value			-3.2838769			-2.88886		-0.5839847		-2.9963058		-0.7737146		-5.1466118		-6.6288767														
Right value			1.59594861			4.79924874		0.73815302		1.8319875		0.28194067		1.16695695		-0.0837266														

Table 4.11: Difference between the interpolated depth from our model and the original survey depth from example three with all soil layer

Sample_3		Layer 1				Layer 2				Layer 3				Layer 4				Layer 5				Layer 6				Layer 7			
X	Y	D 1	D 2	D (2-1)	Sqr	D 1	D 2	D (2-1)	Sqr	D 1	D 2	D (2-1)	Sqr	D 1	D 2	D (2-1)	Sqr	D 1	D 2	D (2-1)	Sqr	D 1	D 2	D (2-1)	Sqr	D 1	D 2	D (2-1)	Sqr
-239	343	40	39.5	0.49	0.24	14	21.9	-7.85	61.7	0	0	0	0	30	13.8	16.2	263	0	4.53	-4.53	20.6	18	16.1	1.91	3.66	27	26	0.97	0.94
-217	-135	26	31	-4.96	24.6	39	15.7	23.3	542	15	8.18	6.82	46.6	27	31	-4	16	0	0	0	0	14	5.92	8.08	65.3	23	41.6	-18.6	344
-192	115	39	27.1	11.9	143	24	22.6	1.43	2.06	0	0	0	0	10	23.3	-13.3	177	0	0	0	0	19	13.7	5.3	28.1	53	33.9	19.1	365
-155	-22	45	36.7	8.27	68.4	30	14.3	15.7	247	0	0	0	0	34	20.2	13.8	192	0	0	0	0	1	15.4	-14.4	207	33	21.5	11.5	133
-112	232	37	35.6	1.36	1.84	41	22.9	18.1	327	0	0	0	0	30	27.6	2.43	5.9	0	0	0	0	1	13.2	-12.2	149	30	48.1	-18.1	327
-89	-233	24	37.3	-13.3	176	30	19.1	10.9	119	10	10.4	-0.37	0.14	28	22.7	5.33	28.4	0	0	0	0	10	24.8	-14.8	219	46	31.3	14.7	215
-17	-360	42	36.5	5.54	30.7	17	36.5	-19.5	381	0	0	0	0	25	28.2	-3.23	10.5	0	0	0	0	13	19.7	-6.75	45.5	29	40	-11	122
32	202	40	43.5	-3.51	12.3	31	20.4	10.6	113	0	0	0	0	16	25.9	-9.91	98.2	0	0.61	-0.61	0.37	18	21.1	-3.1	9.62	30	21.3	8.75	76.5
57	77	26	36.7	-10.7	114	35	40.2	-5.16	26.6	0	0	0	0	27	34.7	-7.73	59.7	12	7.06	4.94	24.4	5	7.96	-2.96	8.76	25	28	-3.04	9.22
115	355	48	33.8	14.2	201	23	41	-18	324	0	5.06	-5.06	25.6	26	23.4	2.6	6.75	0	0	0	0	8	17.7	-9.73	94.6	32	38.1	-6.1	37.2
-332	143	47	45.3	1.72	2.95	40	17	23	527	0	0	0	0	30	30.7	-0.7	0.48	0	0	0	0	6	14.4	-8.44	71.3	36	36.8	-0.85	0.72
-329	-48	24	31.7	-7.66	58.7	11	31.2	-20.2	408	0	0	0	0	29	19.8	9.18	84.2	0	0	0	0	4	9.28	-5.28	27.8	43	34.8	8.23	67.7
-220	-333	24	43	-19	361	17	13.9	3.13	9.82	0	0	0	0	30	32.1	-2.06	4.24	0	0	0	0	10	11.1	-1.06	1.11	39	21.4	17.6	309
-186	-65	41	36.2	4.78	22.9	32	16.2	15.8	251	0	0	0	0	11	29.4	-18.4	339	0	0	0	0	29	8.4	20.6	424	34	29.8	4.22	17.8
-149	-230	45	41.2	3.76	14.2	11	13.6	-2.63	6.91	29	23	6	36	16	20.7	-4.69	22	0	0	0	0	14	17.1	-3.07	9.43	20	47.1	-27.1	734
-97	204	42	36.3	5.68	32.2	15	33.1	-18.1	328	0	0	0	0	21	23.4	-2.42	5.88	0	0.19	-0.19	0.03	15	7.2	7.8	60.8	18	45.3	-27.3	744
-58	-214	43	32.1	10.9	118	15	38.6	-23.6	556	0	3.36	-3.36	11.3	19	28.5	-9.53	90.8	0	0	0	0	29	16.9	12.1	147	17	38.3	-21.3	453
-47	147	31	23.9	7.11	50.6	15	32.9	-17.9	321	0	0	0	0	19	15.1	3.91	15.3	0	0.82	-0.82	0.68	10	8.96	1.04	1.08	27	35.7	-8.69	75.5
13	-245	23	44.7	-21.7	473	46	27.1	18.9	357	0	0	0	0	18	28.5	-10.5	110	0	0	0	0	3	24.4	-21.4	457	22	27.9	-5.9	34.8
45	415	41	39.7	1.29	1.68	0	-0	0	0	0	0	0	0	39	23.3	15.7	247	0	0	0	0	29	17.2	11.8	138	26	47.4	-21.4	459
-42	277	35	40.9	-5.91	35	41	18	23	530	0	6.43	-6.43	41.4	29	29.8	-0.83	0.68	0	0	0	0	22	20.7	1.31	1.71	33	26.1	6.9	47.6
8	53	32	28.9	3.08	9.5	38	33.6	4.39	19.3	0	0	0	0	33	24.8	8.22	67.6	15	15.1	-0.07	0.01	2	16.5	-14.5	209	35	38.8	-3.83	14.7
47	32	30	35.2	-5.22	27.2	45	40.1	4.87	23.7	0	0	0	0	34	21	13	170	7	15.3	-8.28	68.5	2	6.92	-4.92	24.2	46	38.5	7.5	56.3
83	383	36	29.6	6.45	41.6	25	39.4	-14.4	208	0	0	0	0	10	20.4	-10.4	109	0	0	0	0	27	8.77	18.2	332	44	44.6	-0.57	0.32
130	175	33	29.6	3.44	11.8	48	36.9	11.1	123	0	0	0	0	31	22	8.99	80.8	0	0	0	0	2	25.9	-23.9	569	24	33.2	-9.21	84.9
157	-135	41	44.9	-3.93	15.4	11	45.4	-34.4	1183	0	0	0	0	20	23.4	-3.44	11.8	0	0	0	0	1	21.9	-20.9	438	16	39.3	-23.3	544
195	340	37	41.7	-4.75	22.6	41	20.6	20.4	418	0	0	0	0	10	27.4	-17.4	303	0	0	0	0	8	9.89	-1.89	3.56	49	33.8	15.2	232
231	-90	40	36.9	3.09	9.55	17	29.3	-12.3	152	0	0	0	0	39	17.6	21.4	459	0	7.95	-7.95	63.1	28	16.2	11.8	139	53	40	13	168
254	94	28	35.3	-7.32	53.5	24	20.8	3.23	10.4	0	0.14	-0.14	0.02	20	20.5	-0.53	0.29	0	0	0	0	2	27	-25	625	40	49.6	-9.58	91.8
277	-121	22	34.3	-12.3	150	27	23.6	3.36	11.3	0	0.2	-0.2	0.04	24	19.9	4.1	16.8	20	14.5	5.46	29.8	4	19	-15	225	23	44.9	-21.9	480
-327	-257	49	28.7	20.3	413	11	10.7	0.28	0.08	0	0	0	0	12	24.9	-12.9	166	0	0	0	0	7	14.9	-7.86	61.7	26	41	-15	224
-290	320	32	37.5	-5.49	30.1	44	39.6	4.43	19.6	0	0	0	0	21	21.1	-0.12	0.01	0	3.99	-3.99	15.9	10	18.7	-8.73	76.3	21	33.2	-12.2	149
-186	-65	41	36.2	4.78	22.9	32	16.2	15.8	251	0	0	0	0	11	29.4	-18.4	339	0	0	0	0	29	8.4	20.6	424	34	29.8	4.22	17.8
-106	-30	45	39.2	5.8	33.6	14	22	-7.99	63.8	0	0	0	0	22	32.6	-10.6	113	0	2.47	-2.47	6.09	9	13.9	-4.9	24	18	34.5	-16.5	273
8	53	32	27	5	25	38	35.4	2.6	6.76	0	0	0	0	33	29.6	3.43	11.8	15	12	2.97	8.8	2	14.6	-12.6	160	35	41.6	-6.59	43.4
42	99	43	28.1	14.9	221	36	32.2	3.8	14.4	0	0	0	0	35	24.8	10.2	103	9	9.27	-0.27	0.07	7	7.02	-0.02	0	23	25.8	-2.79	7.76

Sample_3		Layer 1				Layer 2				Layer 3				Layer 4				Layer 5				Layer 6				Layer 7			
X	Y	D 1	D 2	D (2-1)	Sqr	D 1	D 2	D (2-1)	Sqr	D 1	D 2	D (2-1)	Sqr	D 1	D 2	D (2-1)	Sqr	D 1	D 2	D (2-1)	Sqr	D 1	D 2	D (2-1)	Sqr	D 1	D 2	D (2-1)	Sqr
127	307	41	37.6	3.41	11.6	47	29.2	17.8	317	11	0	11	121	30	22.1	7.89	62.2	0	0	0	0	19	14.1	4.86	23.6	33	31.9	1.13	1.29
209	-306	29	22.3	6.7	44.8	27	20.5	6.54	42.7	0	0	0	0	26	25.7	0.27	0.07	0	0	0	0	7	25.9	-18.9	356	32	35.4	-3.37	11.4
254	94	28	35.3	-7.32	53.5	24	20.8	3.23	10.4	0	0.14	-0.14	0.02	20	20.5	-0.53	0.29	0	0	0	0	2	27	-25	625	40	49.6	-9.58	91.8
318	308	27	33.7	-6.69	44.7	27	10.3	16.7	280	0	0	0	0	34	29.5	4.45	19.8	0	0	0	0	9	17.3	-8.31	69.1	32	30.7	1.26	1.58
-319	292	36	29.5	6.5	42.2	26	38.4	-12.4	153	0	0	0	0	14	20	-6.02	36.2	0	0	0	0	14	13.2	0.83	0.69	27	30.9	-3.9	15.2
-278	353	42	42	-0.03	0	15	36.6	-21.6	464	0	0	0	0	13	19.3	-6.34	40.2	0	0	0	0	23	22.8	0.18	0.03	42	30	12	143
-206	241	41	34.7	6.32	40	19	27.7	-8.69	75.5	0	0	0	0	10	14	-4.02	16.1	15	11.5	3.45	11.9	27	8.96	18	325	37	31.6	5.41	29.3
-142	-135	49	33.9	15.1	227	23	15.4	7.55	57	0	7.95	-7.95	63.2	28	28.8	-0.84	0.71	0	0	0	0	2	11.5	-9.47	89.6	32	43.1	-11.1	123
-105	115	28	29.3	-1.3	1.68	21	33.3	-12.3	150	0	0	0	0	12	16.2	-4.15	17.2	0	0	0	0	22	14.1	7.89	62.2	19	34.9	-15.9	253
-46	362	29	29.6	-0.56	0.31	44	16.9	27.1	737	0	2.66	-2.66	7.08	36	23.9	12.1	146	0	0	0	0	2	20.5	-18.5	342	46	30.3	15.7	245
43	-209	26	38.5	-12.5	157	42	32	10	101	0	0	0	0	11	26.4	-15.4	238	0	0	0	0	27	15	12	143	34	37.4	-3.4	11.6
130	75	25	34.8	-9.82	96.4	47	28.9	18.1	326	0	0	0	0	35	18.7	16.3	267	0	2.62	-2.62	6.85	22	23.3	-1.25	1.56	15	42.2	-27.2	740
215	-308	22	29.2	-7.16	51.2	19	27	-7.99	63.9	0	0	0	0	36	25.9	10.1	102	0	0	0	0	25	7.11	17.9	320	30	30.5	-0.47	0.22
321	37	39	42	-3.03	9.17	14	24.7	-10.7	115	20	12.9	7.12	50.7	25	12	13	170	0	0	0	0	20	13.7	6.34	40.1	30	26.3	3.68	13.5
-174	142	23	30.5	-7.46	55.6	23	39.2	-16.2	261	0	0	0	0	20	16.6	3.43	11.7	0	1.16	-1.16	1.35	0	15.8	-15.8	250	27	42.9	-15.9	253
-99	41	22	43.4	-21.4	460	30	22.6	7.41	54.9	0	0	0	0	26	21.2	4.77	22.8	0	0	0	0	20	16	3.98	15.9	52	27.4	24.6	607
-66	141	21	34	-13	168	33	18	15	226	0	0	0	0	10	19.3	-9.26	85.7	0	0	0	0	8	15.9	-7.93	62.9	36	29.2	6.82	46.5
19	213	25	41.6	-16.6	276	48	20.6	27.4	751	0	0	0	0	25	25.3	-0.32	0.1	0	0	0	0	7	22	-15	225	18	23.8	-5.76	33.2
83	383	36	29.6	6.45	41.6	25	39.4	-14.4	208	0	0	0	0	10	20.4	-10.4	109	0	0	0	0	27	8.77	18.2	332	44	44.6	-0.57	0.32
141	-3	23	42.5	-19.5	381	36	42.3	-6.3	39.6	0	0	0	0	24	24.5	-0.52	0.27	0	0	0	0	13	11.9	1.14	1.29	15	28.4	-13.4	179
194	45	43	36.5	6.52	42.5	17	39	-22	483	0	0	0	0	36	32.9	3.13	9.79	0	0	0	0	27	6.67	20.3	413	36	28.1	7.89	62.3
261	-344	40	24.4	15.6	243	37	25.8	11.2	124	0	0	0	0	20	32	-12	145	0	0	0	0	3	10.4	-7.37	54.3	18	35.9	-17.9	320
326	-209	29	36	-7.03	49.5	48	38.1	9.89	97.7	0	0	0	0	17	27.3	-10.3	105	10	8.62	1.38	1.9	17	7.54	9.46	89.4	52	34.5	17.5	305
295	225	36	37.9	-1.91	3.63	14	38.3	-24.3	588	0	0	0	0	10	17.7	-7.68	59	0	0	0	0	22	12.2	9.79	95.8	16	25.9	-9.9	97.9
$\sum d$	-359.2	$\sum d^2$	45220	$(\sum d)^2$	128990	\bar{d}	-0.855	S^2	107.19	\bar{S}	10.353	t(0.975)	1.96	Leftvalue	-1.845	Rightvalue	0.135												

Table 4.12: Difference between the interpolated depth from our model and the original survey depth from example one, two and three

Data set	Layer 1	Layer 2	Layer 3	Layer 4	Layer 5	Layer 6	Layer 7
Sample1 (30 boleholes/layer)	∞	∞	∞	∞	∞	∞	∞
Left value	-2.791	-4.742	-3.625	-8.958	0	-1.859	-3.616
Right value	3.1941	6.3688	3.3531	1.082	0	6.0677	4.8108
Sample2 (30 boleholes/layer)	∞	∞	∞	∞	∞	∞	∞
Left value	-4.281	-4.782	-11.89	-9.127	0	-3.693	-7.883
Right value	0.9276	5.7607	-0.323	2.2072	0	7.1868	0.5882
Sample3 (60 boleholes/layer)	∞	∞	∞	∞	∞	∞	∞
Left value	-3.284	-2.889	-0.584	-2.996	-0.774	-5.147	-6.629
Right value	1.5959	4.7992	0.7382	1.832	0.2819	1.167	-0.084

4.1.4.3 Soil Layer Volume Comparison

In the test, we will compare the volume of each soil layer from the image created by the program, with the initially created data to show if there is any difference between the soil volume estimated by the program and the actual volume.

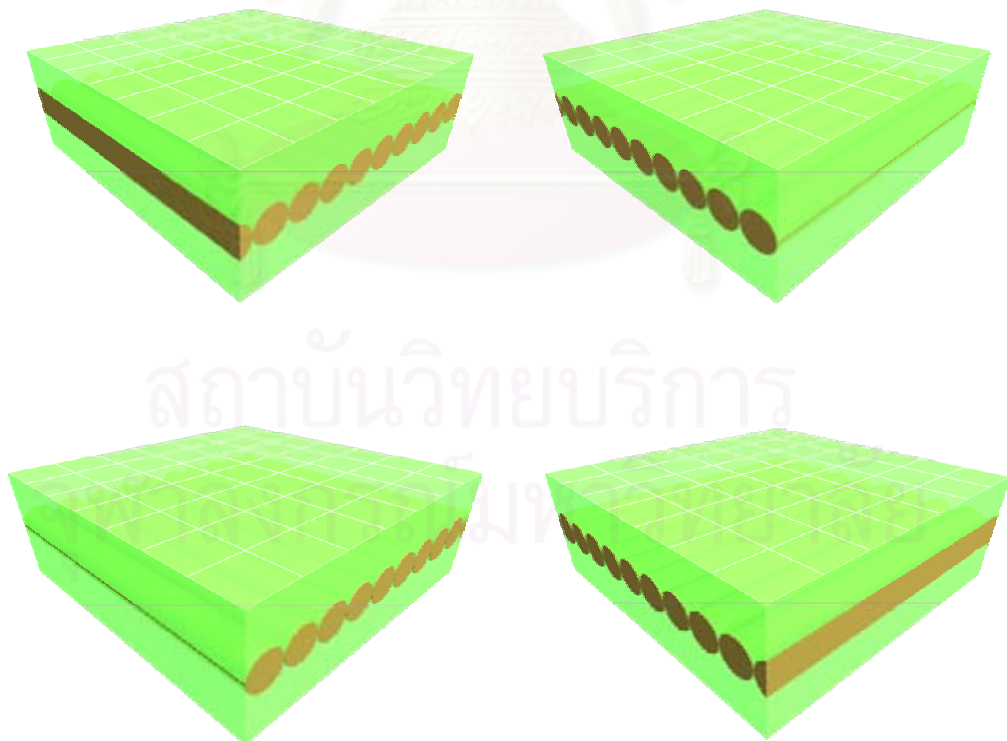


Figure 4.9: Soil layer model in example 1 from all four sides

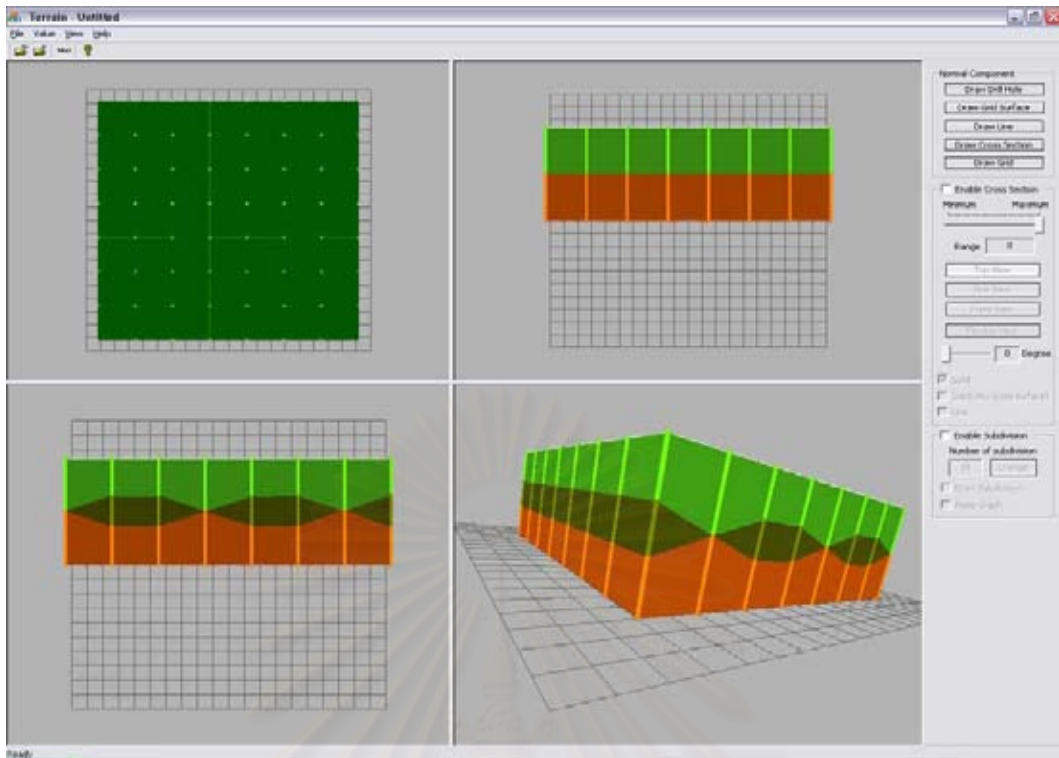


Figure 4.10: Soil layer model after computation with small number of boreholes in example 1

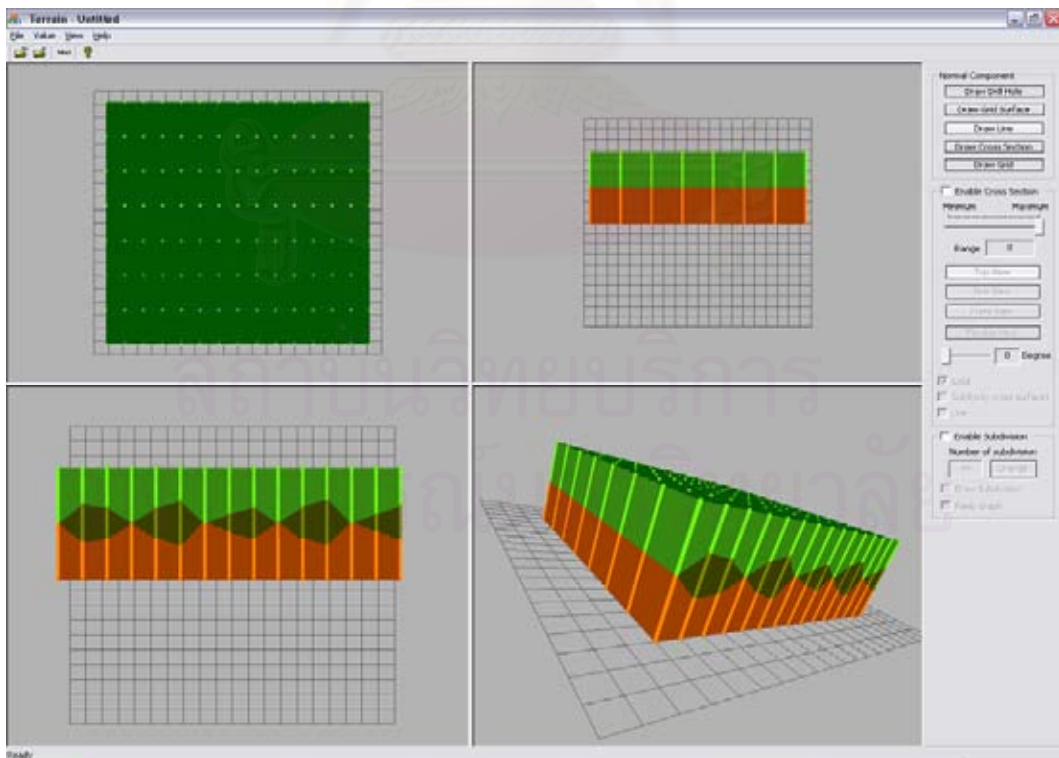


Figure 4.11: Soil layer model after computation with large number of boreholes in example 1

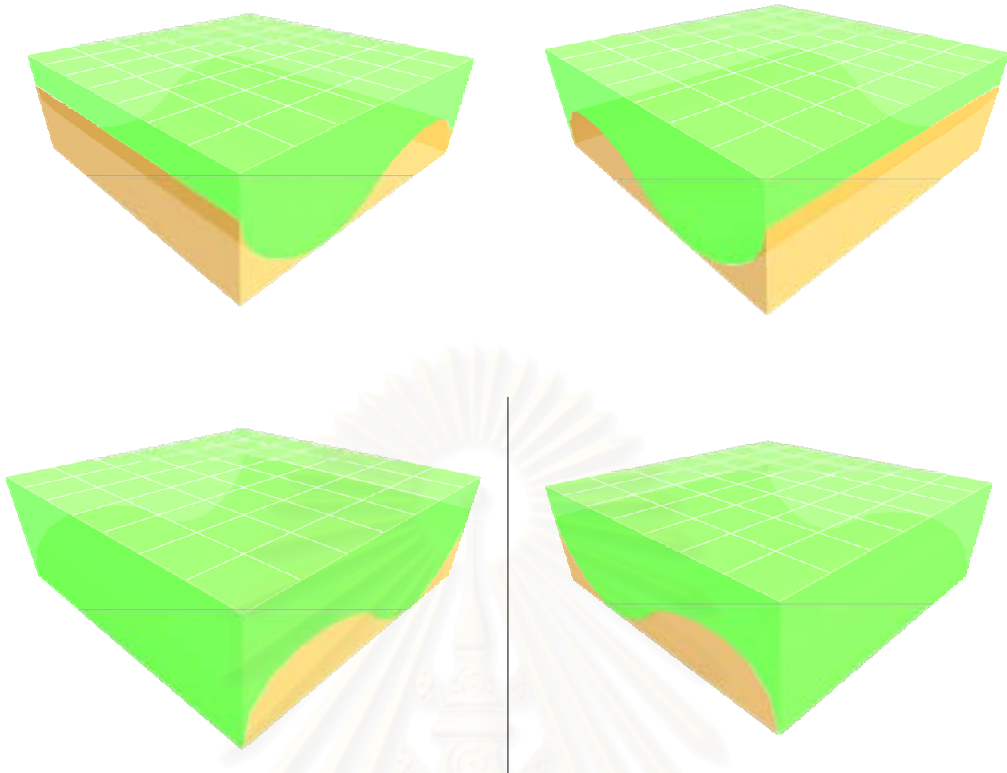


Figure 4.12: Soil layer model in example 2 from all four sides

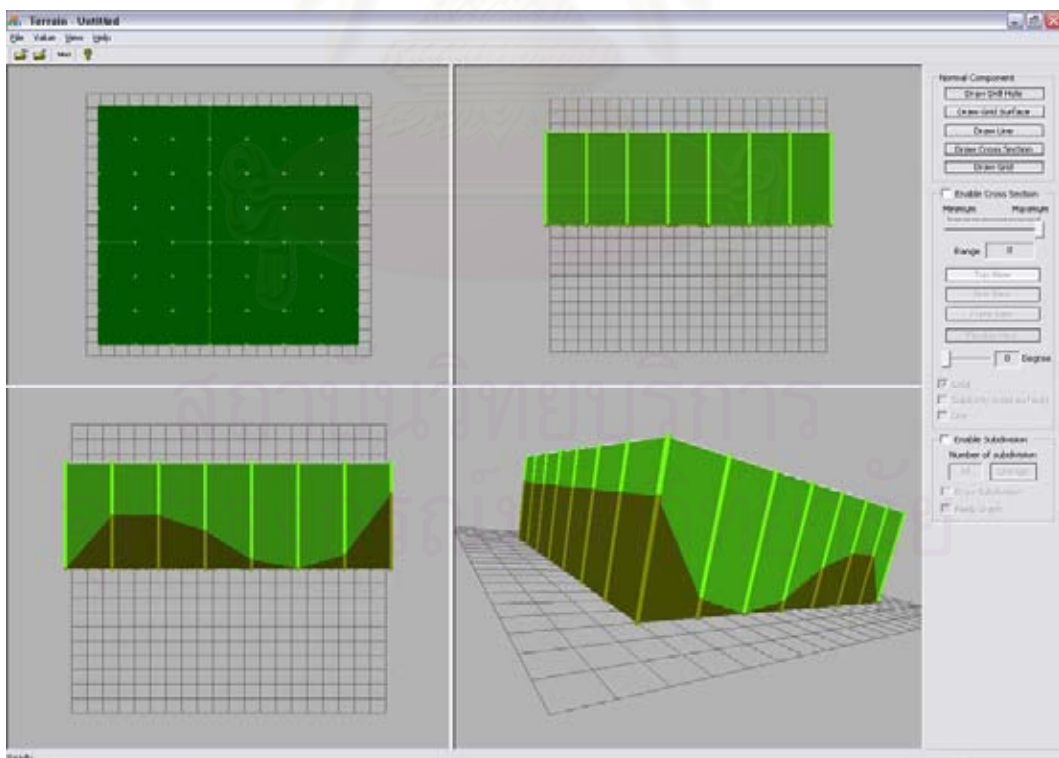


Figure 4.13: Soil layer model after computation with small number of boreholes in example 2

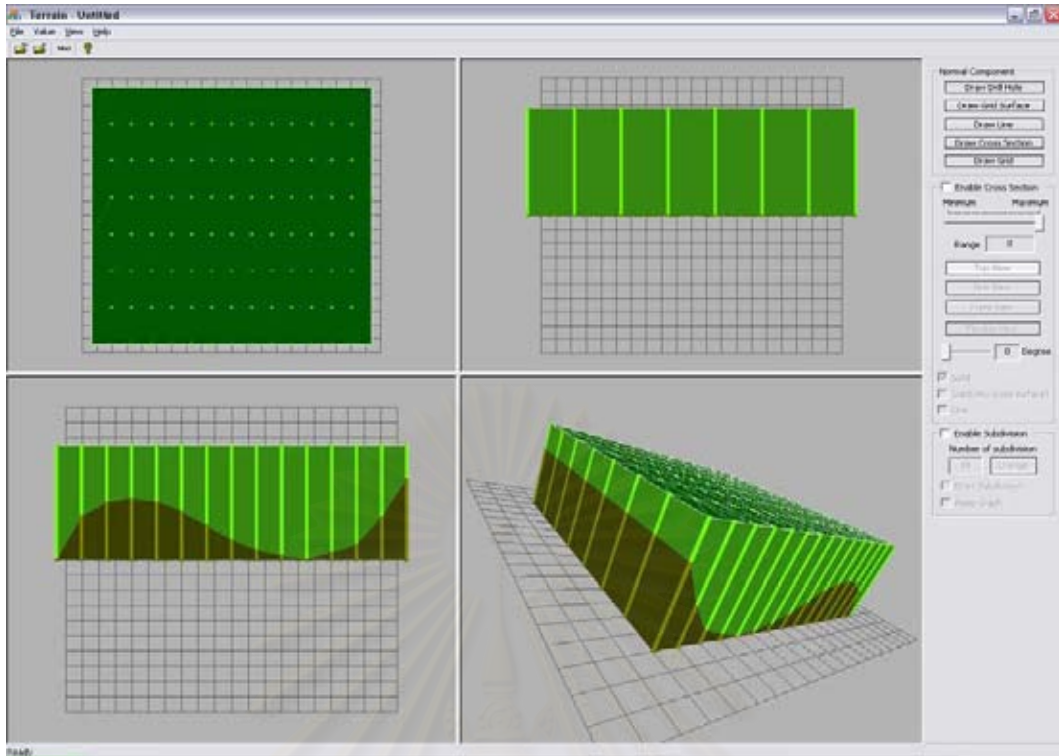


Figure 4.14: Soil layer model after computation with large number of boreholes in example 2

In example 1 from figure 4.9-4.11, the estimated volume differs from the actual model from the imported data. The actual volume of the actual data in figure 4.9 is 2990720 m^3 , 1858561 m^3 and 2990720 m^3 . However, the volume estimated from small amount of boreholes in figure 4.10 is 3201710 m^3 , 1423441 m^3 and 3215855 m^3 respectively. Moreover, the volume estimated from large amount of boreholes in figure 4.11 is 3146455 m^3 , 1541584 m^3 and 3151958 m^3 respectively.

In example 2 from figure 4.12-4.14, the estimated volume differs from the actual model from the imported data. The actual volume of the actual data in figure 4.12 is 5727577 m^3 and 2112422 m^3 . However, the volume estimated from small amount of boreholes in figure 4.13 is 5696091 m^3 and 2143909 m^3 respectively. Moreover, the volume estimated from large amount of boreholes in figure 4.14 is 5702192 m^3 and 2137809 m^3 respectively.

From example, one, two the difference of the estimated volume from the actual data is dependent on the number of boreholes. If there are enough boreholes, it will make the estimation of various positions on the soil layer more accurate, resulting in a better estimate especially for complex arrangement of layers. The accurate of the estimation depends on the number of boreholes, and the interpolation function.

4.2 Sample Results

From figure 4.15 shows creating a model of the soil layer with delaunay triangulation. From figure 4.16 shows creating a model of the soil layers that we can see the internal structure from many angles. From figure 4.17 shows retrieval of internal structure visible from 360 degrees. From figure 4.18 shows retrieval of the internal structure, which can be viewed as a top-view of the geological surface, or as a countour of each layer. From figure 4.19 shows retrieval of the internal structure, this can be viewed as a side-view of the geological surface. From figure, 4.20 shows splitting parts of the geological surface by the depth of the layers, which we can specify, the level of splitting. From figure 4.21 shows the bulding the Reb graph of the geological surface.

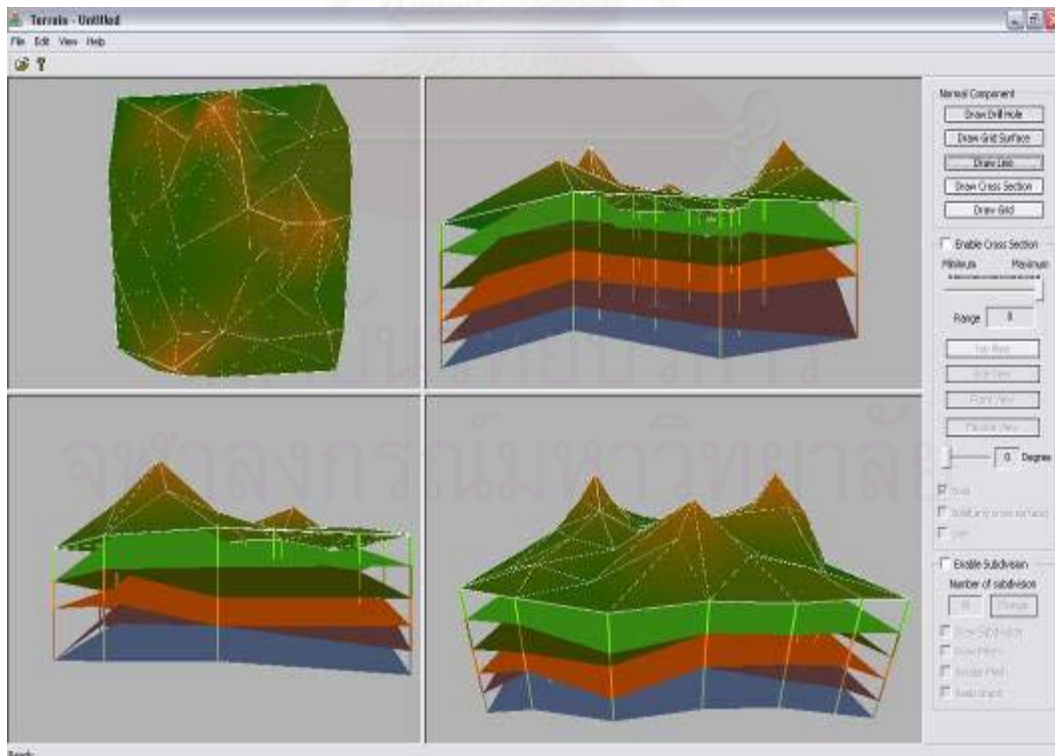


Figure 4.15: Mesh layers of soil layers

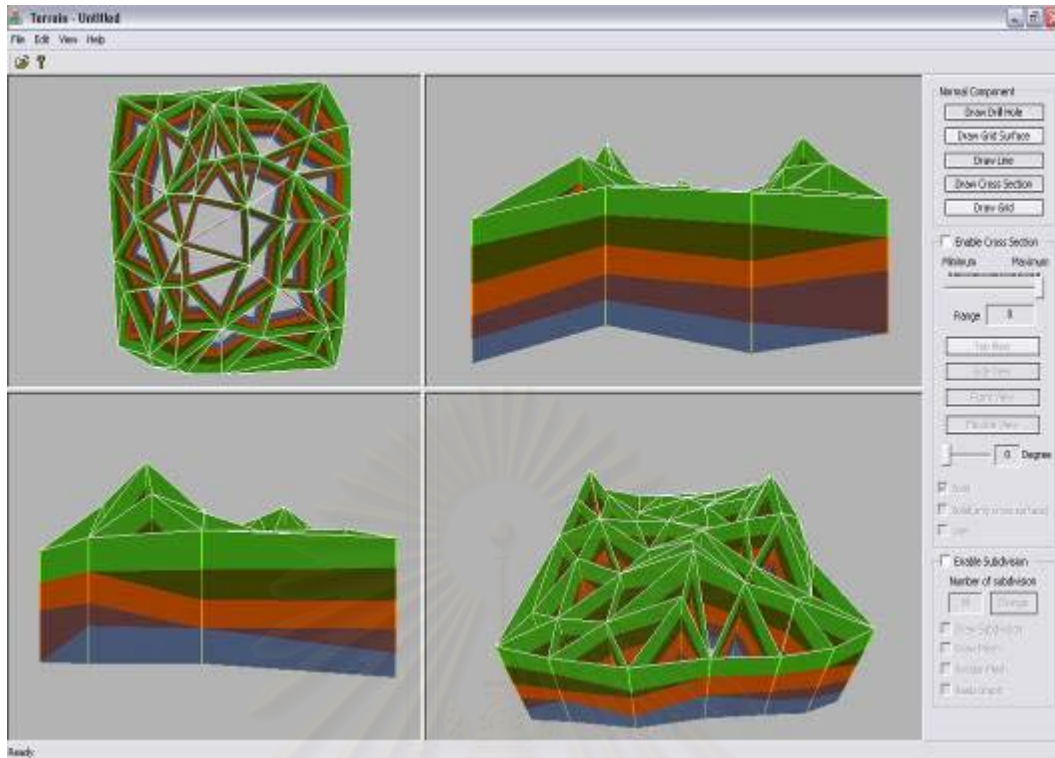


Figure 4.16: Internal structure of soil layers

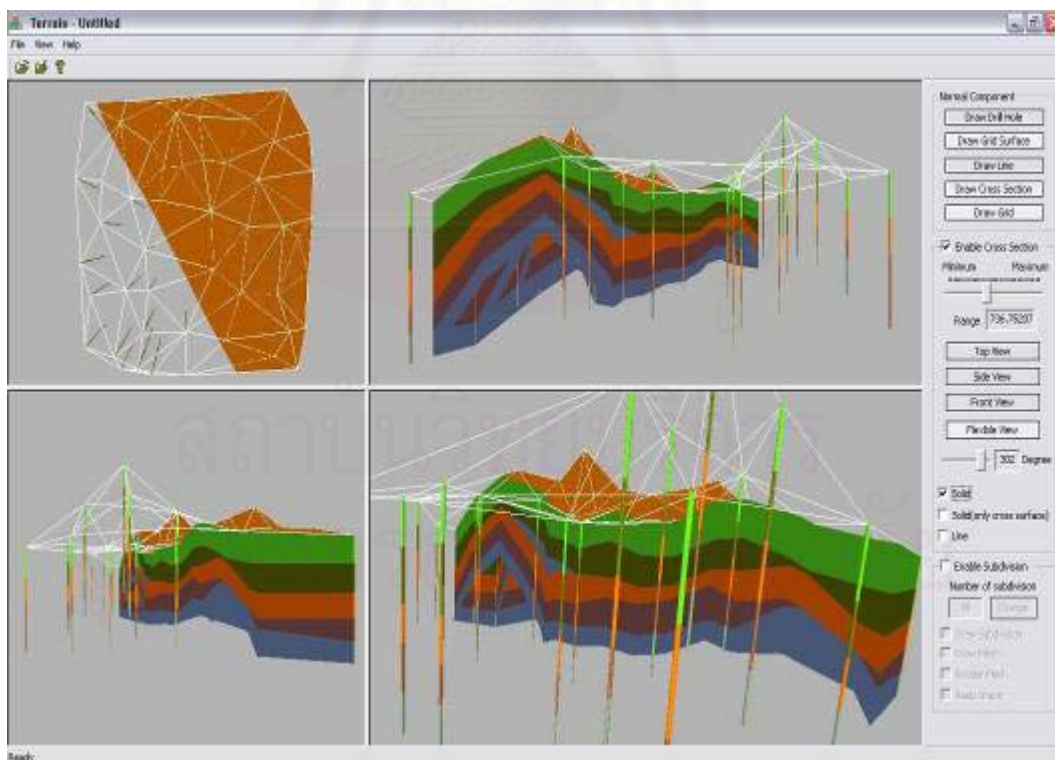


Figure 4.17: Another view of internal structure of soil layers

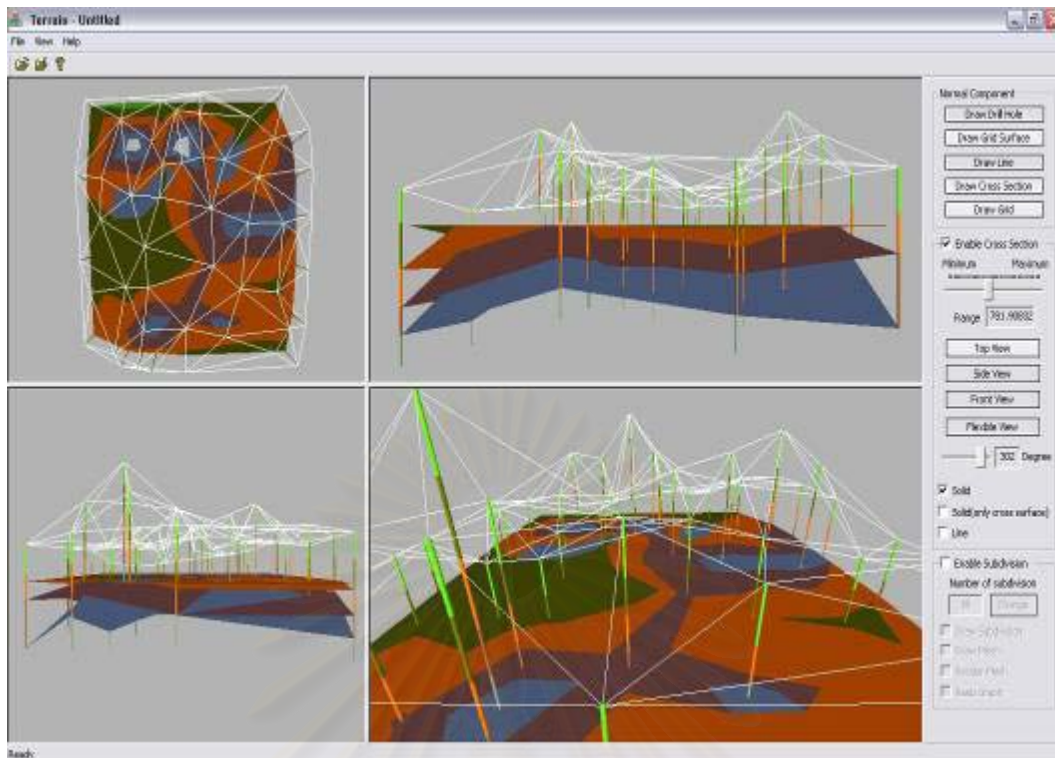


Figure 4.18: Cross-sectional top view of soil layers

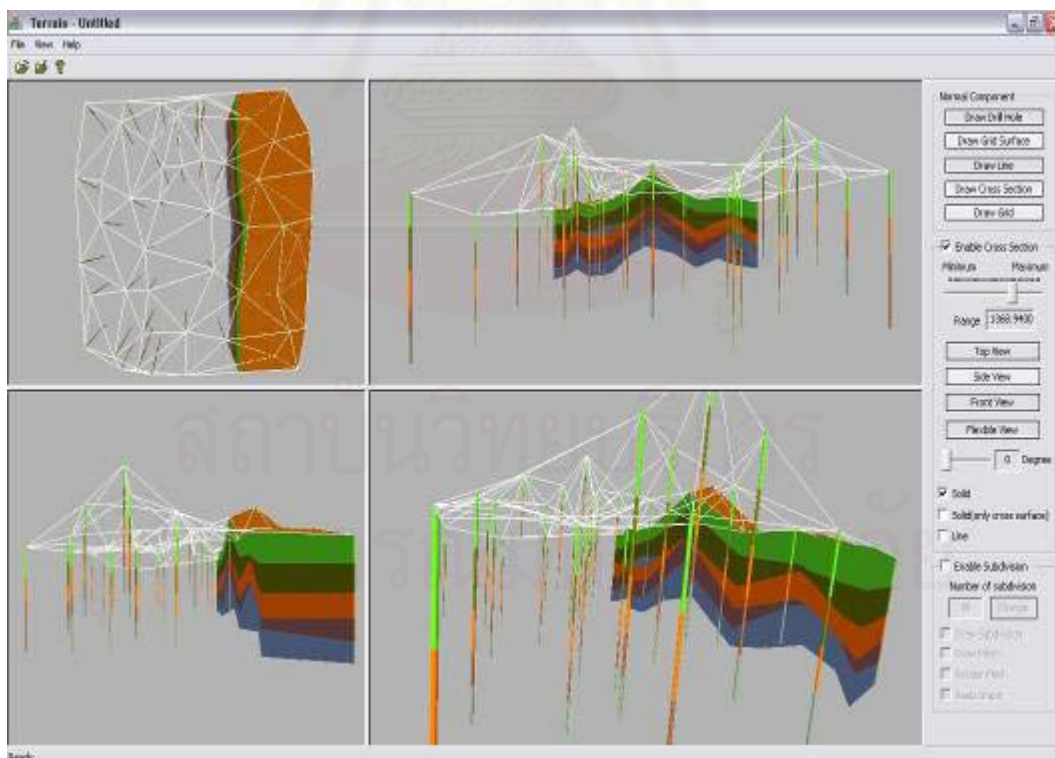


Figure 4.19: Cross-sectional side view of soil layers

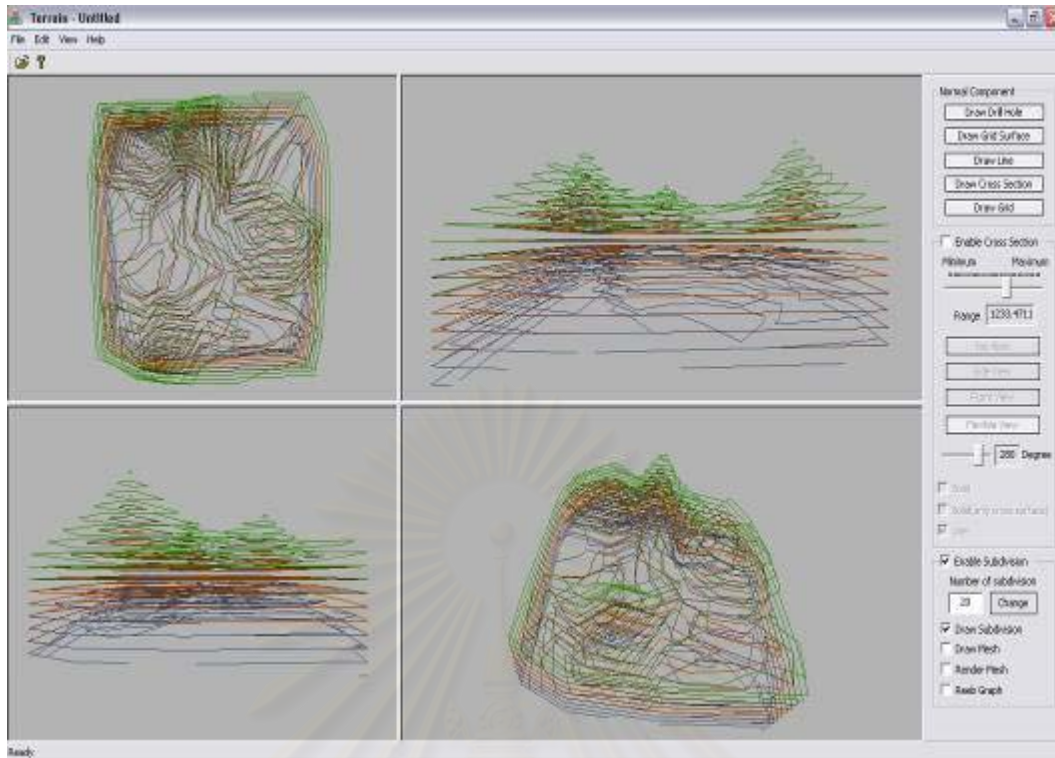


Figure 4.20: Subdivision of soil layer shown with 20 layers



Figure 4.21: Reeb graph for subdivision with 20 layers

4.3 Discussion

Results from testing the z hypothesis show that 90% of the borehole depth estimates are not significantly different from the actual data, with 95% confidence, in all three examples. This shows that the linear approximation can be used with such data. The only data with significant differences is layer 3 in table 4.3 and layer 7 in table 4.4. It should be noted that this is an area where the layers are not organized as usual, but with a small layer in between, as in figure 4.22. The results show that the inaccuracy in estimation results from a different arrangement of soil layers than in other areas. However, from table 4.3 and table 4.4 one sees that the average difference in testing is not significantly different from the actual data. Considering the data of each borehole, it shows that estimating the soil layers with the enhanced Reeb graph model provides estimates close the actual data on average.

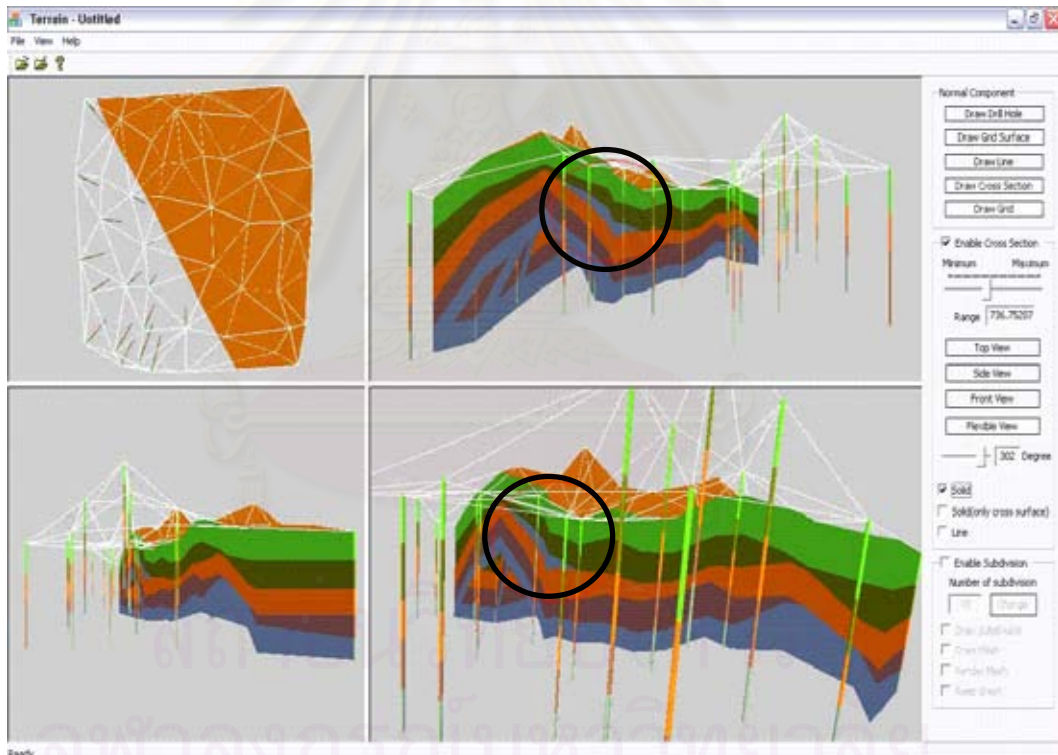


Figure 4.22: Different arrangement of soil layers

From finding the average difference between the estimates and the actual data with statistical estimation in tables 4.6-4.11. We reach the conclusion that the difference of the data is near zero for almost every pair, following the hypothesis tested with the z test. Some pairs of boreholes have a negative bottom and top confidence, which may

results from the soil layer between the usual layers in figure 4.22, which may conclude that the inaccuracy in linear estimation may be insufficient data.

Time capacity

Procedure of creating delaunay triangulation can use speed of evaluate surface reconstruction of hydrogeological information is $O(n \log n)$.

The Delaunay Triangulation of a set P of n points in the plane can be computed in $O(n \log n)$ time, using $O(n)$ space.

$T(n)$ = Time spent on point location + Time to create the expected number of triangles

$$T(n) = O(n \log n) + O(n)$$

$$T(n) = O(n \log n + n)$$

$$T(n) = O(n \log n)$$

Define amount of many boreholes that create properly relations between the joins in soil layers and boreholes.

Limitation of this research

The estimation used with the reeb graph in this resetch uses linear estimation. Although it produces good results with the sample data, some cases may require high degree estimation functions, on a case-by-case basis. The enhanced Reeb graph model we have presented can be used with other estimations other than linear functions. Also, the accuracy with the presented model depends on the amount of input data, because the model depends on the relations between soil layers in each borehole for estimation. This makes the estimation for any position depend on all other positions.

CHAPTER V

CONCLUSION AND FUTURE WORK

This section concludes the thesis and provides some discussion on the experimental results. Future works are also suggested.

5.1 Conclusion

An enhanced Reeb graph proposed in this thesis is an extension of a Reeb graph on a height function. This system utilizes the graph as the skeleton of an object because an enhanced Reeb graph has both topological and geometrical information. The Reeb editor defines this graph easily. Homotopy is the very powerful means to create surfaces from the cross-sectional planes. Surfaces can be constructed from information of both the enhanced Reeb graphs and homotopy.

This research presents a 3D model of multi-layer geographical information, which properly displays the internal structure of the data, for use in effective analysis of hydrological and geological information, and a method to approximate the height of the soil layer as well as properly categorize the soil layers, to create proper relations between soil layers and drill holes.

From the experiment, we find that the accuracy of the enhanced Reeb graph in estimating position and volume of soil layers depends on the number of boreholes and the interpolation function, in other words, it Requires specifying the number of boreholes and the function that actually corresponds to the complexity of the soil layers of the input data, which requires water resource engineering knowledge.

5.2 Future Work

The presented model can be improved in the creation of multi-layer surfaces to improve the detail and realism, by other methods of interpolation such as Non Uniform Rational B-Spline (NURBS), Catmull-Rom Spline homotopy which can construct natural surfaces or using the brightness of light to create the surface, or using subdivision surfaces for more detail. Moreover, the model can be improved in the surface reconstruction with many data.

REFERENCES

- [1]. G. L. Miller, Steven E. Pav and N. J. Walkington. Fully Incremental 3D Delaunay Refinement Mesh Generation. Proceedings, 11th International Meshing Roundtable, Sandia National Laboratories (15-18 September, 2002): 75-86.
- [2]. L. Demaret, N. Dyn, Michael S. Floater, and A. Iske. Adaptive Thinning for Terrain Modelling and Image Compression. Journal of Computational and Applied Mathematics 145 (August 2002, 2004): 505–517.
- [3]. L. Nonato, R. Minghim, M. C. F. Oliveira, and G. Tavares. A Novel Approach for Delaunay 3D Reconstruction with a Comparative Analysis in the Light of Applications. Computer Graphics Forum 20 2 (June 2001).
- [4]. O. G. Staadt, M. H. Gross, and R. Weber. Multiresolution compression and reconstruction. Proceedings of the 8th conference on Visualization '97 Phoenix Arizona United States (1997): 337-346.
- [5]. S. Baloch, H. Krim, I. Kogan, and D. Zenkov. Rotation Invariant Topology Coding of 2D and 3D Objects Using Morse Theory. International Conference on Image Processing (ICIP05) (2005).
- [6]. T. Nieda, A. Pasko, and T.L. Kunii. Detection of critical points for shape metamorphosis animation. 10th International Multimedia Modelling Conference (MMM) (2004): 93-100.
- [7]. Y. Shinagawa, T.L. Kunii, and Y.L. Kergosien. Surface coding based on Morse theory. Computer Graphics and Applications, IEEE 11 (1991): 66-78.
- [8]. K. Cole-McLaughlin, H. Edelsbrunner, J. Harer, V. Natarajan, and V. Pascucci. Loops in Reeb graphs of 2-manifolds. ACM Symposium on Computational Geometry (2003): 344-350.
- [9]. R. Abraham, J.E. Marsden and T. Ratiu. Manifolds, Tensor Analysis and Applications. Springer-Verlag (1988).
- [10]. J. Milnor. Morse Theory. Princeton University Press (1963).
- [11]. A.B. Hamza and H. Krim, Topological modeling of illuminated surfaces using Reeb graph. International Conference on Image Processing (ICIP 2003) 1 (14-17 September, 2003): 769-772.

- [12]. P. Kanonchayos, T. Nishita, S. Yoshihisa, and T.L. Kunii. Topological morphing using Reeb graphs. Cyber Graphics, Proceedings of the First International Symposium on Cyber Worlds (CW 2002) (2002).
- [13]. S. Dumrongkittikul, T. Tirasirachai, A. Jongjarernmongkol, and P. Kanongchaiyos. 3D Object Reconstruction System Using Cross-sectional Data. Presented at 1th International forum on Animation and Multimedia in TAM2005 (2005).
- [14]. S. Biasotti. Reeb graph representation of surfaces with boundary. International Conference on Shape Modeling and Applications (SMI 2004), IEEE Computer Society Genova, Italy (7-9 June 2004).
- [15]. Y. Shinagawa and T.L. Kunii. Constructing a Reeb graph automatically from cross sections. Computer Graphics and Applications, IEEE 11 (1991): 44-51.
- [16]. S. Tamura. Homotopy modeling based on enhanced Reeb graph. Senior of Department of Information Science Faculty of Science University of Tokyo (1997).
- [17]. Y. Shinagawa and T.L. Kunii. The Homotopy Model: A Generalized Model for Smooth Surface Generation from Cross Sectional Data. Visual Computer 7 3 (1991): 72-86.
- [18]. James H. Clark. Parametric Curves, Surfaces and Volumes in Computer Graphics and Computer-Aided Geometric Design. Technical Report 221 Computer Systems Laboratory, Departments of Electrical Engineering and Computer Science, Stanford University, Stanford, California 94305 (Nov 1981).
- [19]. Catmull Edwin and Rom Raphael, A class of local interpolating splines, in R.E Barnhill and R.F. Riesenfeld (eds.) Computer Aided Geometric Design. Academic Press (1974): 317-326.
- [20]. Phillip J. Barry and Ronald N. Goldman. A Recursive Evaluation Algorithm for a class of Catmull-Rom Splines. ACM Computer Graphics 22 4 (August 1988): 199-204.
- [21]. Fuchs.H, Z.M. Kedem and S.P. Uselton. Optimal Surface Reconstruction from Planar Contours. Communications ACM 20 (1977): 693-702.
- [22]. Christiansen HN and Sederberg TW. Conversion of complex contour line definitions into polygonal element mosaics. Comput.Graph 12 (1978): 187-192.

- [23]. Y. Shinagawa. A Study of a Surface Construction System Based on Morse Theory and Reeb Graph. PhD thesis Department of Information Science, Faculty of Science University of Tokyo (1992).
- [24]. L. A. Treinish. Interactive, Web-Based Three-Dimensional Visualizations of Operational Mesoscale Weather Models.
- [25]. S. Biasotti, B. Falcidieno, and M. Spagnuolo. Extended Reeb Graphs for Surface Understanding and Description. Proceedings of the 9th International Conference on Discrete Geometry for Computer Imagery (2000): 185-197.
- [26]. Bernd Hamann and Jiann-Liang Chen, Data Point selection for piecewise linear curve approximation. Computer Aided Geometric Design 11 3 (1994): 289-301.
- [27]. Gerald Farin. Curves and Surfaces for Computer-Aided Geometric Design. Academic Press 4 (1997)
- [28]. H. Pottmann, S. Leopoldseder, and M. Hofer. Approximation with active B-spline curves and surfaces. 10th Pacific Conference on Computer Graphics and Applications (PG'02) (2002): 8-25.
- [29]. S. Biasotti. Topological techniques for shape understanding. Central European Seminar on Computer Graphics (CESCG 2001) (2001).

BIOGRAPHY

Mr. Rungwit Laichuthai was born on September 28, 1983 in Bangkok. I graduated Bachelor Degree from Department of Computer Engineering, Faculty of Engineering at Kasatsart University in 2005 and post graduted the Master Degree from the Department of Computer Engineering, Faculty of Engineering at Chulalongkorn University in 2005.



สถาบันวิทยบริการ
จุฬาลงกรณ์มหาวิทยาลัย